UNITED STATES DEPARTMENT OF THE INTERIOR

GEOLOGICAL SURVEY

PREPARED IN COOPERATION WITH THE UNITED STATES DEPARTMENT OF ENERGY

Isotope Geochemistry of Carbonate Minerals in Nonmarine Rocks; Northern Green River Basin, Wyoming

By

Warren W. Dickinson[1]

Open-File Report 85-532

This report is preliminary and has not been reviewed for conformity with U.S. Geological Survey editorial standards and stratigraphic nomenclature

[1]Denver, Colorado 80225

1985

CONTENTS

CONTENTS--continued

ILLUSTRATIONS

ILLUSTRATIONS--continued

TABLES

Isotope Geochemistry of Carbonate Minerals in Nonmarine Rocks; Northern Green River Basin, Wyoming

By

Warren W. Dickinson

ABSTRACT

Petrographic and mineralogic analyses have been made on carbonate minerals in nonmarine rocks of the northern Green River Basin. Ratios of stable carbon and oxygen isotopes were measured in near-surface waters, in organic matter of shales, and in carbonate minerals of sandstones, shales, and fractures.

Normal hydrostatic pressures in the basin indicate an open hydrochemical system above 8,000 ft, whereas overpressuring below 10,000 ft implies a relatively closed system. Extensive reductions in porosity and permeability with depth not only lead to overpressuring but also enhance pore water evolution by reducing the water/rock ratio.

In sandstones, $\delta^{13}C$ and $\delta^{18}O$ of calcite cements generally become more positive with increasing depth. The increase of ^{13}C in deeper cements indicates that pore waters receive less ^{12}C from soil and atmospheric CO_2 and more ^{13}C from the ubiquitous grains of detrital limestone. Similarly, increased concentrations of ^{18}O in deeper cements requires equilibration with ^{18}O-enriched pore fluids, which evolve by less input of ^{16}O from meteoric waters and a greater input of ^{18}O from silicate and carbonate diagenesis at elevated temperatures.

With increasing depth, measured $\delta^{18}O_{calcite}$ in sandstone cements and in bulk shales converge from opposite directions toward a predicted $\delta^{18}O_{calcite}$, which was calculated from a closed system model of pore water. Deviation of measured $\delta^{18}O_{calcite}$ indicates: (1) that there is some lag in equilibration and (2) that above the overpressured zone, authigenic calcite may approach isotopic equilibrium with waters from an open system. This suggests that some portion of the calcite in both sandstones and shales continually recrystallizes during burial and approaches isotopic equilibrium with pore waters in open and restricted hydrochemical systems.

Shifts in the isotopic composition of dolomite in sandstones and shales, although difficult to interpret because of the complex nature of the dolomite, also suggest partial equilibration with burial.

Similar isotopic values between fracture calcites and calcite cements in sandstones indicates that local wall-rock materials were the source for fracture filling cements. Fracturing was a recent event, and the precipitation of filling cements was a relatively rapid geologic process.

INTRODUCTION

More than 15,000 ft of Upper Cretaceous and Tertiary nonmarine rocks have accumulated in the northern Green River Basin of west-central Wyoming (fig. 1). At depths generally below 10,000 feet they contain large reserves of natural gas in low permeability, overpressured sandstones and siltstones. Economic recovery of these reserves will depend largely on technological developments that will allow exploitation of natural permeability and artificial enhancement of the sandstones. However, for this to happen a better understanding for all geological aspects of the rocks is necessary. The isotope geochemistry of the carbonate minerals, calcite and dolomite, is one aspect of these rocks that is the focus of this thesis.

The Upper Cretaceous and Tertiary sandstones of the basin consist mostly of recycled sedimentary rocks and first-cycle arkose, which were deposited in a variety of alluvial plain environments. Although the total volume of carbonate is low in these rocks, it is present in various amounts throughout most of the gas-bearing reservoirs. Because significant amounts of secondary porosity may result from the dissolution of carbonate minerals (Schmidt and McDonald, 1979), information about them may help exploitation of the low permeability reservoirs.

I have examined outcrops and core from five wells in the basin. My intent is to demonstrate the source of intergranular and fracture filling carbonate cement in sandstones and to relate the isotopic composition of the carbonate minerals to diagenesis in open and restricted hydrochemical systems. To accomplish this goal, isotopic ratios of carbon and oxygen have been measured in near-surface waters, in organic matter of shales, and in carbonate minerals of sandstones, shales, and fractures. In addition, detailed petrographic analyses have been made on the carbonate minerals.

Stable isotopes of carbon and oxygen are useful in understanding the origin of carbonate cements. All modern evidence indicates that carbonate diagenesis takes place by dissolution and reprecipitation, which involves an intermediate transfer step by solution (Land, 1980). Because of this process, stable isotopes in authigenic carbonates contain a history of the fluids and temperatures of precipitation.

In general, it is not practical to measure absolute isotopic ratios of a mineral. Instead, the δ (delta) notation is used to compare the isotopic composition of the sample to an accepted standard. For example $\delta^{18}O$ is defined as

$$\delta^{18}O = \frac{(^{18}O/^{16}O)_{sample} - (^{18}O/^{16}O)_{standard}}{(^{18}O/^{16}O)_{standard}} \times 1000$$

where $\delta^{18}O$ is the relative difference in $^{o}/oo$ (parts per thousand) between the isotopic ratio in a sample and the ratio in a standard. In a similar fashion,

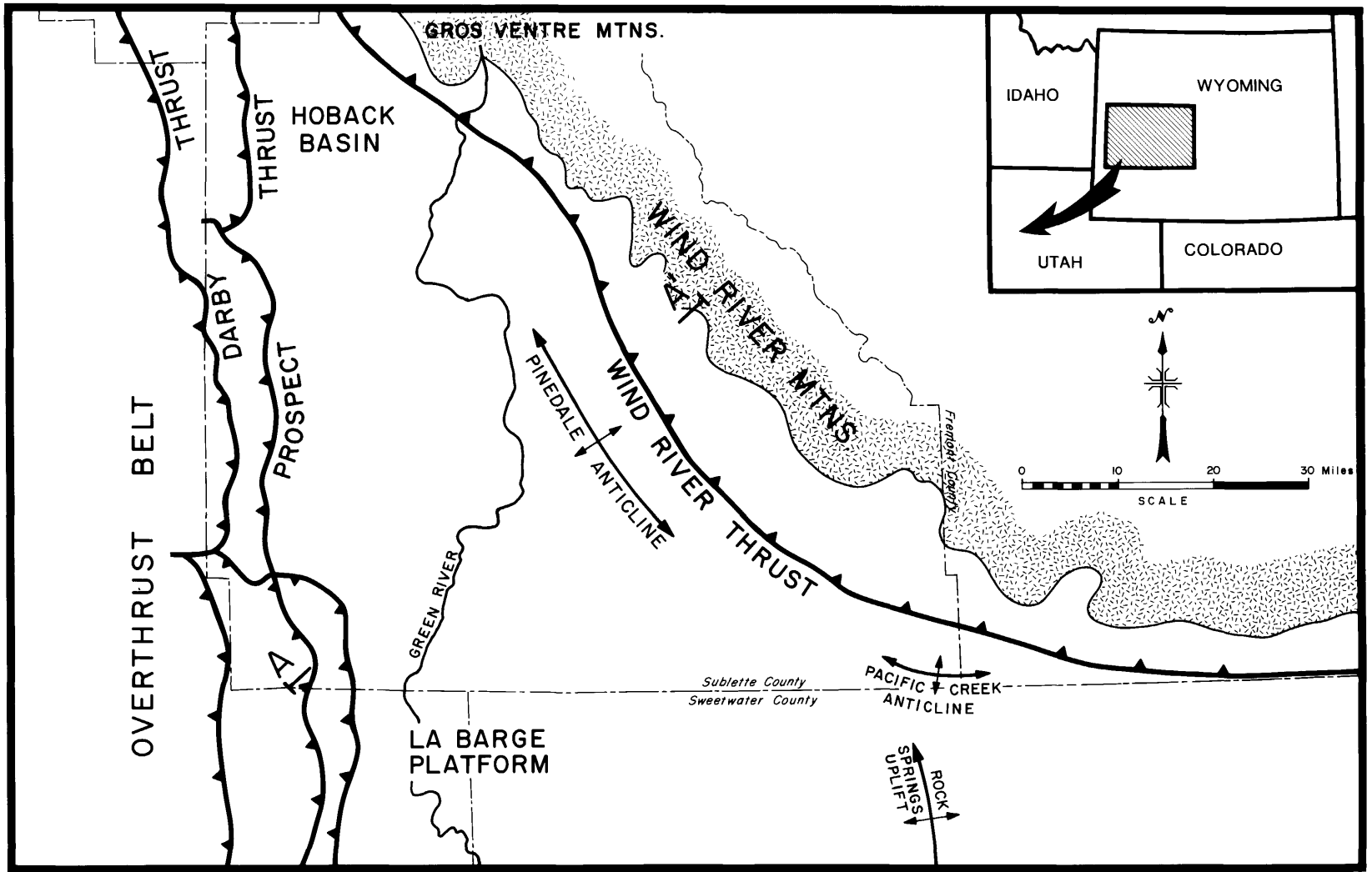

Figure 1.--Major structural and physiographic features of the northern Green River Basin. Cross section A-A' shown in Figure 2.

$^{13}C/^{12}C$ ratios are reported as $\delta^{13}C$. In this report, PDB is used as the standard for both carbon and oxygen in carbonate minerals. Although the supply of PDB, a Cretaceous Belemnite, has long since been exhausted, the values of other reference standards are always related back to it. The isotopic composition of PDB, $\delta^{13}C = 0$, $\delta^{18}O = 0$ by definition, is close to that of many marine carbonates. A positive δ value indicates enrichment in the heavy isotopes (^{13}C, ^{18}O) relative to the standard, and such substances are colloquially referred to as "heavy" in carbon or oxygen. Conversely, negative δ values are depleted in the heavy isotopes and often referred to as "light". For water and substances other than carbonates, SMOW (Standard Mean Ocean Water) is used as the oxygen reference standard. SMOW has a $\delta^{18}O$ of approximately -29.9 on the PDB scale.

Stable isotopes of carbon are most useful in identifying the source of carbon and hence the origin of carbonate minerals. In general, $\delta^{13}C$ allows distinction between light carbon derived from organic matter and heavy carbon derived from limestones, dolomites, and inorganic substances. The isotopic composition of sedimentary carbonates reflects a mixing or dominance of carbon from these sources.

Oxygen isotopes are useful in determining temperatures of precipitation if the $\delta^{18}O$ values of two minerals of interest (includes water) are known. The $\delta^{18}O$ of water can be used to help identify the source and the extent to which water has been modified by diagenetic reactions. For example, mineral-water reactions will have little effect on the isotopic composition of waters that flow rapidly through a pore network. On the other hand, such reactions should significantly modify $\delta^{18}O$ of stagnant pore waters. The $\delta^{18}O$ of diagenetic minerals reflects not only temperature but also shifts in the $\delta^{18}O$ of pore water.

In this study the effective use of oxygen isotopes is limited because $\delta^{18}O$ has only been measured in near-surface waters, calcites, and dolomite. However, if the assumption is made that some portions of the carbonate minerals continually recrystallize with burial, shifts in the $\delta^{18}O$ of deep pore waters may be reflected in the $\delta^{18}O$ of diagenetic carbonates. Such a shift is observed in the carbonate cements of this study. I will show that it is caused mainly by a shift in $\delta^{18}O_{water}$ from the open hydrochemical system of the normally pressured zone to the restricted system of the overpressured zone.

A major problem in studying the isotopic composition of carbonates in clastic rocks is the separation of an adequate quantity of a particular phase for analysis. One way to partly avoid this problem is to correlate a large number of bulk isotopic analyses with their carbonate mineralogy, which has been petrographically determined. Using these data and a consistent laboratory method of measurement, relative differences in isotopic compositions between samples can be observed.

This introduction is followed by a discussion of background material which includes the stratigraphic, hydrologic, and hydrocarbon producing aspects of the basin. Mineralogical and isotopic data for carbonates in sandstones, shales, and fractures are presented in the next four sections. Following these, the general principles of isotope geochemistry are considered, and models are constructed in preparation for an interpretation of the isotopic data presented in the previous sections. The discussion, which provides most of the interpretations and conclusions of the report, relates the isotopic composition of the carbonates to the models, and geology of the basin.

GEOLOGIC SETTING

The northern Green River Basin lies between the Wyoming - Idaho thrust belt on the west, the Wind River Range on the east and the Gros Ventre Range on the northeast (fig. 1). The southern boundary, which was arbitrarily chosen, extends from Pacific Creek on the southwestern flank of the Wind River Range westward to the La Barge Platform and roughly coincides with the Sublette - Sweetwater County line. The Hoback Basin, a physiographic basin at the northern end of the structural Green River Basin is also included in this area.

The deepest part of the northern Green River Basin is east of the Pinedale anticline and contains about 32,000 feet of sedimentary rocks (fig. 2). Of this, about 24,000 ft are Late Cretaceous, Paleocene and Eocene in age and include, the Hilliard, Mesaverde, Ericson, Lance, Ft. Union and Wasatch formations. Middle Eocene rocks are exposed over most of the area. Older rocks in the subsurface have been truncated by erosion and thrust faults and are not exposed along the margins of the basin (fig. 2).

Tectonics and Sedimentation

During the Paleozoic and early Mesozoic, the area of the northern Green River Basin was part of a vast continental shelf on the western edge of the North American craton upon which accumulated a relatively thin veneer (about 6,000 ft) of sediments consisting mostly of marine carbonates but with some clastics. To the west, the rapidly subsiding Cordilleran miogeosyncline became the site for nearly uninterrupted deposition of marine carbonates. By Late Triassic time, pulses of uplift in south central Idaho initiated the breakup of the miogeosyncline (Armstrong and Oriel, 1965) and marked the beginning of a new orogenic period.

In latest Jurassic and earliest Cretaceous time, thrusting in southeastern Idaho produced highlands that destroyed the Cordillerian miogeosyncline (Armstrong and Oriel, 1965). This tectonism spread eastward into Wyoming and created a permanent high that gradually exluded marine sedimentation. The last marine invasion into the northern Green River Basin area occurred during Coniacian time (85 m.y.; Dorr and others 1977). This transgression was followed by a period of rapid terrestrial deposition.

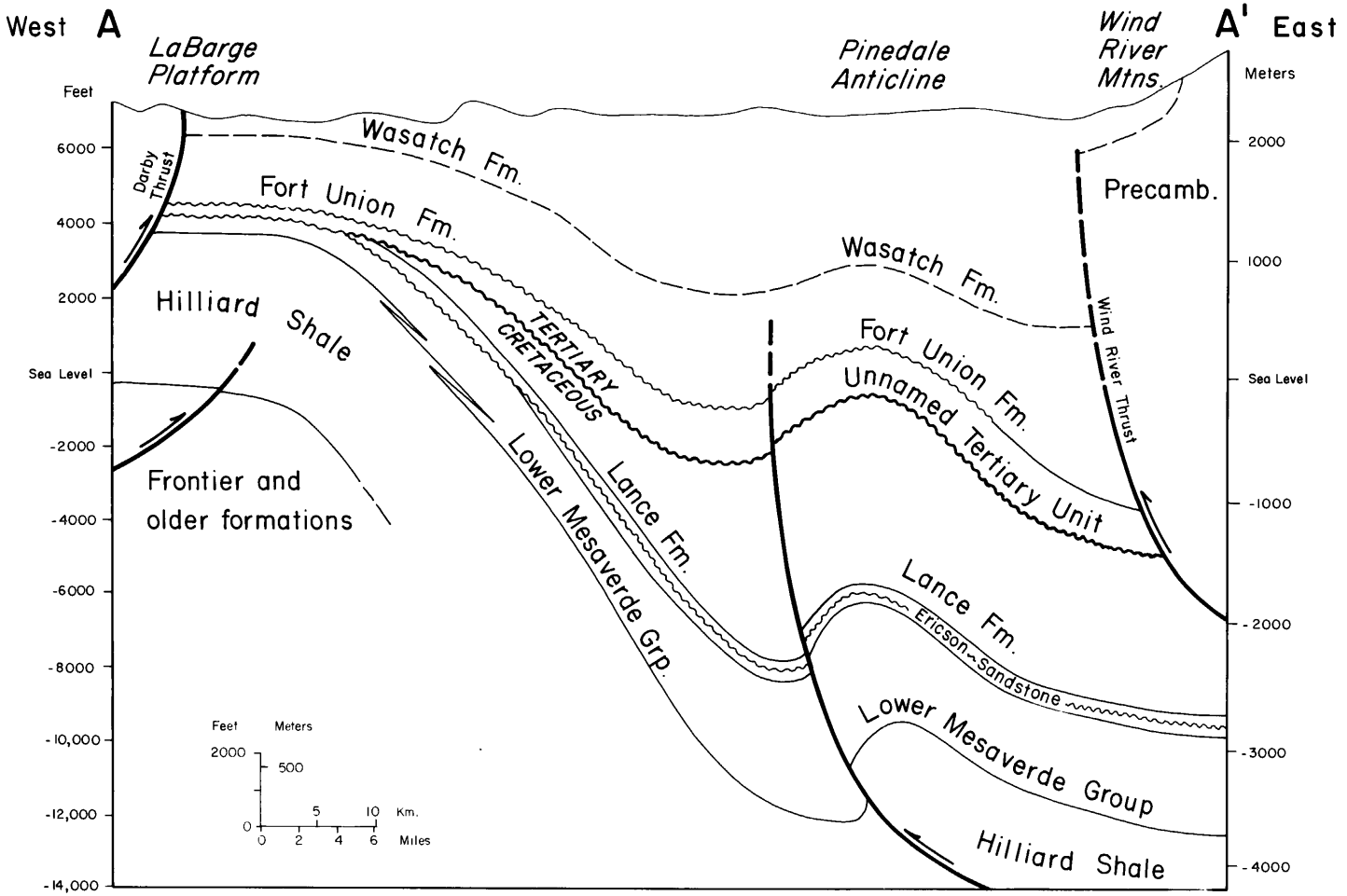

Figure 2--West to east cross section A-A′ through the northern Green River Basin (after Law, 1984) for location see Figures 1 or 3.

It is clear that large amounts of sediment accumulated in the northern Green River Basin during periods of tectonic activity in Late Cretaceous and early Tertiary times. To explain this and the development of the basin, Shuster and Steidtmann (1984) have modified existing flexural models. They suggest that subsidence of the area began by a depression of the lithosphere caused by loading from the Darby, and Prospect thrust plates on the west and Wind River thrust plate on the northeast (fig. 1). Erosion of the rising thrust plates coupled with subsequent deposition in the adjacent depression could have redistributed this load and modified the basin into its present shape (Shuster 1983).

For most of the time between the latest Cretaceous and present, the area has been an intermontane basin and the site for synorogenic deposition. The basin received sediment from the west, north, and east at a rate that was in accordance with local tectonic activity. Dorr and others (1977) and Shuster and Steidtmann (1984) indicate that there was no deposition in the northern end of the basin after early Eocene time. However, the presence of Oligocene, Miocene, and possibly Pliocene deposits suggest that basin filling continued along the south and southwestern flanks of the Wind River Range (Zeller and Stevens, 1969) albeit at a slow rate after the Eocene. In either case, burial history after the Eocene is difficult to interpret because of widespread erosion caused by several thousand feet of regional uplift in the late Pliocene (Love, 1960). Undoubtedly, filling proceeded at various rates and times throughout the basin, but post-Eocene sediments were thin because major tectonism had ended by mid-Eocene time.

Sediment Source and Deposition

Sandstone composition varies throughout the basin and depends largely on the type and location of the source rocks. In general, Upper Cretaceous to Tertiary sandstones grade in composition from lithic to arkosic. A large increase in arkose commonly marks the Cretaceous - Tertiary boundary. Lithic sandstones are of interest to this report because they contain up to 10 percent of carbonate rock fragments. Most of the lithic debris in the basin came from the west as a result of repeated uplift by low angle thrusting and subsequent erosion of thick Paleozoic sediments. Detrital carbonate grains found in Upper Cretaceous and Paleocene sandstones probably came from the Paleozoic carbonates that were deposited in the miogeosyncline.

Erosion of the Wind River and Gros Ventre Ranges, which were initially uplifted during the Late Cretaceous (Love, 1960), added large amounts of arkosic debris but only minor amounts of lithic debris to the basin. This is because the Paleozoic section on the east side of the basin is much thinner than on the west, and it was not subjected to the repetitive erosion caused by multiple thrust faults. As the Wind River and Gros Ventre ranges uplifted along single, high angle thrusts, the thin sedimentary section was rapidly stripped to expose Precambrian igneous and metamorphic rocks. Judging from the volume of arkose and lack of lithic fragments in the Tertiary sandstones

of the Wagon Wheel #1 well (fig. 3), the Precambrian of the Wind River Range was fully exposed by mid-Paleocene time. While upper Paleocene and younger sediments in the eastern part of the basin are entirely arkosic, rocks of equivalent age in the western part of the basin, which were much farther from arkosic sources, contain both arkose and detrital carbonate. In the northern part of the basin, arkosic sediments did not dominate until the Eocene, when transport directions shifted from eastward to southward (Dorr and others 1977).

Alluvial fan, alluvial plain, and flood plain environments generally characterize Late Cretaceous and early Tertiary deposition in the basin. Thin coal beds are common in Paleocene and older sediments but rare in Eocene rocks. Although large Eocene lake deposits are restricted to the southern Green River Basin, a few small lake deposits of Paleocene and Eocene age are exposed in the Hoback Basin (Dorr and others 1977), but none have been observed in the central portion of the northern Green River Basin (B. E. Law, oral commun. 1983).

The composition and texture of the basin sediments are typical of those resulting from synorogenic deposition and proximity to source rocks. Characteristically, the sandstones are poorly sorted in core from 5 wells (fig. 3). Grain size, which overall coarsens upward or with decreasing age, reflects the approaching source rocks as thrust plates encroached on the basin from the west and the east. In the Wagon Wheel, Wasp, and Pacific Creek wells (fig. 3), sand/shale ratios calculated from logs have an average value of 1:2.4. Although most of the sands and shales are lenticular and not traceable for more than a mile in the subsurface, other logs and core suggest this average ratio is representative for the Upper Cretaceous and Tertiary most parts of the central basin.

Sandstone Reservoirs

In most parts of the northern Green River Basin at depths below 9,000 ft, the Upper Cretaceous and Tertiary rocks contain large reserves of natural gas in low-permeability, overpressured sandstones (Spencer, 1983). Neither structure nor stratigraphy are important for gas entrapment. Rather, the occurrence of gas appears to result from a dynamic balance between organic richness, temperature and low-permeability. Exploration and development of these reservoirs has been hindered by the low-permeability and discontinuous nature of the sandstones. In the late 1960's the Wasp and Wagon Wheel wells were drilled for the purpose of nuclear stimulation which was never completed because of poor results elsewhere. However, because gas reserves are present, the sandstones have been the subject of considerable research. The low permeability of these sandstones has led not only to overpressuring but also initiated a relatively closed hydrological system.

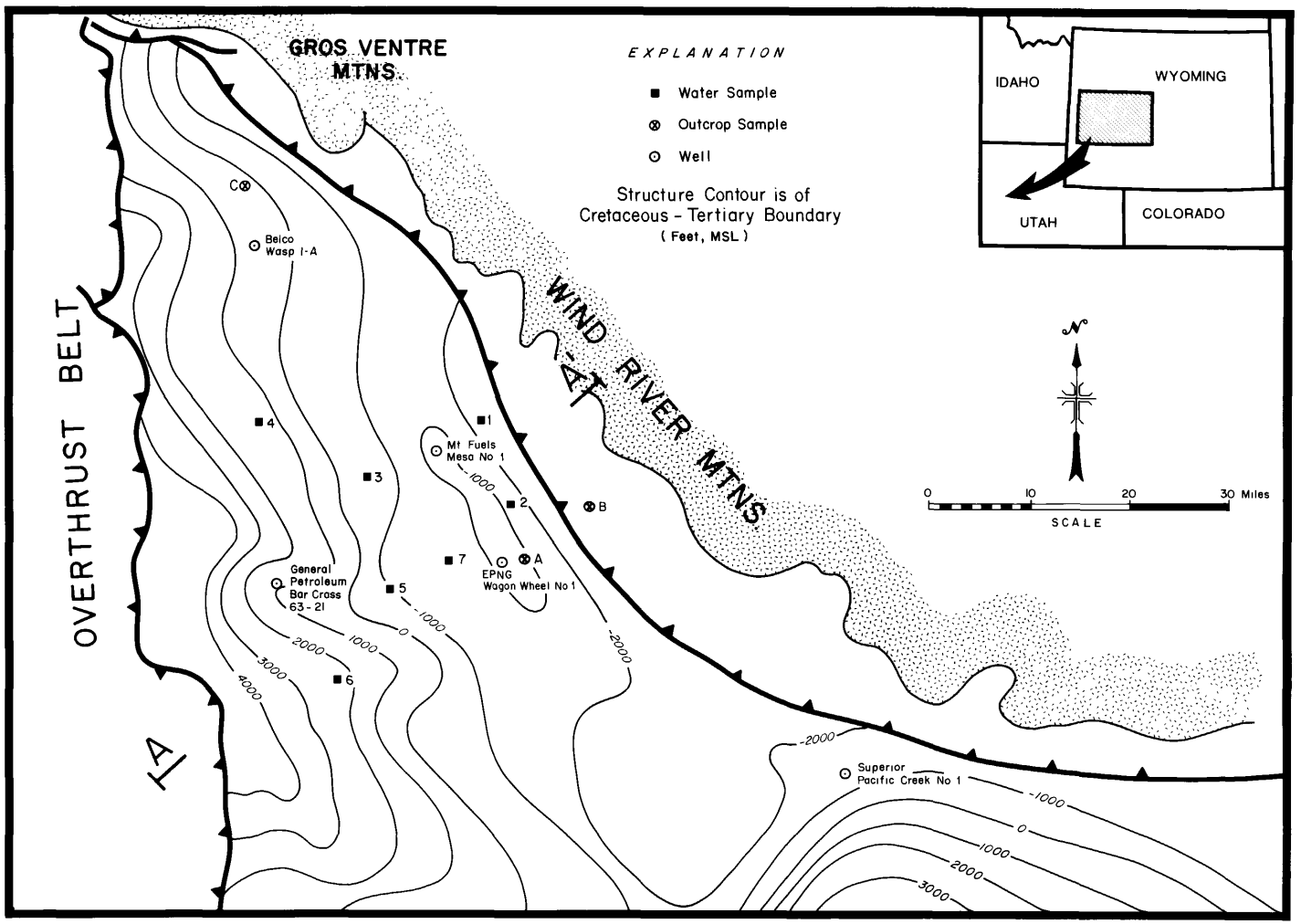

Figure 3—Northern Green River Basin showing location of outcrop samples, of wells sampled for water, and for core analysis. Structure compiled from Bucurel (1981) Law (1981), and Law (unpub. 1982).

Porosity and Permeability Loss

In the basin, porosity decreases with increasing depth both laterally within the same formation and vertically through different formations. The quantity and depth distribution of core porosity data are sufficient from the Wagon Wheel well to show this relationship (fig. 4). Porosities decrease with depth from 20 percent to 2 percent and average 7.9 percent. These measurements are good estimates of in situ conditions because overburden pressure has little effect on porosity (Thomas and Ward, 1969). Even though there is a considerable range of porosity within each cored interval, maximum sandstone porosity decreases with depth. This trend, which may be biased towards the "clean" sandstones, is also supported by log-calculated porosities (figs. 5 and 6).

Throughout the basin, there is a lack of reliable permeability data because the conventional methods, which are often used, cannot accurately measure the extremely low permeabilities of the reservoir sandstones (Thomas and Ward, 1969). In spite of this, conventional measurements clearly indicate that maximum permeability decreases with depth (fig. 7). The limit of resolution for conventional measurements is about 0.01 millidarcy (md). Methods developed by Thomas and Ward (1969) allow resolution beyond this limit and show that in situ stress from overburden pressure greatly reduces permeability. Permeabilities of reservoir sandstones, which have been either measured by in situ methods or calculated from drill-stem tests are about an order of magnitude lower than conventional measurements and range from 0.001 md to 0.02 md (Ahmed and others 1981). By comparison, the permeability of many mudrocks is within this range.

In the Wagon Wheel well there is a positive correlation (0.71) between porosity and permeability (fig. 8). Presumably, the diagenetic processes that are observed to reduce porosity in thin section also reduce permeability. Porosity reduction proceeds by three principal processes: 1) grain deformation and compaction; 2) precipitation of calcite and silica cements early in the burial history; and 3) filling and coating of residual and secondary pores by illite, chlorite, microcrystalline quartz, and ferroan carbonates (Dickinson and Gautier, 1983).

I made no attempt to interpret the complex sequence of pore-filling cements which differs from zone to zone. However, it is apparent that the dominant pore reducing process depends largely on the depositional environment and initial composition of the sediment. For example, more than half of the sandstone core, which I examined from five wells, lacked obvious sedimentary structures (fig. 9a, b). Most of these sandstones are the product of flood plain deposition, soft sediment deformation, and bioturbation caused by infaunal digging and pedogenesis. These processes result in the homogenization of sand and mud to form a mixture that is poorly sorted and depleted in porosity. The initial composition of many sandstones, which received detritus from sedimentary rocks, included a large percentage of ductile, framework grains such as clay or shale clasts. When compressed

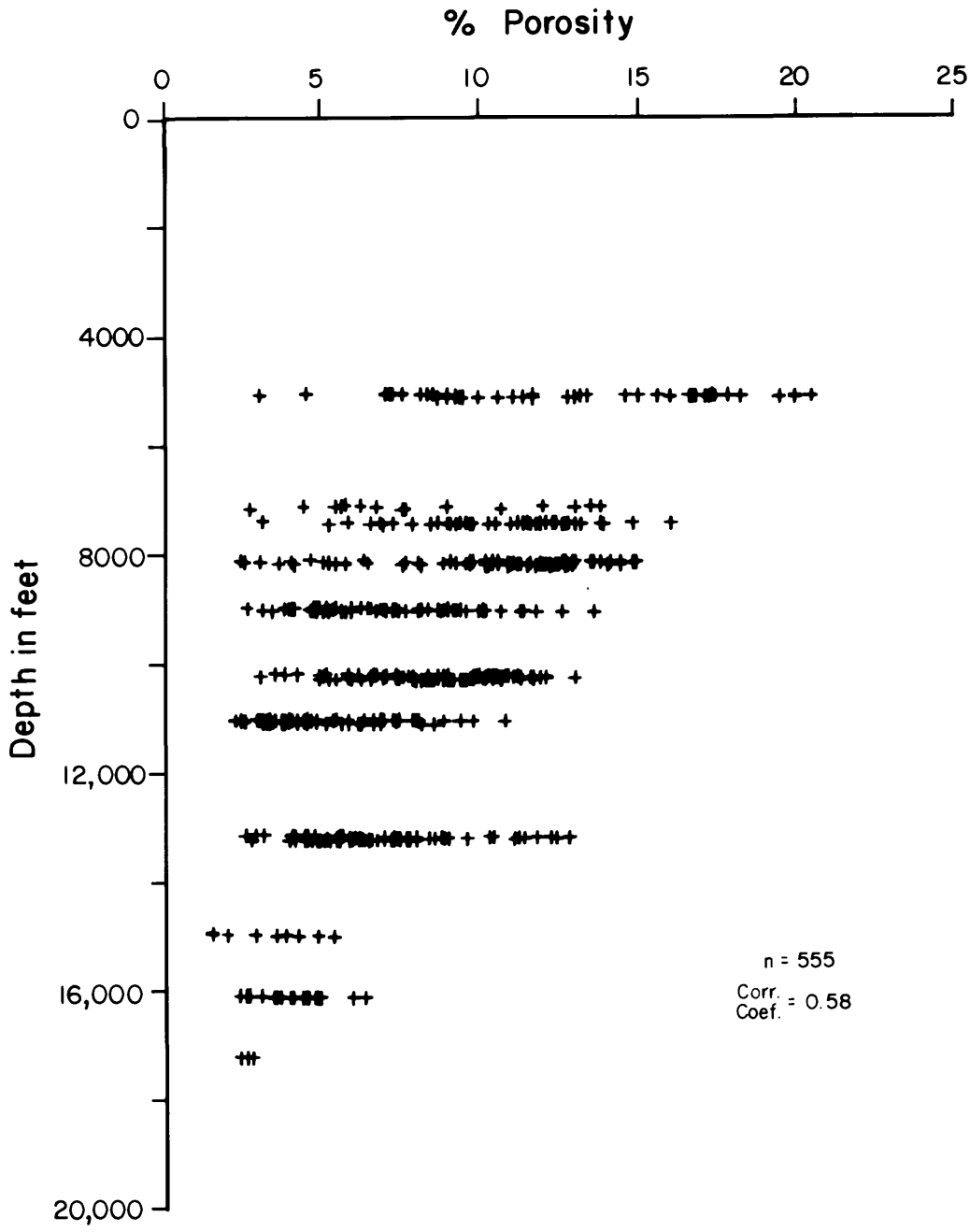

Figure 4--Measured helium porosity of sandstones in core from EPNG, Wagon Wheel #1 well.

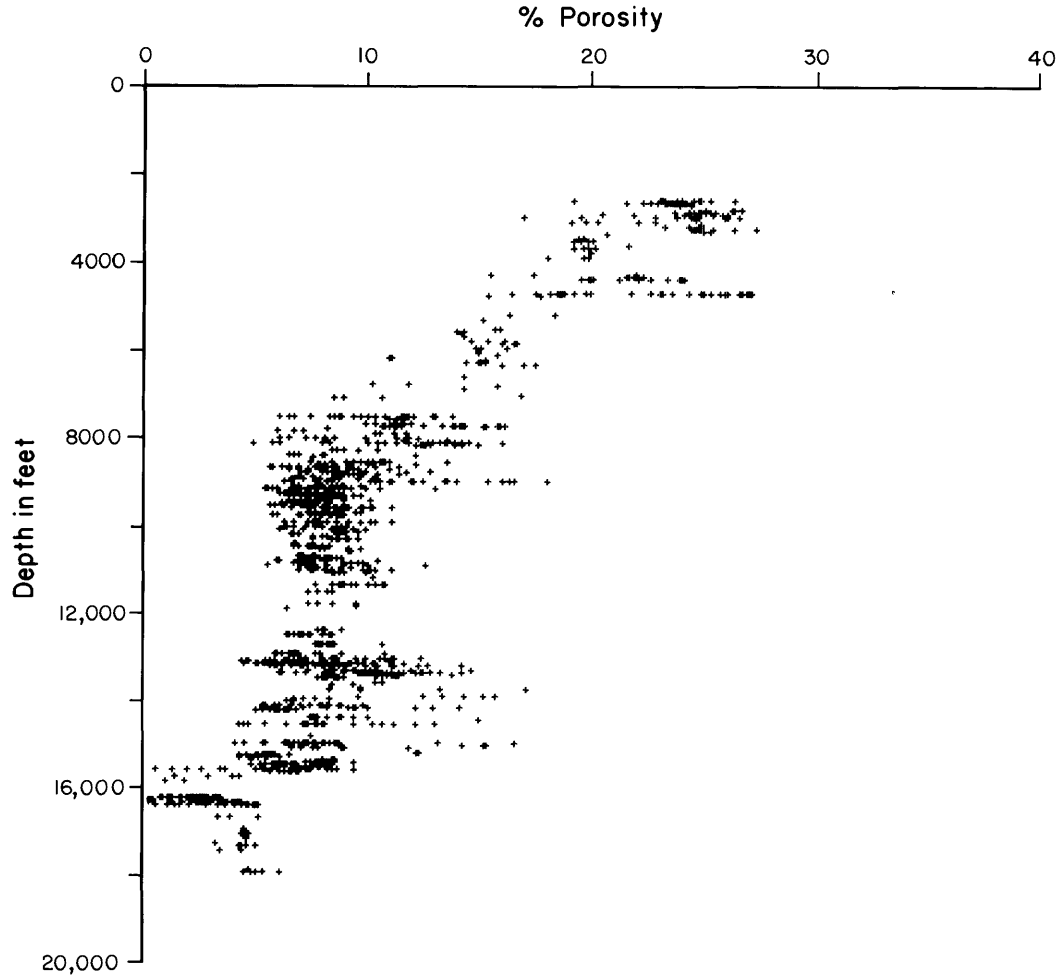

Figure 5--Log measured, sidewall neutron porosity of sandstones in Wagon Wheel #1. A three-point smoothing routine removed some of the scatter that resulted from depth shifts and hand digitizing of a paper print. Plot shows porosity values at one foot increments in sandstones, which were chosen as rocks with less than 50 API units on the gamma ray log.

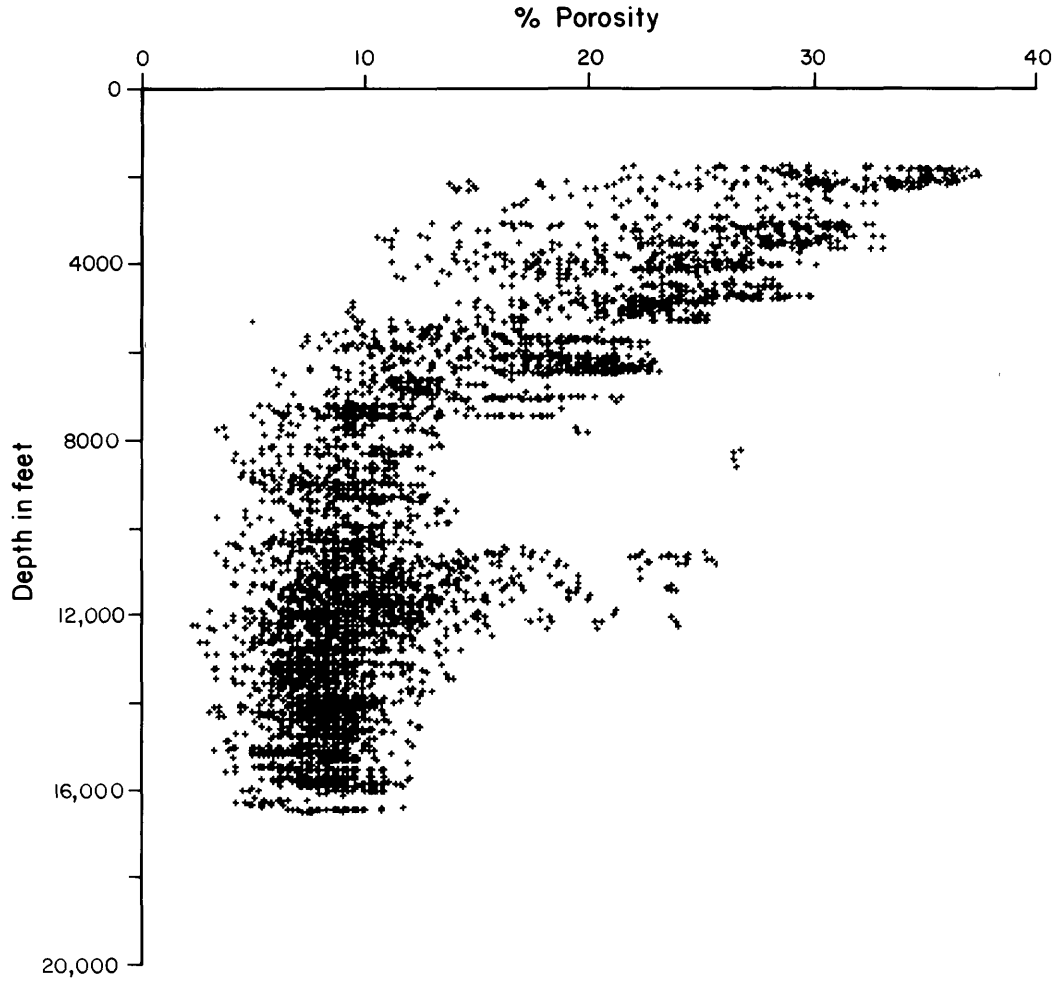

Figure 6--Log measured and calculated sonic porosity of sandstones in the Apache #36-1 well (about 3 miles east of the Belco WASP 1-A, Fig. 3). A grain density of 2.68 was used to calculate porosity from sonic travel time. Points are porosity values at one foot increments in sandstones, which were chosen as rocks with less than 50 API units on the gamma ray log. The zone of increased porosity around 12,000 ft is due to the Ericson Sandstone, a quartz arenite, which is significantly different than the overlying and underlying rocks.

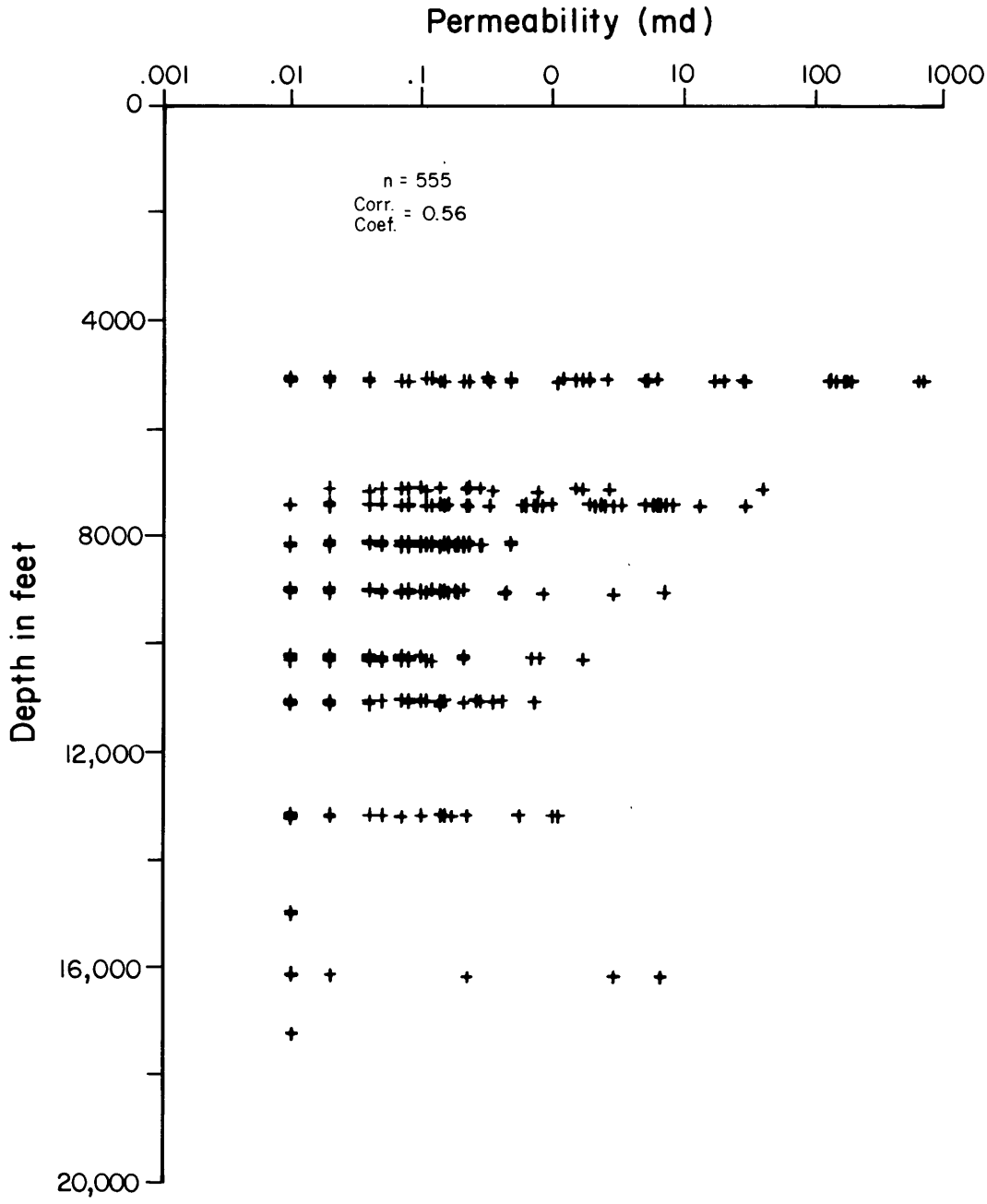

Figure 7--Conventional (not stressed to simulate overburden pressure) permeability of sandstones in core from Wagon Wheel #1.

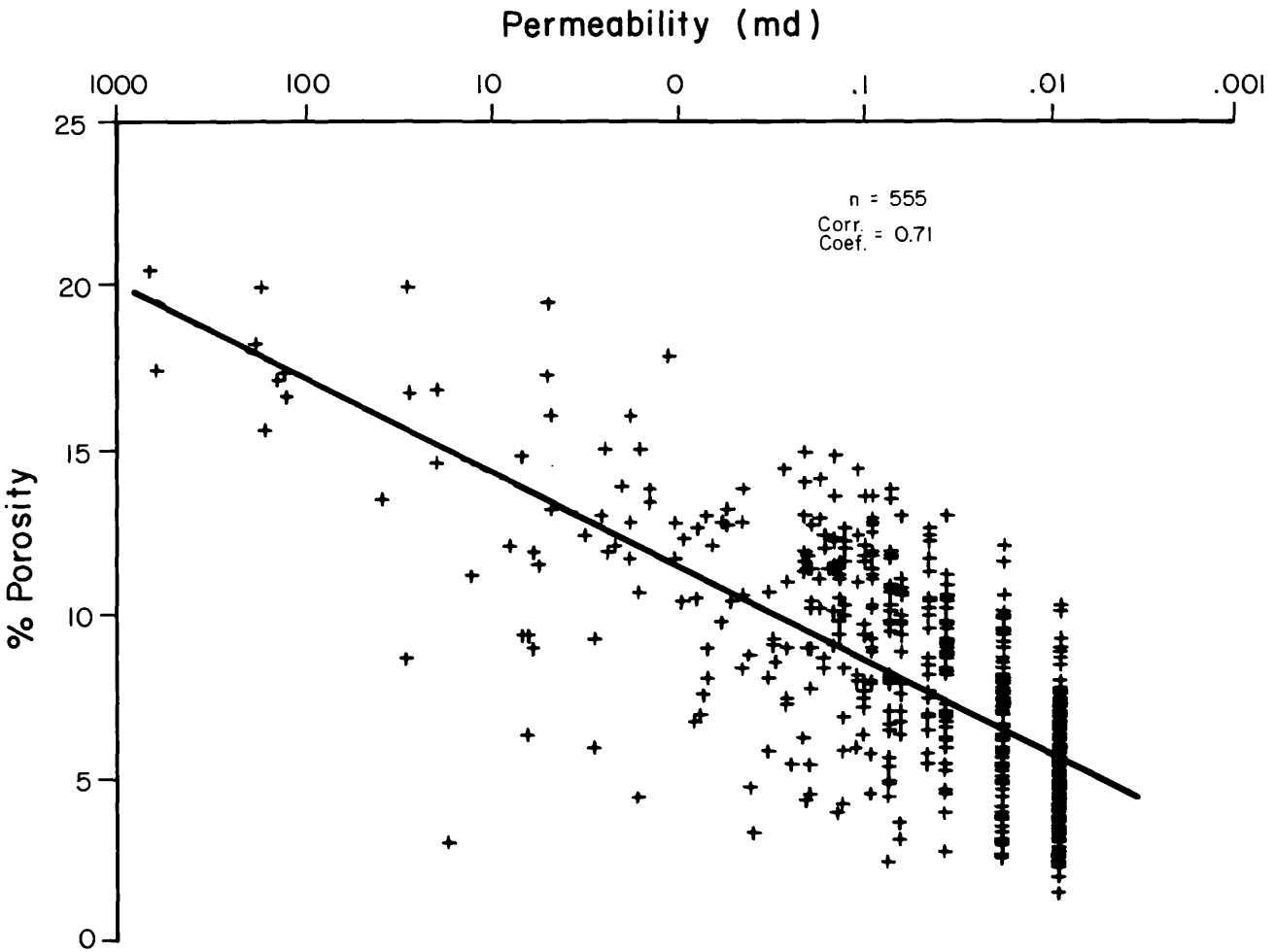

Figure 8--Conventional (not stressed to simulate overburden pressure) permeability versus porosity in sandstone core from Wagon Wheel #1. The high density of points "stacked" at .02 and .01 millidarcys reflects the artificial limit of conventional permeability measurements.

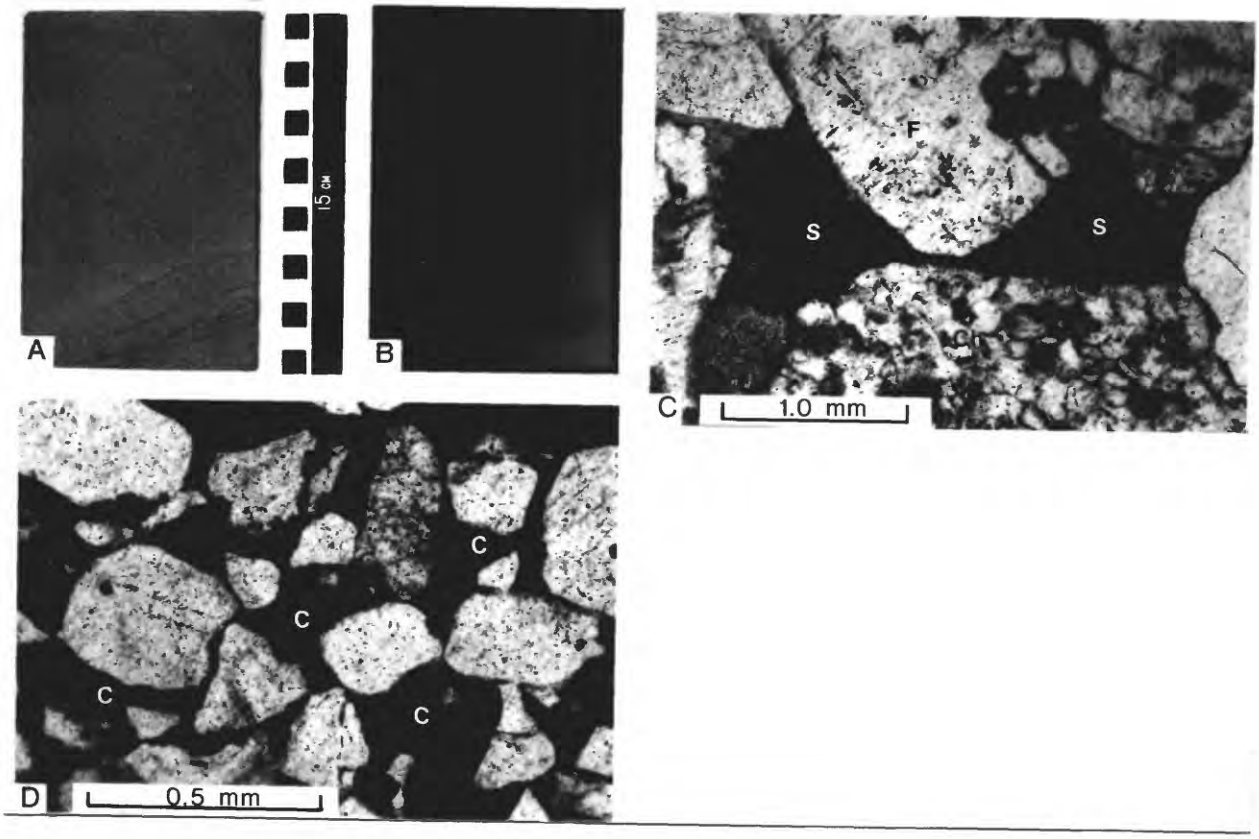

Figure 9--Examples of porosity reducing processes in Upper Cretaceous and Tertiary sandstones of the northern Green River Basin. A) slab of core shows a massive and poorly sorted sandstone resulting from soft-sediment deformation above contorted ripple lamination. B) Radiograph of same slab shows lack of structural detail in the "homogenized" part of the sandstone. C) Pseudomatrix forms when a ductile grain of shale (S) is compressed between stronger grains of chert (Ch) and feldspar (F). D) Sample, WASP-197 at depth 12,514′ in the overpressured zone showing early inclusion-rich, fine grained calcite cement (C, dark pink stain), which has precipitated before significant compaction of framework grains. Minus-cement porosity is 24 percent.

between stronger grains of quartz, chert, and other brittle rock fragments, these grains deform and flow into adjacent pore space (fig. 9c). Sandstones that contain 45 percent ductile grains can lose all original porosity simply by ductile grain deformation (Jonas and McBride, 1977). On the other hand, early cementation was the dominant process of porosity loss in quartz-rich sandstones which were initially well sorted and contained few ductile grains (fig. 9d). Because these sandstones escaped the effects of initial compaction and syndepositional mixing, they were more porous and permeable than their poorly sorted counterparts. As a result, large volumes of water passed through them carrying dissolved solids that precipitated and led to early cementation.

The net reduction in porosity from 2,000 to 18,000 ft illustrated in figures 4 to 6 is interpreted as a continuous loss of primary and secondary porosity. Most of the primary (original from deposition) porosity in these rocks is probably lost between the surface and about 5,000 ft deep. However, large volumes of meteoric water also circulate within this zone and may remove enough dissolved solids by the dissolution of grains and cements to cause a net gain in the amount of secondary porosity. Thus, as primary porosity is continually lost, secondary porosity is continually generated so that net porosity is both lost and redistributed with burial. Below 5,000 ft little primary porosity exists and there is a continual loss of secondary porosity. The slight increase in porosity at about 13,000 ft is due to the presence of a quartz arenite which is lithologically distinct from the overlying and underlying rocks.

Gas Generation and Overpressuring

Observations by Law and others (1980) indicate that large gas accumulations in the basin are associated with fluid pressures which are greater than hydrostatic pressure (overpressuring). They found that the top of overpressuring commonly is coincident with temperatures of 88° to 93°C (190° to 200°F) and a vitrinite reflectance of about R_o = 0.8 (fig. 10). The similarity in carbon isotopic ratios between desorbed gas from cored shales and well-head gas suggests that gas is currently being generated from local rocks rich in organic carbon (Law, 1984). Overpressuring is thought to result from the thermal generation of gas in low-permeability rocks (Law and others 1980; McPeek, 1981; Law, 1984). If this is the case, the extent of overpressuring depends on the permeability of the rocks and the rate of gas generation, which is controlled by temperature and organic richness. Gas accumulates because it is generated at a rate that exceeds its ability to escape.

Overpressuring is important because it not only indicates the presence of gas but also indicates a relatively closed hydrologic system. The low permeability and discontinuous nature of the sandstones prevent direct fluid migration to and from the surface. Obviously, migration takes place over geologic time, but I have no estimate of how "closed" the system is. However,

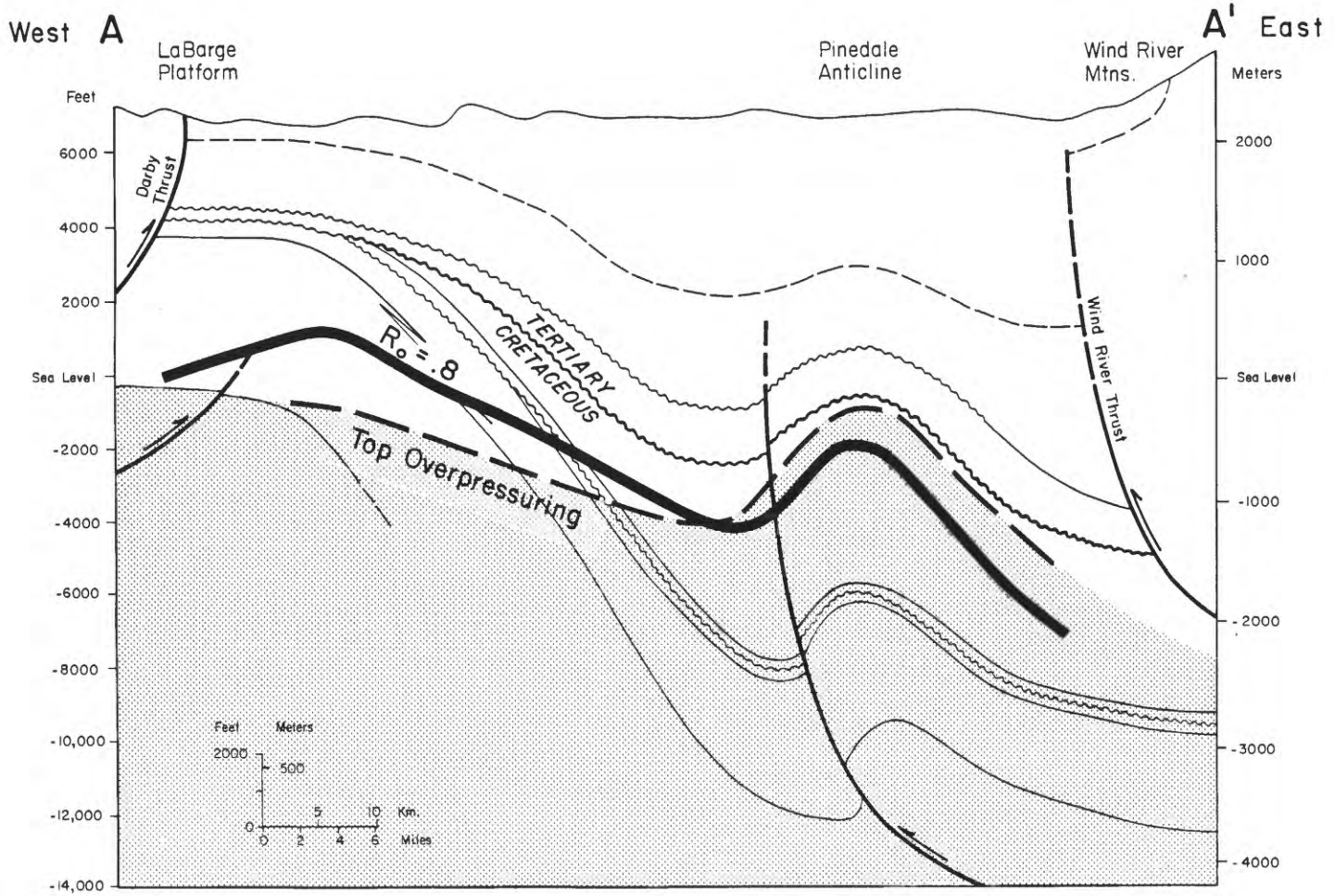

Figure 10--Cross section A-A′ (see fig. 3 for location) showing the relationship of the top of overpressuring to a vitrinite reflectance of R_o = 0.8 percent. The two are commonly coincidental and truncate formation boundaries (after Lickus and others, 1984).

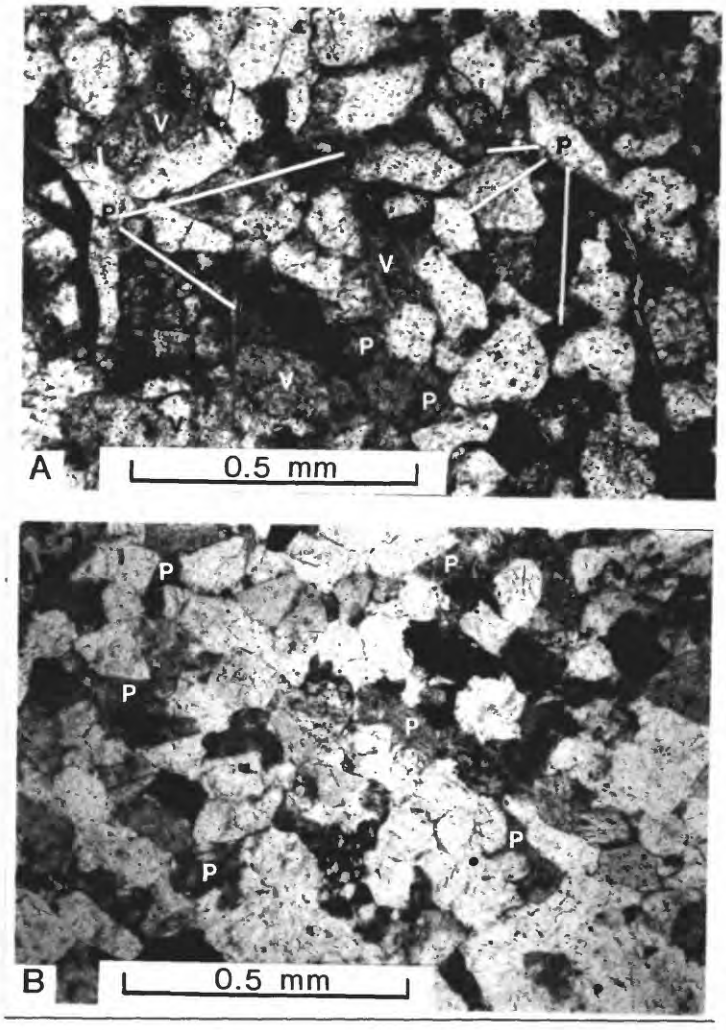

Figure 11--Contrasting porosities and permeabilities between normally pressured and overpressured sandstones with similar grain size from the Lance Formation. A) Normally pressured sandstone at depth 4,004′ in Bar Cross #63-21. Connected pores (P, blue epoxy) and dissolution of famework grains (V) give this sandstone relatively high porosity and permeability. B) Down-dip, overpressured sandstone at depth 10,980′ in Wagon Wheel #1. Compaction, quartz cementation, and clay-filled pores (P, blue epoxy) have reduced porosity and permeablilty.

Table 1.--Selected isotopic composition of near-surface waters Sublette Co., Wyoming

Sample	Location	Well Depth (ft.)	$\delta^{13}C$ °/oo PDB	$\delta^{18}O$ °/oo SMOW	δD °/oo SMOW	^{14}C % Modern	Tritium TU*
1	NW 1/4 sec. 30 T.34 N., R.109 W.	75	-10.2	-17.4	-134	56.6 ± 0.9 (4,700 yrs.)†	2.4 ± 4.2
2	NW 1/4 sec. 5 T.31 N., R.109 W.	80	-11.5	-20.1	-159	---	16.9 ± 4.2
3	NW 1/4 sec. 24 T.32 N., R.111 W.	60	-6.7	-20.2	-156	15.2 ± 0.4 (15,600 yrs.)†	5.4 ± 4.1
4	SE 1/4 sec. 21 T.33 N., R.112 W.	---	-9.7	-19.3	-155	---	<1 ± 4.1
5	SW 1/4 sec. 20 T.30 N., R.110 W.	104	-5.0	-20.8	-162	4.8 ± 0.4 (25,100 yrs.)†	3.1 ± 4.2
6	SW 1/4 sec. 6 T.28 N., R.111 W.	200	-9.9	-20.3	-157	---	4.5 ± 4.1
7	NE 1/4 sec. 5 T.30 N., R.109 W.	450	-7.2	-20.4	-157	---	<1 ± 4.1
	Average	162	-8.6	-19.8	-154		

Note: Unpublished data from B.A. Kimball U.S.G.S. (WRD).
* Tritium Unit = (PCI/L)/3.22
† Apparent age (no "dead" carbon correction)
--- no data available

with measured permeabilities in the microdarcy range and relative permeabilities even lower, it is probable that the migration of gas or water occurs more by diffusion than by darcy flow.

The distinct petrographic differences between normally pressured and overpressured sandstones support the premise of nearly closed conditions in the overpressured rocks. Dissolution features prevalent in the normally pressured rocks are lacking in the overpressured rocks (fig. 11). Although the rocks of each pressure regime had similar provenance and depositional environments, they have undergone different diagenesis. Because of the low permeability, large volumes of material can neither be removed from nor brought to the overpressured sandstones. On the other hand, the greater fluid flow in the normally pressured rocks permits significant removal of material by dissolution and precipitation of large volumes of externally supplied cement. Although diagenesis obscures much of the evidence, the high minus-cement porosity of some overpressured sandstones such as figure 9d, suggest that they were once in an open system.

Hydrology

The isotopic composition of pore waters greatly aides interpretation of the isotopic composition of the carbonate minerals. Unfortunately the actual pore waters from the rocks of interest are rarely available, and this is especially true in the northern Green River Basin where deep pore waters usually cannot be extracted for analysis. However, near-surface waters in the basin offer a possible starting point for data which can be extrapolated to deeper rocks. In addition, paleohydrologic conditions can be inferred from the present conditions and the geologic history of the area.

Present Conditions

Widespread aquifers having uniform characteristics are absent from the northern Green River Basin and most useable ground water comes from lenticular, fine- to coarse-grained Eocene arkose of the Wasatch Formation (Welder, 1968). These waters, which are usually less than 500 ft deep, contain predominantly sodium-bicarbonate and generally have less than 500 ppm total dissolved solids (TDS). In seven wells that were sampled during this study (fig. 3), the water levels were not deeper than 50 ft and hydraulic conductivities are estimated at 50 to 100 gal/day/ft. As with most sampling proceedures it is important to remember that the water samples represent the most permeable horizons and may not be similar to the pore waters in the nearby low-permeability horizons. Nevertheless, the isotopic composition of the water samples reveals several interesting features (table 1).

In spite of their moderate discharge rates and shallow depths these ground waters are relatively old. In most of the samples (table 1) tritium is undetectable within analytical error, indicating that the water entered the aquifer prior to 1953 (pre-bomb water). Although the apparent ages from ^{14}C are erroneously old because of dilution with "dead" (no detectable ^{14}C)

carbon, the error should be minimized by the paucity of detrital carbonate and organic matter in the aquifers. If these ages are approximately correct, there is a strong possibility that the surface environment during recharge was different from the present and this could affect the interpretation of the ground water evolution.

Carbon isotopic ratios in ground water are a function of pH, CO_2 partial pressure (P_{CO_2}), and the dominant source of carbon contained in the carbonate species. Essentially, there are two pathways from which carbon can enter ground water: 1) There are sources that provide carbon to the water either before or during recharge. These include mainly atmospheric CO_2 ($\delta^{13}C \simeq -7^o/oo$, PDB) and soil CO_2, which is a combination of CO_2 from decomposing organic matter ($\delta^{13}C \simeq -15$ to $-35^o/oo$, PDB) and plant root respiration ($\delta^{13}C \simeq -21$ to $-26^o/oo$, PDB). In areas of lush vegetation, soil CO_2 is the dominant source, but in arid climates it is a minor source. In addition, runoff from limestone terrane and the dissolution of atmospheric dust derived from the erosion of carbonate rocks may contribute carbonate species with $\delta^{13}C$ from 0 to $-9^o/oo$, PDB. 2) Carbon can also enter ground water from sources within the aquifer by the dissolution of carbonate minerals or the production of CO_2 from oxidation of organic matter. However, the isotopic values of carbon from these sources are identical to those values of carbon from recharge.

Without detailed modeling it is difficult to interpret the evolution of $\delta^{13}C$ in table 1, but some inferences are possible. Deines and others (1974), emphasized the dependence of ground water $\delta^{13}C$ on the presence or absence of a fixed P_{CO_2} (open or closed system of Garrels and Christ, 1965 Ch. 3). Judging from the age of the waters, it is likely that they have been in a closed system, isolated from the atmospheric CO_2 reservoir. Thus, $\delta^{13}C$ of the waters may be interpreted as a balance between $\delta^{13}C$ from the initial recharge and $\delta^{13}C$ from carbon sources within the aquifers. Caliches derived from aeolian carbonate dust (Gardner, 1972), although important in many parts of the southwestern United States, have not been reported in the study area. Pearson and Hanshaw (1970) report $\delta^{13}C$ values of -15 to $-19^o/oo$ (PDB) for CO_2 from arid west Texas soils, which are similar to those in the northern Green River Basin. Limestones in the vicinity of Yellowstone (50 miles north) have an average $\delta^{13}C = +.51^o/oo$, PDB (Friedman, 1970), whereas unaltered detrital carbonate grains from this study have an average $\delta^{13}C = -.33^o/oo$, PDB. Although the arkosic aquifers, which contain little organic matter and few detrital carbonate grains, appear to be a poor source for carbon, the volume of carbonate dissolving over long periods of time must be sufficient to increase the $\delta^{13}C$ of the waters. For example, if the flow of ground water roughly parallels surface drainage, then samples 2, 7, and 5 (table 1) respectively, descend along a flow path. The fact that $\delta^{13}C$ of these samples becomes less negative down the flow path probably is the result of increased distance from the recharge zone as more and more detrital carbonate grains dissolve and contribute ^{13}C to the waters. The old apparent age of sample 5 is partly due to the contribution from "dead" detrital carbonate.

The values of $\delta^{18}O$ and δD in table 1 appear to agree with the distribution of these isotopes in meteoric surface waters from North America (fig. 12). The isotopic composition of rainwater is controlled mostly by a process of Rayleigh distillation. As moisture moves away from the sea into higher latitudes and cooler climates, the $\delta^{18}O$ and δD of rain or snow falling from it becomes progressively more negative. This is caused by a combination of factors: 1) isotopic fractionation during condensation and evaporation due to differences in vapor pressure between isotopes; 2) decrease in air temperature and a resulting increase in isotopic fractionation; 3) re-evaporation of rainwater on the ground; and 4) transpiration by plants (Faure, 1977 p. 328; Drever, 1982 p. 338; Hoefs, 1980 p. 103).

There is an excellent linear relationship between $\delta^{18}O$ and δD for most surface waters because the condensation of moisture approximates an equilibrium process and hydrogen fractionation is proportional to oxygen fractionation. Taylor (1974) gives this relationship for the meteoric water line: $\delta D = 8\delta^{18}O + 5$. Values of $\delta^{18}O$ and δD in table 1 differ from the meteoric line by an average of $0.2^{o}/oo$ and $1.6^{o}/oo$, respectively. This close agreement indicates that there has been no mixing with non-meteoric water and no significant isotopic modification resulting from diagenetic reactions or differential water movement (membrane filtration) through the aquifer.

While the $\delta^{18}O$ and δD values (table 1) lie on the meteoric line, they may differ (an amount not apparent from figure 12) from local precipitation, which unfortunately was not collected. Such differences would be apparent if recharge occurred at higher elevations or in the past under different climatic conditions (Gat, 1971). For example, in two samples of runoff from the Yellowstone area the average δD is $-148^{o}/oo$ (Friedman and others 1964), and by calculation, $\delta^{18}O = -19.1^{o}/oo$. If these values also represent the average precipitation for the northern Green River Basin, then in relation, the average ground water values of $\delta^{18}O = -19.8$ and $\delta D = -154$ (table 1) are slightly depleted and suggest that recharge was at a higher elevation or a lower temperature. Such detail would be necessary for a more complete interpretation of the hydrologic system.

Although waters deeper than 500 feet exist in the basin, little is known about their composition because of the ample supplies at shallow depths. It is clear that there are fewer and fewer aquifers with increasing depth. There are probably several reasons for this. First, lenticular sandstones cannot efficiently transport water to great depths. Second, recharge of deep sands, which are not exposed at the surface, would have to be by vertical migration (seepage) or by access along a fault. And third, the reduction of porosity and permeability with increasing depth presents a formidable barrier to descending meteoric waters. However, the few water samples from deep, normally pressured sandstones have a surprisingly low TDS. Waters from 6,900 ft in the Wagon Wheel well and from 9,700 ft at Jona Gulch (about 25 miles southeast of Wagon Wheel well, fig. 3) have less than 4,000 TDS, yet hydraulic conductivities are on the order of .01 to .001 gal/day/ft^2 (0.5 to 0.05 md) so

migration is slow. Although the low TDS of these waters suggests a meteoric origin, conclusive evidence is lacking because the entire northern Green River Basin has no more than six water analyses from below 5,000 ft and none have stable isotopic data.

With one possible exception no water has been recovered from drilling tests in the overpressured, gas-bearing sandstones (B. E. Law, oral commun., 1982). However, geophysical and core measurements show that many of these sandstones have water saturations of 50 percent to 70 percent. During formation tests and pumping, this water is irreducible or non-extractable because of the small pores and low permeabilities.

Past Conditions

After the Cretaceous seas retreated from the northern Green River Basin in Santonian time (85 m.y.; Dorr and others 1977), deposition probably remained near sea level until the mid-Eocene. Moore (1960) indicates that deposition of the Hoback Formation (Upper Paleocene in the Hoback Basin) took place between 1,000 and 1,500 ft above sea level. Stream flow during this time was generally to the south but may have also been towards the east depending upon uplift along the Wind River thrust fault. Undoubtedly, with highlands nearby most of the time, an abundance of meteoric water percolated through the accumulating basin sediments.

Several lines of evidence allow reasonable estimation for the isotopic composition of the Upper Cretaceous and Tertiary meteoric waters. The $\delta^{13}C$ of paleo-recharge water can be estimated from the isotopic composition of modern soil CO_2 which has been compiled by Deines and others 1974 for a variety of environments. In the Late Cretaceous and Paleocene the basin was heavily forested and humid, with a warm temperate climate, but it became drier by early Eocene (Dorr and others 1977). During these times, $\delta^{13}C$ of recharge water was probably close to $-20^{o}/oo$ (PDB) - more negative than the present because of abundant plant growth in the soil zone. From mid-Eocene to Pliocene, recharge $\delta^{13}C$ was probably -20 to $-15^{o}/oo$ or slightly less negative as a result of different vegetation when the grasses evolved in the area of the central United States. Shifts in $\delta^{13}C$ were paralleled by shifts in $\delta^{18}O$ which occurred when the seas retreated, and the area cooled as a result of global cooling, continental rotation, and increased elevation. During the Late Cretaceous and early Paleocene, $\delta^{18}O$ of rainwater was probably between -5 to $-7^{o}/oo$ (SMOW) and comparable to the present Gulf Coast (figs. 12 and 13). From Eocene through Pliocene, evidence from Taylor (1974) indicates that meteoric $\delta^{18}O$ became increasingly more negative from -7 to $-15^{o}/oo$ (fig. 14). With several thousand feet of regional uplift beginning in the Pliocene (Love, 1960), $\delta^{18}O$ became even more negative and since then has probably remained within 2 or $3^{o}/oo$ of its present value ($\simeq -19^{o}/oo$, SMOW) depending upon the regional weather patterns. Presumably, with drier conditions after the Pliocene, $\delta^{13}C$ of meteoric waters became more positive to reflect the decrease in vegetation.

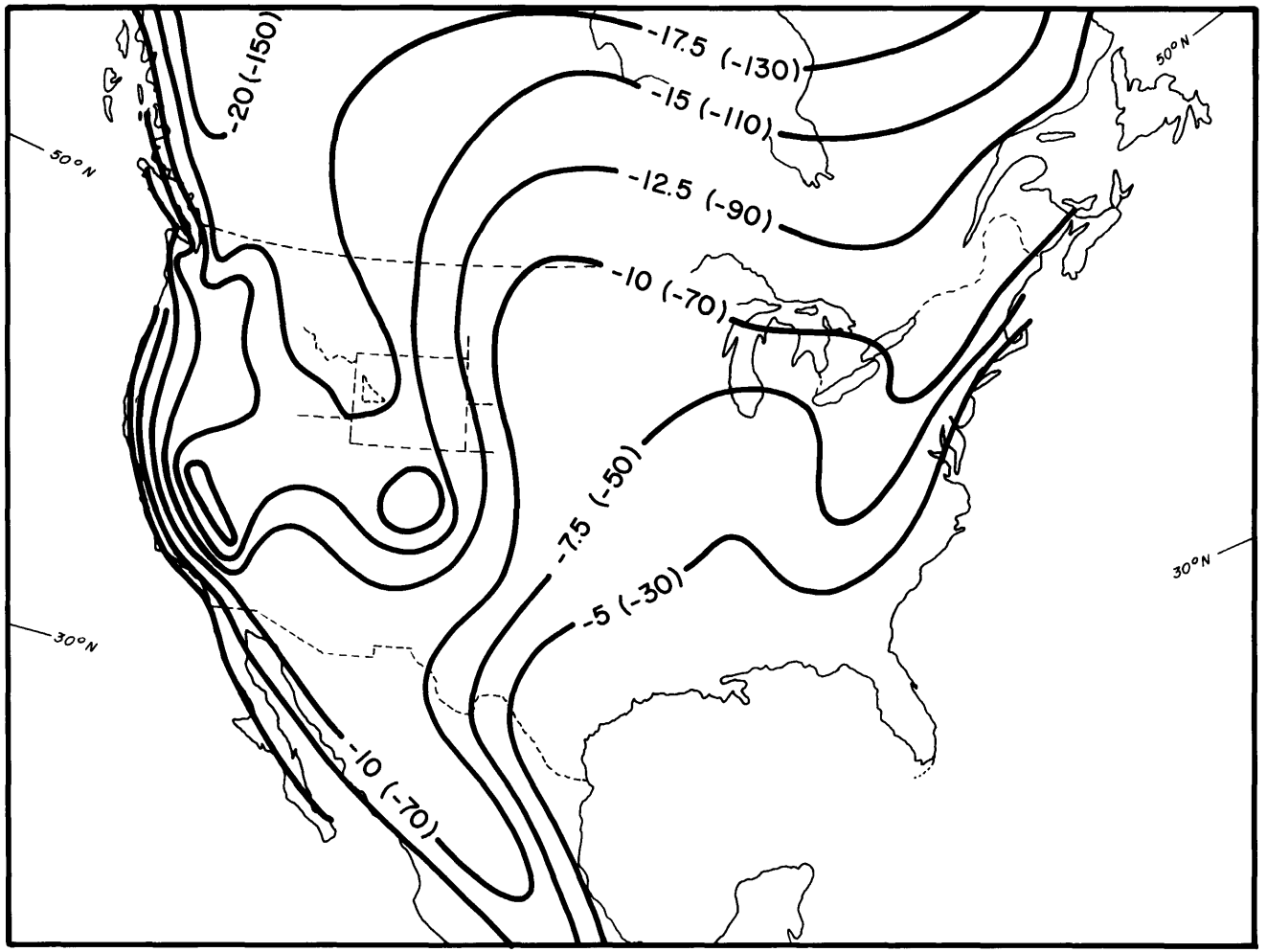

Figure 12--Distribution of $\delta^{18}O$ and δD (in parentheses) in meteoric lake, stream, and river, and spring waters of North America (modified from Sheppard and others, 1969).

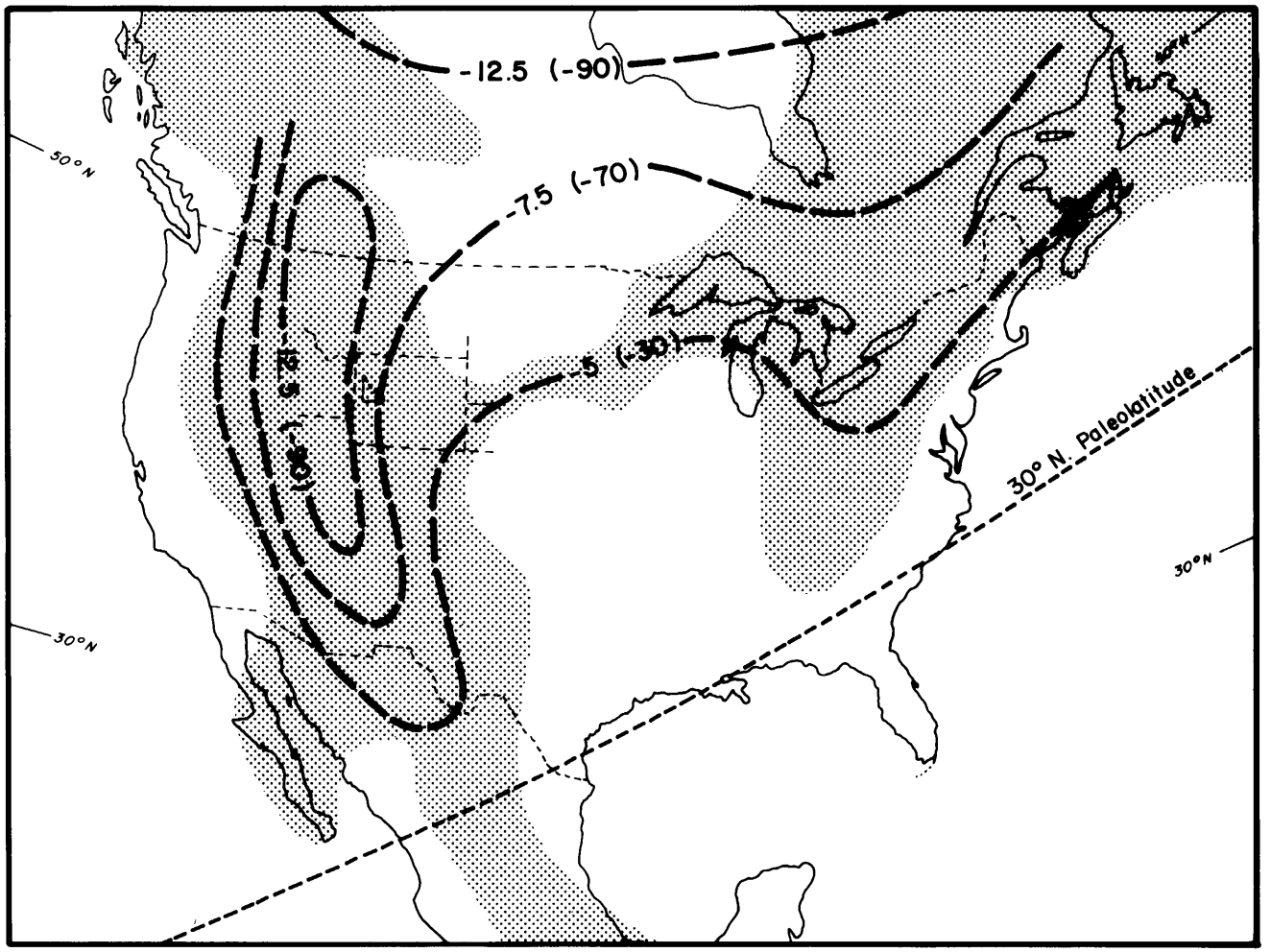

Figure 13--A probable, Upper Cretaceous and Paleocene distribution of $\delta^{18}O$ and δD (in parenthesis) in meteoric waters. Maximum transgression of the sea and paleogeography are from Erickson (1978).

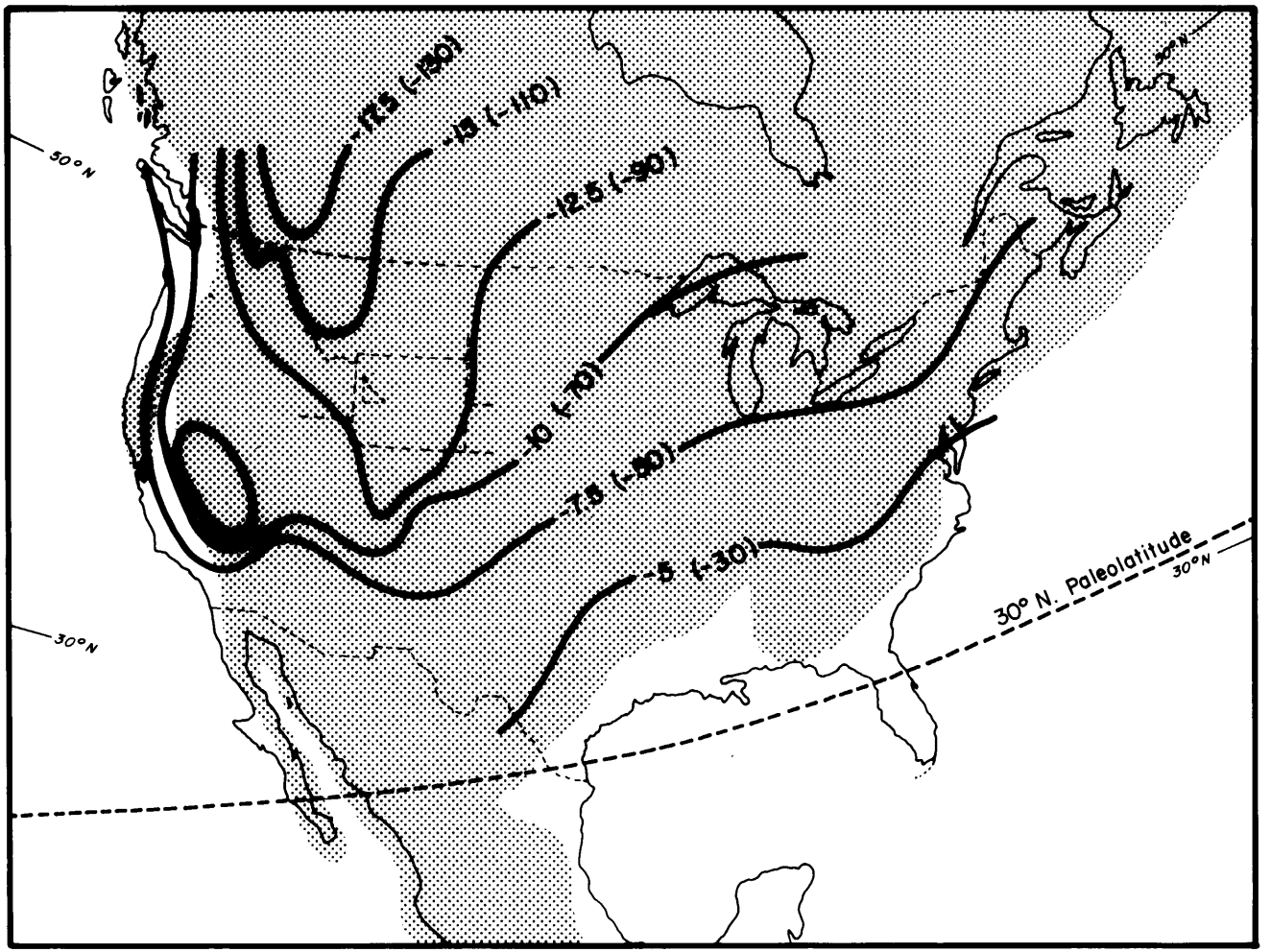

Figure 14--Eocene through Pliocene distribution of $\delta^{18}O$ and δD (in parenthesis) in meteoric waters (adapted from Taylor, 1974). Maximum transgession of the sea is from Dott and Batten (1981).

SAMPLING AND ANALYSIS

In the northern Green River Basin, core from Upper Cretaceous and Tertiary rocks is sparse, but where available, it commonly covers a large depth interval within a single well. Stratigraphic control between wells is poor not only because the wells are far apart but also because the rocks are predominantly fluvial in origin. Bedding is extremely lenticular, and with few exceptions, sandstones are not traceable for more than a mile in the subsurface. In addition, pollen grains, which are the only identifiable fossils, are sparse and therefore make poor biostratigraphic markers. For these reasons, it seemed feasible and logical to study vertical rather than lateral trends in carbonate geochemistry.

I used a combination of petrographic and geochemical techniques to study carbonates in sandstones, shales, and fractures. Samples were taken from core in 5 wells and 3 outcrops (fig. 3). Wagon Wheel core, which spans the greatest depth of the five wells, was sampled in most detail and used as a model for the other wells. Cored intervals rich in carbonate were macroscopically identified and plugged for analysis. Thin sections of the sandstone plugs were stained for carbonate using Dickson's (1966) method and characterized by 300 point counts. For whole rock analyses, about 6 grams from each plug was sawed within 5 mm from the thin section, crushed with an electric mortar and pestal, and sifted to less than 44 microns (325 mesh).

An aliquot of the crushed sandstone and shale samples from Wagon Wheel core was X-rayed for carbonate minerals. A small amount of halite (15 percent of sample weight) was added to these samples to provide an internal standard. X-rays of the main calcite and dolomite peaks were measured by step-scanning (0.01^{o} 2θ increments with a 5 second count per stop) between the angles of 28 and 32 degrees 2θ. A Phillips, variable-slit powder diffractometer was used for analysis. D-spacings of the main calcite and dolomite peaks were calculated from the halite standard for later determination of Fe, Mg and Ca content. Error in measurement was estimated from two samples each of which was re-packed and scanned 5 times. The average standard deviation between the two samples was 0.0024Å for calcite and 0.0033Å for dolomite.

Using petrographic and X-ray data, I selected crushed sandstones and shales for bulk isotopic analysis of calcite or dolomite or both. These samples were reacted with 100 percent phosphoric acid to liberate CO_2 for mass spectrometer measurement of carbon and oxygen isotope ratios (McCrea, 1950). It was assumed that only carbonate minerals reacted with the acid to yield CO_2. The double extraction technique (Epstein and others 1964; Walters and others 1972), which is based on solubility differences between carbonates, was used to separate the CO_2 that evolved from mixtures of calcite and dolomite. CO_2 collected after 1 hour of acid digestion was considered to be from calcite, while CO_2 collected after 4 days was considered to have evolved from dolomite. To avoid contamination, CO_2 generated between 1 and 6 hours was pumped off.

Relative concentrations of ^{13}C and ^{18}O in CO_2 were measured on a Finnigan Mat-251 (PM) mass spectrometer and reported in parts per thousand ($^o/oo$) by the following relationships:

$$\delta^{13}C = \frac{(^{13}C/^{12}C)_{sample} - (^{13}C/^{12}C)_{standard}}{(^{13}C/^{12}C)_{standard}} \times 1000$$

$$\delta^{18}O = \frac{(^{18}O/^{16}O)_{sample} - (^{18}O/^{16}O)_{standard}}{(^{18}O/^{16}O)_{standard}} \times 1000,$$

where the standard, NBS-19 has a value of $\delta^{13}C = +1.96^o/oo$ and $\delta^{18}O = -2.30^o/oo$ relative to PDB. For laboratory error in measurement, the standard deviation of 24 samples of NBS-19 was $0.05^o/oo$ for $\delta^{13}C$ and $0.15^o/oo$ for $\delta^{18}O$. The standard deviation between two separate measurements of 11 carbonate samples, which were randomly chosen from the sandstone cores, was $0.22^o/oo$ for $\delta^{13}C$ and $0.41^o/oo$ for $\delta^{18}O$.

For shale samples, the isotopic composition of organic carbon was also determined. To remove carbonate carbon, crushed samples were leached for about 12 hours in 1N HCl. The acid solution was separated from the shale by filtering through a fiberglass Millipore filter. Dried samples were checked for carbonate residue with a drop of concentrated HCl. The samples were then burned in a vacuum combustion system to convert the organic carbon to CO_2 for mass spectrometer analysis (Craig, 1953). Isotopic values of the organic carbon samples are reported relative to PDB and have a laboratory error of about $\pm 0.15^o/oo$.

Because it was not possible to physically separate analytical quantities of either the calcite or the dolomite phase, bulk isotopic analyses of sandstones were evaluated by utilizing thin-section data to characterize the carbonate mineralogy. However, after mild crushing detrital carbonate grains in some sandstones could be removed by hand. Dolomite grains were identified by their color, texture, and low solubility in acid. Alizarin red stain was used to identify detrital limestone grains. A controlled test showed this stain to have no effect on the isotopic composition. Micrite grains, which could be recognized by their texture, were chosen to reduce the possibility of analyzing recrystallized grains. X-ray analyses were used to aid evaluation of the isotopic composition of shale. In fractures, phase separation was not a problem and sufficient quantities of calcite could be either scraped or drilled for analysis.

Rate of CO_2 Generation

The variable rate at which CO_2 evolves during acid digestion of carbonate mixtures makes it possible to obtain isotopic ratios of calcite and dolomite from the same sample. This rate depends largely on the acid solubility and

particle size of carbonates in the mixture. The isotopic composition of the CO_2 changes with the isotopic composition of the carbonates that are dissolving. Epstein and others (1964) and Walters and others (1972) determined rates of CO_2 generation and isotopic ratios in mixtures of pure calcite and dolomite for various particle sizes. However, in the northern Green River Basin the carbonates are not mixtures of these pure end-members but are mixtures of solid solutions. Therefore, it was necessary to test the relationship between the isotopic ratios and rate of CO_2 generation.

Gas from six samples, each having a petrographically distinct suite of carbonate phases, was collected at selected times during acid digestion. As the calcite phases dissolved the reaction slowed, and a longer time between each collection was necessary to obtain measurable quantities of CO_2 from the dolomite phases. The volume of CO_2 and its $\delta^{13}C$ and $\delta^{18}O$ were measured from each collection (table 2) and plotted versus time in figures 15 and 16. Isotope values obtained from bulk extractions compare reasonably well with those values that are located on the flatter portion of the sequential extraction curves. To make valid comparisons between samples it is important to be consistent with particle size and extraction time.

For control in the above test, I used a fracture-filling calcite (sample WWF-18), which consisted of what petrographically appeared to be a single carbonate phase. The $\delta^{13}C$ and $\delta^{18}O$ of CO_2 from four collections taken during the acid dissolution of this sample were similar and within the limits of analytical error. This indicates two things. 1) Small fractionations of oxygen, which are caused by the diffusion of reaction products away from particle surfaces (Walters and others 1972), were not observed. 2) The reaction between calcite and phosphoric acid proceeds by a stripping mechanism. Therefore, if the calcite is assumed to be homogenous, CO_2 may be collected and measured before complete acid digestion of the sample.

In general, the separation of carbonates by solubility differences is not a precise method to obtain isotopic ratios. While it is possible to separate with some certainty the extremes - calcite and dolomite - it is not possible to separate Fe-calcite from detrital calcite or Fe-dolomite from detrital dolomite. Even with controlled particle sizes, the solubilities of these phases overlap and cause mixing of isotopic ratios. It is significant that errors resulting from laboratory procedure are far smaller than those which could result from separation by solubility differences. However, with consistancy of method, relative differences in isotopic ratios of "calcites" and "dolomites" between samples can be observed.

The slopes of the curves in figures 15 and 16 are primarily controlled by the proportions of carbonate phases with different solubilities. If the solubilities of intermediate carbonate phases such as Fe-calcite or ankerite were known, it might be possible to estimate their relative positions on the curves. For example, circumstantial evidence suggests that ankerite is less soluble than dolomite. If this is true, then the negative trend in $\delta^{18}O$ after 3 days in sample WW-148 (fig. 16b) might have resulted from the dissolution of

Table 2.--Isotopic composition and volume of CO_2 from sequential and bulk extractions

Sample	Sequential Extraction					Bulk Extraction		
	Reaction Time (hours)	Volume of Gas (cc)	Volume % of Reaction	$\delta^{13}C$ o/oo PDB	$\delta^{18}O$ o/oo PDB	Reaction Time (hours)	$\delta^{13}C$ o/oo PDB	$\delta^{18}O$ o/oo PDB
	0.25	6.00	44.60	-1.30	-11.90			
	.50	1.20	9.55	-1.11	-11.14			
	1.00	0.89	6.57	-0.98	-10.41	1.08	-1.18	-11.91
	1.50	.43	3.18	-0.72	-9.15			
Wagon Wheel	3.25	.53	3.90	-0.38	-7.24			
7969	6.17	.40	3.28	-0.01	-4.90			
	28.33	1.50	12.12	0.35	-3.11			
	48.08	0.73	5.85	.44	-2.56			
	97.38	1.00	8.22	.45	-2.52	96.00	0.41	-2.93
	122.38	1.30	2.67	.39	-2.54			
	0.25	9.80	65.99	-4.02	-14.09			
	.50	1.80	11.92	-4.16	-14.53			
	1.00	1.10	7.46	1.50	0.45			
	1.50	0.45	3.01	-3.71	-13.67	1.35	-3.61	-14.52
Wagon Wheel	3.00	.36	2.45	-3.18	-12.25			
76	6.00	.20	1.33	-1.94	-9.08			
	26.08	.43	3.12	-0.04	-4.39			
	95.00	.55	4.01	.37	-3.48			
	120.22	.10	.66	---	---	120.00	0.46	-3.25
	0.25	9.40	52.90	-3.25	-15.12			
	.50	2.30	12.94	-3.12	-14.97			
	1.00	1.20	7.12	-3.05	-14.46	1.25	-2.71	-14.58
	1.50	0.57	3.18	-2.75	-13.55			
Wagon Wheel	2.00	.30	1.78	---	---			
104	4.00	.40	2.25	-1.52	-9.81			
	28.30	1.60	9.84	-0.09	-5.70			
	54.08	0.76	4.59	.17	-4.97			
	74.93	.30	1.97	.12	-5.08			
	148.25	.55	3.37	.35	-4.38	144.00	0.51	-4.05
	0.25	3.90	21.11	-1.02	-13.00			
	.50	1.00	5.45	-0.69	-10.98			
	1.00	0.97	5.21	---	---			
	1.66	.83	4.50	.04	-7.83			
	2.12	.51	2.72	.11	-7.44			
Wagon Wheel	4.08	1.10	5.93	.15	-7.04			
171	26.08	4.90	28.94	.30	-5.89			
	47.92	2.20	13.28	.46	-4.57			
	72.70	.90	5.33	---	---			
	146.00	1.20	7.47	.47	-4.05	120.00	0.44	-4.98
	0.25	5.00	29.71	-0.52	-11.63			
	.50	0.80	5.07	-0.55	-10.50	0.50	-0.55	-11.45
	1.00	.79	4.71	-0.34	-9.40			
	1.50	.48	2.38	-0.12	-8.20			
	3.00	.87	5.18	-0.01	-7.21			
Wagon Wheel	6.00	.87	5.18	-0.01	-6.41			
148	28.25	2.90	18.51	0.13	-5.55			
	53.45	1.50	9.78	.23	-5.03			
	93.92	1.46	9.43	.22	-5.16	96.00	.20	-5.40
	143.75	1.10	6.95	.18	-5.52			
	169.08	0.40	2.59	.13	-5.83			
	0.25	54.20	71.53	-3.91	-13.01			
Wagon Wheel	.50	12.20	16.05	-3.91	-12.99			
F-18	1.00	8.10	10.70	-3.90	-12.96			
	2.00	1.3	1.70	-3.96	-12.98	2.25	-3.96	-12.88

--- indicates no data.

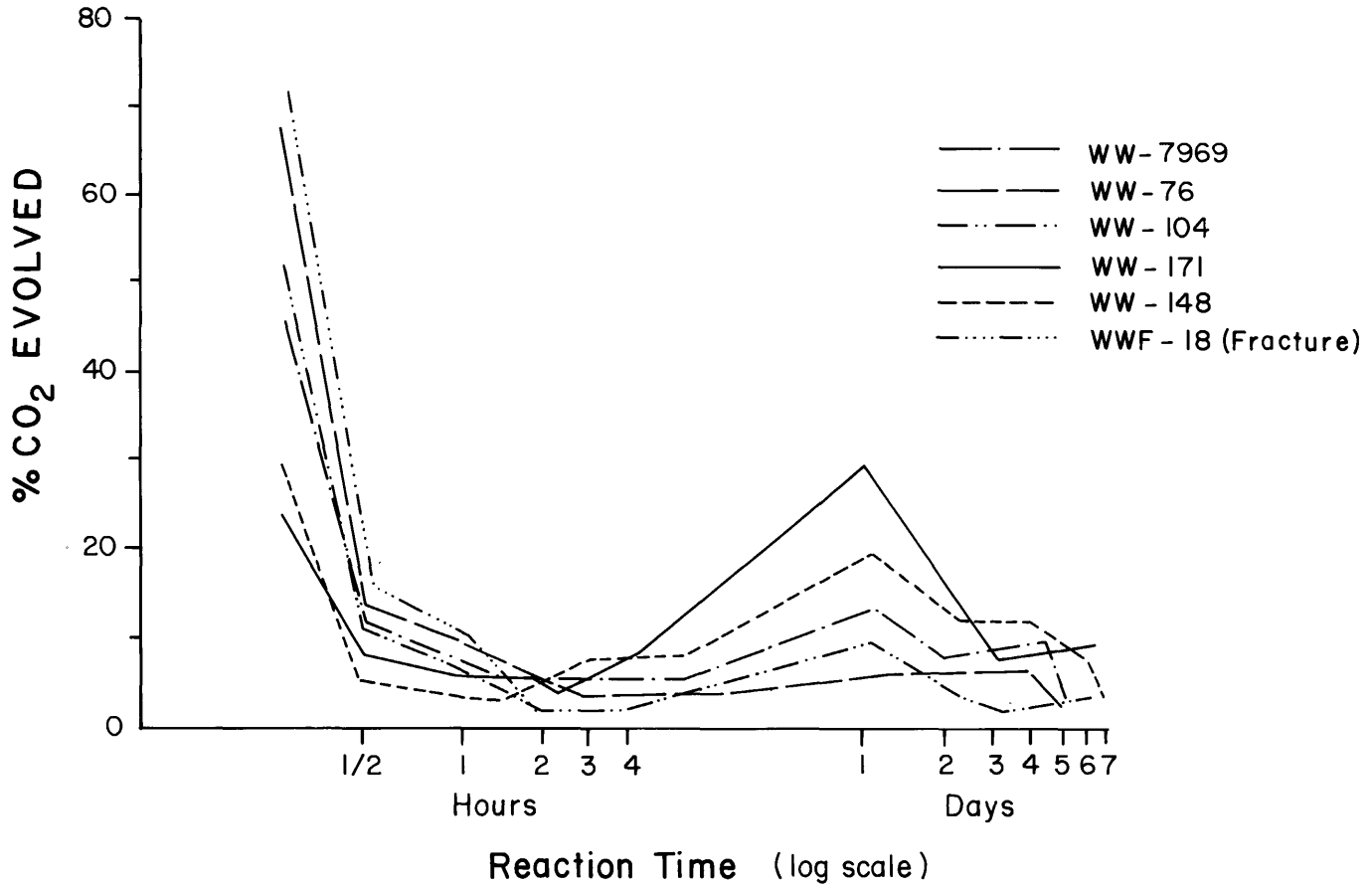

Figure 15. Percent of total CO_2 gas collected sequentially during acid dissolution. The % CO_2 evolved is (sample ml CO_2/total ml CO_2) x100. Data listed in Table 2.

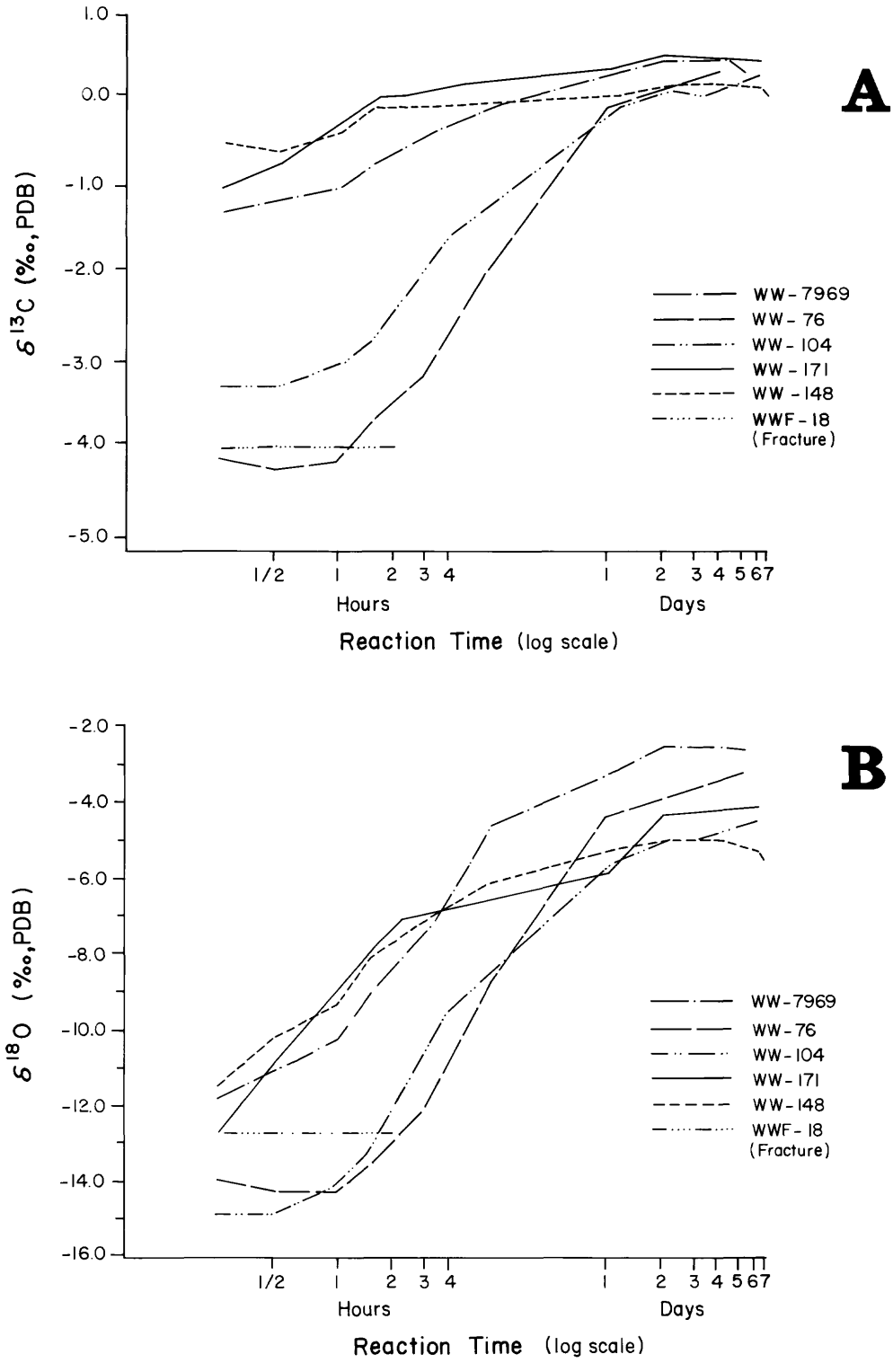

Figure 16--Measured $\delta^{13}C$ (A) and $\delta^{18}O$ (B) of CO_2 gas which was sequentially collected from the reaction tube for seven days. Data listed in Table 2.

ankerite, which is depleted in ^{18}O relative to dolomite. However, the same conclusion could also be reached by comparing the isotopic values of several samples that have different proportions of dolomite and ankerite.

SANDSTONES

Carbonate minerals are present in the Upper Cretaceous and Tertiary sandstones as detrital grains of limestone and dolomite; as calcite cement, which contains various amounts of iron; and as rhombic dolomite grains, which are monocrystalline detrital grains with authigenic overgrowths (table 3). Total carbonate of the study samples ranges between 3 and 45 percent and averages 18 percent, which, because of sampling bias, is higher than the surrounding rocks. Estimates from petrographic work suggest that in the Tertiary arkosic sandstones, total carbonate is probably less than 2 percent, whereas in the Upper Cretaceous lithic sandstones it is about 10 percent. Thus, as igneous debris flooded the basin, the total amount of carbonate in the sandstones decreased from the Late Cretaceous to Eocene.

Variation in provenance also caused a major shift in the composition of carbonate minerals. With increasing depth or age, total calcite decreases while total dolomite increases (fig. 17). Point count data indicate this variation is due mainly to a decrease in calcite cement with a subsequent increase in rhombic dolomite. Surprisingly, there is no relationship between calcite cement and its most probable source, detrital limestone. However, this lack of relationship may result from not being able to recognize those detrital grains that have completely dissolved away.

Because of the synorogenic depositional patterns, most of the detrital limestone and dolomite grains came from thick Paleozoic carbonate rocks which lay to the west of the subsiding basin. These grains, many of which contain glauconite pellets (fig. 18a), probably represent the source for the well rounded glauconite grains that are common in the Upper Cretaceous nonmarine sandstones of the basin.

In the Upper Cretaceous and Tertiary sandstones there are essentially three ways that carbonate minerals may form: 1) by replacement of other non-carbonate grains, 2) by direct (and passive) precipitation into a pore or onto the surface of a detrital grain, and 3) by recrystallization of a previous carbonate phase.

Processes two and three of the above require further explanation. In this section, isotopic evidence will demonstrate that calcite phases have undergone diagenetic changes in composition. Presumably, these changes occur because calcite tends to stablize or equilibrate with the changing geochemical conditions of burial. This equilibration commonly has been perceived as taking place by either of two diagnetic processes: 1) complete dissolution of one calcite phase and subsequent filling of the resultant void by another calcite phase, and 2) the dissolution of one calcite phase and concomitant precipitation of another calcite phase immediately adjacent to sites of

Table 3.--Isotopic composition and mineralogy of carbonate in sandstones

Well or Surface Location	Sample Number	Depth (feet)	Temperature °C	Isotopic Ratios (°/oo, PDB)				Mineralogy (%)							
				Calcite		Dolomite		Fe-free	Fe-poor	Fe-rich	Detrital	Rhombic	Dolomite	Detrital	Total
				$\delta^{13}C$	$\delta^{18}O$	$\delta^{13}C$	$\delta^{18}O$	Calcite	Calcite	Calcite	Calcite	Core	Overgrowth	Dolomite	Carbonate
	2*	7,044	60	-0.92	-18.02	---	---	21.00	0.0	0.0	0.0	0.0	0.0	0.0	21.00
	6*	7,046	60	-1.78	-17.72	---	---	21.00	0.0	0.0	0.0	0.0	0.0	0.0	21.00
	20*	7,114	61	-0.24	-17.32	---	---	14.88	0.65	0.0	0.13	0.0	0.0	0.0	15.67
	7969	7,264	62	-1.18	-11.91	0.41	-2.93	3.67	0.33	0.0	6.33	0.0	0.0	5.00	15.33
	30	7,344	62	-1.66	-11.43	---	---	1.00	7.50	0.0	2.00	0.0	0.0	0.50	11.00
	31	7,350	62	-1.54	-14.42	---	---	0.40	7.00	4.00	2.00	0.0	0.0	0.40	13.80
	34	7,366	62	-0.51	-16.44	---	---	0.50	25.00	0.0	3.25	0.0	0.0	0.0	28.75
	36	7,379	62	-1.60	-13.00	---	---	0.50	1.75	3.00	1.50	0.0	0.0	0.50	7.25
	8710	7,633	64	-3.10	-13.24	0.58	-1.77	13.13	0.0	0.0	9.10	1.00	0.0	11.62	34.85
EPNG	52	8,084	67	-3.71	-14.49	---	---	0.00	1.00	4.00	2.33	0.0	0.0	0.0	9.33
Wagon	53	8,088	67	-3.67	-13.51	---	---	1.00	2.00	6.00	4.00	0.0	0.0	0.0	13.00
Wheel #1	59	8,124	67	-2.84	-14.18	---	---	2.75	4.75	1.00	2.50	0.0	0.0	0.25	11.25
	60*	8,128	67	-2.98	-13.34	---	---	2.00	4.00	2.40	0.80	0.0	0.0	0.0	9.20
	68*	8,934	73	-4.37	-15.52	---	---	1.40	3.00	14.00	2.00	0.0	0.0	1.00	21.40
	69	8,944	73	-3.22	-12.40	---	---	0.40	0.60	2.80	1.80	0.0	0.0	0.40	6.00
	76	8,989	73	-3.61	-14.52	0.46	-3.25	1.50	2.50	8.75	3.75	0.75	0.0	2.50	19.75
	80	10,153	81	-3.03	-13.75	---	---	0.25	1.00	4.75	0.75	1.50	0.0	2.25	10.50
	89	10,217	82	-2.35	-13.15	0.63	-3.64	1.50	2.00	8.25	1.75	1.00	0.75	2.50	17.75
	95*	10,978	87	-2.67	-14.89	0.73	-4.12	1.60	2.60	11.00	0.60	0.0	0.0	4.00	19.80
	104*	11,028	87	-2.71	-14.53	0.51	-4.05	1.20	2.20	13.60	1.40	1.00	0.0	1.00	20.40
	110	11,068	87	-0.95	-10.38	0.69	-3.67	1.25	1.00	2.75	1.00	0.0	0.0	3.00	9.00
	148	14,951	114	-0.55	-11.45	0.20	-5.40	0.50	0.0	0.0	3.50	6.50	2.50	4.00	17.00
	155*	16,083	122	-2.46	-11.12	0.32	-5.09	0.20	0.20	0.0	0.0	8.00	0.60	3.40	12.40
	156*	16,087	122	-0.16	-10.18	0.31	-4.91	0.25	0.25	0.0	0.0	6.40	2.22	6.40	15.52
	171	17,176	129	---	---	0.44	-4.98	0.0	0.0	0.0	0.0	16.33	4.67	0.0	21.00
	172*	17,178	129	-0.40	-10.57	0.37	-5.25	0.0	0.0	0.50	0.0	6.00	2.00	2.75	11.25
	175*	17,959	134	-1.53	-13.88	0.65	-3.70	6.00	3.00	4.00	0.0	9.00	6.00	2.00	30.0
	F-39*	17,960	134	-0.92	-13.44	0.60	-4.50	9.00	2.00	2.00	0.0	17.00	3.00	6.00	39.00
	1	8,720	73	-3.64	-14.95	---	---	9.00	2.00	0.0	7.00	0.0	0.0	2.00	20.0
	2	9,140	76	-5.37	-15.50	---	---	19.00	0.0	0.0	6.00	0.0	0.0	2.00	27.00
Mt. Fuels	3	9,654	79	-4.95	-15.63	---	---	7.00	3.50	0.0	3.50	0.0	0.0	2.00	16.00
Mesa #1	4	11,230	89	-2.07	-11.36	0.34	-4.49	3.50	0.0	0.0	1.50	0.0	0.0	3.00	8.00
	5	11,265	90	-2.80	-12.15	0.32	-4.10	3.00	0.0	1.00	5.00	2.00	0.0	4.00	15.00
	6	11,886	94	-1.93	-12.06	0.84	-3.23	3.00	0.0	0.0	7.00	0.0	0.0	2.00	12.00
	7	11,956	94	-3.35	-16.52	---	---	16.00	0.0	0.0	2.00	0.0	0.0	1.00	19.00

Table 3.--Isotopic composition and mineralogy of carbonate in sandstones--Continued

Well or Surface Location	Sample Number	Depth (feet)	Temperature °C	Isotopic Ratios (°/oo, PDB)				Mineralogy (%)							
				Calcite		Dolomite		Fe-free Calcite	Fe-poor Calcite	Fe-rich Calcite	Detrital Calcite	Rhombic Dolomite Core	Dolomite Overgrowth	Detrital Dolomite	Total Carbonate
				$\delta^{13}C$	$\delta^{18}O$	$\delta^{13}C$	$\delta^{18}O$								
	19*	10,546	101	-3.66	-16.83	---	---	11.50	7.50	0.0	2.00	0.0	0.0	3.00	24.00
	45	11,467	109	-4.39	-18.30	---	---	1.50	10.0	4.00	5.00	0.0	0.0	3.50	24.00
	197*	12,514	118	-6.00	-18.99	---	---	19.50	4.50	0.0	0.0	0.0	0.0	0.0	24.00
	246*	13,250	124	-5.67	-14.45	---	---	29.00	3.00	3.50	1.50	0.0	0.0	7.00	44.00
Belco	259	13,336	125	---	---	-1.15	-5.99	0.0	0.0	0.0	0.0	2.50	3.00	5.50	11.00
WASP 1-A	337	13,866	130	-1.56	-14.68	-0.25	-6.88	7.50	3.00	2.00	3.50	5.50	0.50	4.00	26.00
	357	14,002	131	-2.51	-16.75	---	---	4.00	7.50	3.00	6.50	2.00	0.50	5.50	29.00
	390*	14,171	132	-1.53	-13.89	-0.09	-5.24	0.0	0.0	3.00	0.0	10.0	2.00	5.50	20.50
	427	14,358	134	-1.07	-12.79	0.11	-5.76	2.50	3.00	3.00	1.50	8.00	0.0	8.00	26.00
	20	14,566	109	-1.81	-11.67	-0.30	-5.77	4.00	3.00	0.50	3.50	4.50	0.0	4.50	20.0
	25	18,038	134	-0.96	-12.06	0.30	-4.19	1.00	0.0	0.0	1.00	3.00	0.0	2.00	7.00
Superior	28	18,641	138	-0.71	-11.85	0.68	-3.58	11.00	0.0	0.0	11.00	3.00	0.0	6.00	31.00
Pacific	30*	18,778	139	-0.73	-12.05	0.71	-4.41	19.50	0.0	0.0	1.00	3.00	0.0	5.00	28.50
Creek #1	38	19,743	146	-0.79	-12.52	0.75	-3.80	6.00	1.00	0.0	8.00	4.00	0.0	1.00	20.0
	42*	20,447	151	-4.27	-13.51	---	---	3.00	0.0	0.0	0.0	0.0	0.0	0.0	3.00
General	2*	3,995	39	-5.39	-17.41	---	---	11.50	2.00	0.0	1.50	0.0	0.0	0.0	15.00
Petroleum	8	4,018	40	-3.95	-14.59	---	---	2.00	0.0	0.0	2.50	0.0	0.0	0.50	5.00
Bar Cross	10*	4,024	40	-5.93	-17.15	---	---	20.0	0.0	0.0	2.00	0.0	0.0	1.00	23.00
63-21	13	5,076	47	-5.13	-13.45	2.33	-7.26	15.0	0.0	0.0	11.00	0.0	0.0	8.00	34.00
	16	5,562	50	-2.94	-11.59	-1.19	-6.33	5.00	0.50	1.50	3.00	8.50	2.50	3.00	24.00
	19	6,921	59	---	---	-4.15	-10.77	0.0	0.0	0.0	0.0	9.0	5.0	2.5	16.5
Center sec. 3, T. 30 N., R. 108 W.	A*	0	4	-14.20	-17.06	---	---	22.5	0.0	0.0	0.0	0.0	0.0	0.0	22.5
SW 1/4 sec. 11, T. 31 N., R. 107 W.	B*	0	4	-6.70	-15.63	---	---	15.0	0.0	0.0	0.0	0.0	0.0	0.0	15.0
Center sec. 25, T. 37 N., R. 112 W.	C*	0	4	-8.09	-16.55	---	---	41.0	0.0	0.0	0.0	0.0	0.0	0.0	45.0

--- indicates no data.
* sample containing over 90% calcite cement (solid dots Fig. 23).

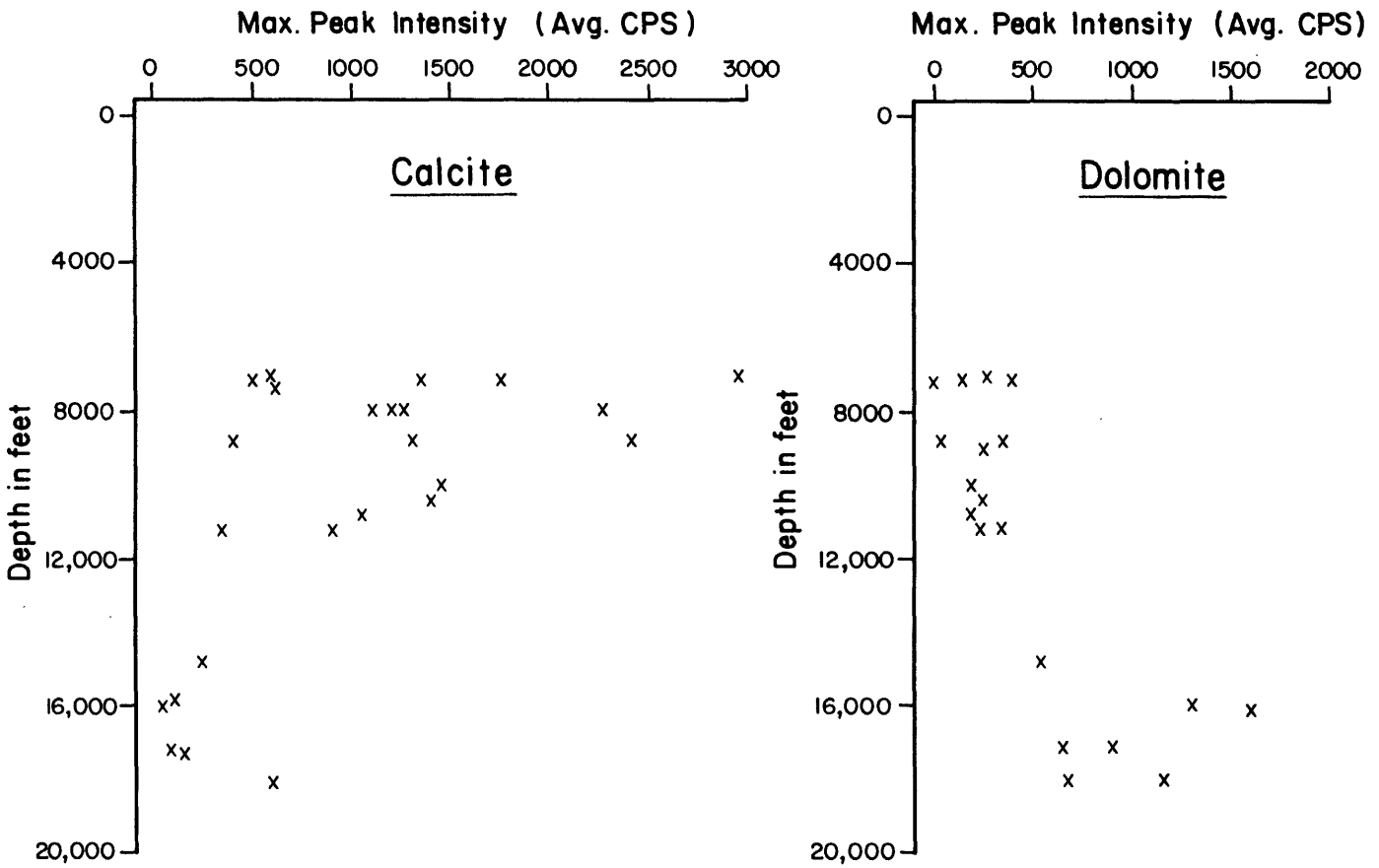

Figure 17--Sandstones from Wagon Wheel #1 (Table 5) showing relative decrease in the amount of calcite and increase of dolomite as a function of depth. Maximum peak intensity in average counts per second (CPS) is for the $D_{(104)}$ reflection. Standard deviation for the error in measurement is 97 CPS for calcite and 59 CPS for dolomite. See Chapter 3 for methods.

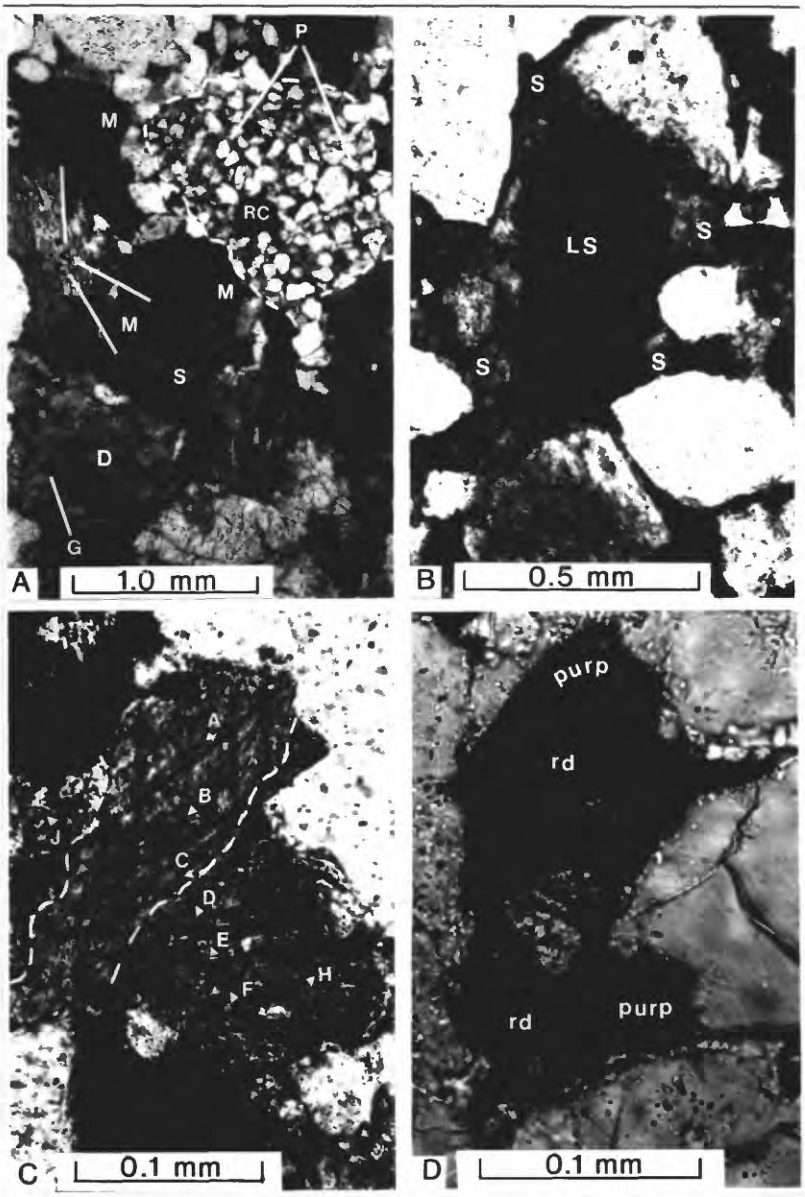

Figure 18--Carbonate constituents in the Upper Cretaceous and Tertiary sandstones. A) Detrital limestone grain with micrite (M) that has undergone partial recrystallization to sparry calcite (S) either before or after sandstone deposition. Remnant clast of calcareous sandstone (dashed outline), which has undergone dissolution, now consits of small quartz grains, pores (P, blue epoxy) and relict calcite cement (RC). Grain of well-rounded, polycrystalline detrital dolomite (D) contains a glauconite pellet (G). B) Recrystallized grain of detrital limestone (LS) with skeletal fragments. Sparry calcite cement (S) and recrystallized grain are in optical continuity. C) Relict, iron-free calcite cement (points A & B, light pink) surrounded by iron-bearing calcite cement (points C-J, royal blue). Dashed line marks boundary between cements. Microprobe points A-J correspond to Wagon Wheel #148, area 4 in table 6. D) Pore-filling calcite cement showing diffuse zonation. Stained calcite is transitional from red (rd) in center to purple (purp) at rim.

dissolution. The former process has frequently been termed "void-filling", whereas the latter process has been referred to as "neomorphism" (e.g., Folk, 1965; Bathurst, 1975). Wilkinson, and others (1984) have demonstrated that these two processes are really no more than portions of a continuum, defined solely on the basis of the size of the fluid-filled void space that separated the two phases during transformation.

The distinction between void-filling calcite and neomorphic calcite in these sandstones is largely arbitrary. However, the term "void-filling" calcite will be used where the filling of primary porosity was evident. The term "recrystallization" is favored instead of "neomorphism" because the inversion of aragonite to calcite (part of Folk's 1965 definition of neomorphism) has not been observed. Hence, in the following discussions the term "recrystallization" is used where one calcite phase is replaced by another calcite phase regardless of the size of void space that existed.

Detrital Limestone

Detrital limestone grains consist mostly of micrite, sparry calcite, and an occasional fragment of a marine fossil. Some detrital grains are fragments from a continuum of rocks ranging from quartz-bearing limestones to calcareous sandstones. Where the calcite in these grains has dissolved away, an aggregate of small, well rounded quartz grains is left behind in the sandstone (fig. 18a). Most detrital grains have suffered some degree of recrystallization. In places the recrystallization clearly post-dates deposition (fig. 18b); but in other places the evidence for timing of the recrystallization is ambiguous (fig. 18a). In many sandstones below 10,000 ft it is difficult to distinguish void-filling cement from detrital limestone grains that have been compacted into pseudomatrix and recrystallized. Although these identification problems lead to erroneous point count data, all recognizable recrystallized grains were included as detrital grains.

Large detrital grains selected for isotopic analysis were hand-picked from several zones in Wagon Wheel core (table 4, fig. 19). Isotopic compositions of the these grains compare reasonably well with the average isotopic composition of limestones sampled by Friedman (1970) near Yellowstone Park, and with the average isotopic composition of marine Paleozoic limestones reported by Keith and Weber (1964). This similarity supports the interpretation that the carbonate grains were locally derived from the erosion of Paleozoic limestones. Unfortunately, large grains suitable for hand-picking could not be found in the deep core. However, since detrital grains in the deep rocks probably came from similar Paleozoic sources, their original isotopic composition should be comparable with those analyzed from shallow depths.

For marine limestone samples, Keith and Weber (1964) found that $\delta^{18}O$ decreased from -1.2 to -9.7°/oo (PDB) from Recent to Cambrian in age. They suggested that this decrease resulted from post-depositional recrystallization and oxygen exchange with depleted meteoric waters. On the other hand, the

Table 4.--Detrital carbonate grains from Wagon Wheel core

Sample number	Depth (ft)	Isotopic Ratios (°/oo, PDB)			
		Limestone		Dolomite	
		$\delta^{13}C$	$\delta^{18}O$	$\delta^{13}C$	$\delta^{18}O$
7969	7,264	-0.88	-8.46	0.41	-2.93
7969	7,264	1.06	-7.67	1.59	-1.99
31	7,350	0.48	-9.25	---	---
4	7,352	-0.58	-7.01	-0.67	-4.10
8152	7,447	-0.10	-7.97	0.78	-2.89
6	8,096	-6.21*	-9.26*	---	---
8991	8,991	-1.59*	-10.15*	---	---
15	10,161	-1.96	-9.40	0.48	-3.94
	Average	-0.33	-8.29	0.52	-3.17
Keith and Weber (1964)†		0.08	-6.99	---	---
Friedman (1970)††		0.51	-9.56	---	---

* Recrystallized; not included in average.
† Average of 154 Paleozoic marine limestones.
†† Average of 14 limestones near Yellowstone Park.
--- indicates no data.

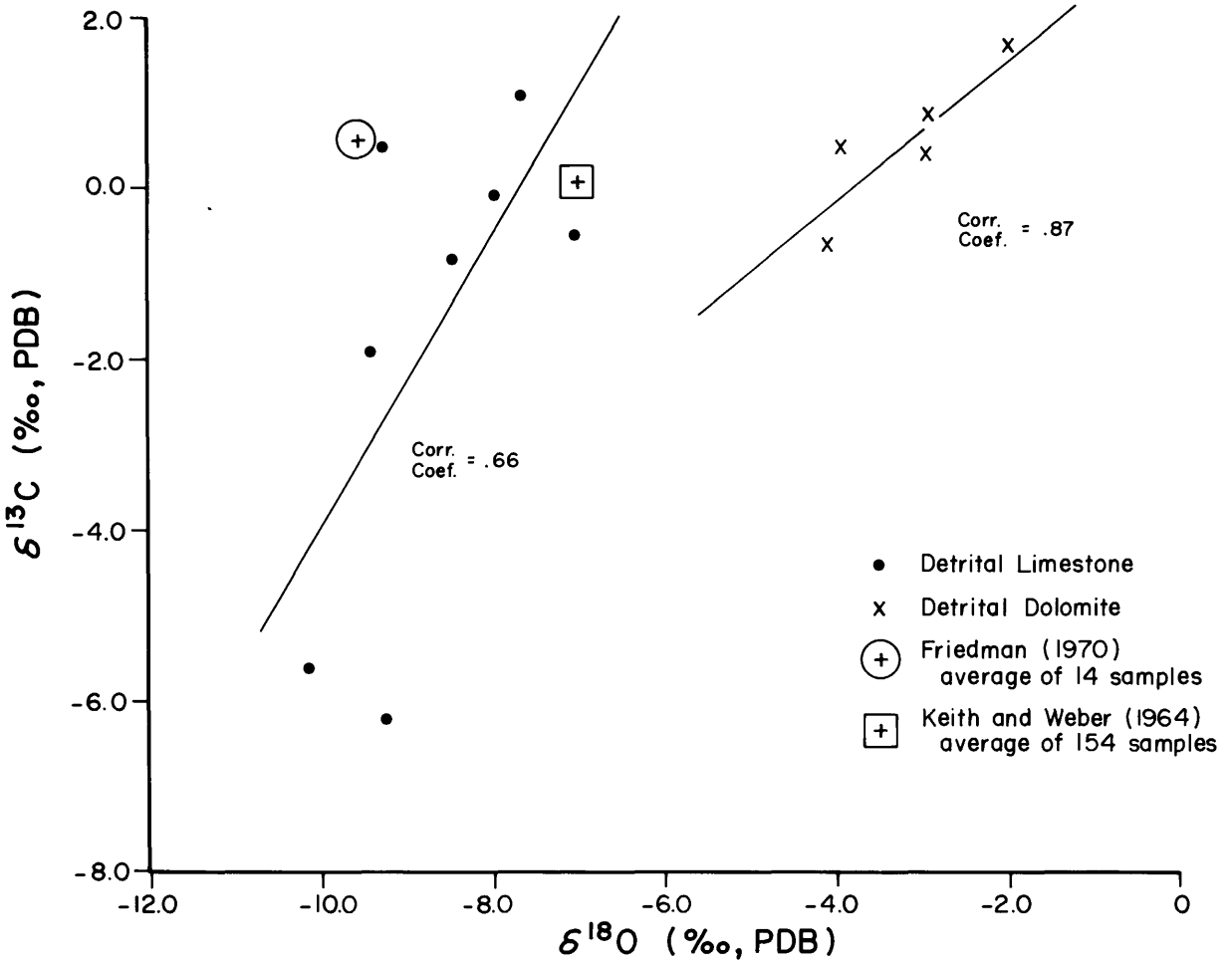

Figure 19--Isotopic composition of detrital carbonate grains that were hand-picked from sandstones in Wagon Wheel #1. Data are listed in Table 4.

same samples all have similar values of $\delta^{13}C$. This similarity suggests that carbon in the recrystallized cement comes from the limestone itself. The carbon reservoir of the marine limestone is large and would mask any contribution of organic carbon which might be present in meteoric water.

The negative $\delta^{13}C$ of samples 6 and 8991 (table 4) implies recrystallization and aquisition of a considerable amount of light carbon (^{12}C) from organic matter. The isotopic composition of the detrital grains, once eroded and isolated from their source, would be controlled largely by the composition of the ground waters. However, based on carbon isotopic values alone, it would be impossible to distinguish grains of recrystallized marine limestone from grains of fresh-water limestone. It is assumed that these samples contain recrystallized marine limestones because fresh-water limestones have not been reported in this part of the basin and because of the large volume of Paleozoic marine limestones in the western source area.

Although most of the hand-picked detrital grains (table 4) show no visible signs of having been recrystallized, the positive correlation between $\delta^{18}O$ and $\delta^{13}C$ indicates partial recrystallization with meteoric waters. The general trend during diagenesis of marine carbonates is a depletion in ^{13}C and ^{18}O as a result of reequilibration with meteoric waters that are impoverished in these isotopes (Land, 1980).

Calcite Cement

In general, pore-filling calcite cements in the sampled rocks contain numerous inclusions and have a mottled, coarsely crystalline texture. Total cement ranges from 0 to 41 percent but averages about 8 percent. Where it constitutes more than 20 percent of the sandstone, the cement typically is poikilotopic (framework grains completely enclosed by large crystals of cement). Sandstones with poikilotopic cement characteristically have both high minus-cement porosities (porosity without chemical cement) and floating grains indicating that cementation occurred at high porosities before much consolidation (fig. 9d). Most quartz overgrowths pre-date all generations of calcite cement. Calcite replacement of feldspar grains is common in the Tertiary arkosic sandstones, whereas recrystallization of detrital limestone grains is common in the re-cycled sandstones of Late Cretaceous age.

Iron Content

Determination of iron and magnesium concentrations in carbonate minerals often allows distinction between various authigenic phases and may reveal important diagenetic relationships. Petrographic, X-ray diffraction, and microprobe analyses are most useful for this purpose.

When stained using Dickson's (1966) method, calcite cements may be petrographically distinguished on the basis of their color, which is a rough indication of iron concentration. Three categories of color were used to characterize the cements (table 3), and following work by Lindholm and

Finkelman (1972) a quantitative weight percent FeO was assigned to them as follows: 1) red to pink for iron-free calcite with less than 0.5 weight percent FeO, 2) mauve for iron-poor calcite with 1-2 weight percent FeO, and 3) purple to royal blue for iron-rich calcite with 2.5-3.5 weight percent Fe. Using these percentages, point count data from table 3 may be normalized to give total FeO concentration in the calcite for each sample.

Bulk X-ray diffraction analyses were also used to determine total iron and magnesium concentrations in calcite and dolomite because of the many ambiguities and errors that arise from carbonate stain color (Dickson, 1966; Lindholm and Finkelman, 1972). Substitution of Fe^{2+} and Mg^{2+} for Ca^{2+} in these minerals causes variations in their interplanar atomic spacing (d spacing) that may be detected by subtle shifts in the peak position of X-rays emitted from the (104) atomic plane. Because these shifts in peak position have been correlated with numerous chemical and microprobe analyses (Matsumoto and others 1978), a reasonably accurate determination of iron, magnesium, and calcium concentrations is possible. To find the molecular (mol) percent of $FeCO_3$ from $d_{(104)}$ spacings, I used a convenient ternary diagram constructed by Matsumoto and others (1978) for the system $CaCO_3$-$MgCO_3$-$FeCO_3$. However, because both Fe^{2+} and Mg^{2+} cause similar shifts in d-spacings, X-ray analysis must be supplemented with microprobe or some similar elemental analysis. Cations such as Mn^{2+} or Zn^{2+} will also cause similar shifts, but compared with Mg^{2+} and Fe^{2+}, their concentrations are relatively low in most calcites and can be neglected. The $d_{(104)}$ spacing for calcite and dolomite in Wagon Wheel samples are listed in table 5, and microprobe analyses for two of these samples are in table 6.

From the above work it is clear that carbonate staining methods delineate iron concentrations near the resolution limit of both microprobe and X-ray analyses. On carbonates containing 1-2 weight percent FeO, 20 second microprobe counts have standard deviations between 3 and 7 percent, while shifts in X-ray peaks are on the order of 0.05 degrees 2θ. In view of the errors involved with using these methods, the apparent similaritie in iron concentrations is remarkable (fig. 20). Although low, the concentrations of $MgCO_3$ may be large enough to augment the shift in peak position and cause additional scatter in figure 20. Samples containing only small amounts of visible ferroan calcite could have shifted X-ray peaks because of magnesium, which cannot be recognized by staining.

The paragenetic relation between many cements, which have various iron concentrations as indicated by stain coloration, is unclear because they occupy separate pores. However, where different cements occupy the same pore, relict iron-free calcite typically is surrounded by a younger generation of iron-bearing calcite (fig. 18c). Relict iron-free calcite commonly has a corroded texture suggesting that it once occupied the entire pore before dissolution and the subsequent precipitation of iron-bearing calcite. These observations are significant because they provide the best evidence that calcite cements inherit new geochemical characteristics by a process of

Table 5.--Slow scan X-ray analysis of carbonate in Wagon Wheel #1 sandstones

Sample No.	Depth (ft)	Calcite		Dolomite	
		$d_{(104)}$ Å	Maximum Peak Intensity*	$d_{(104)}$ Å	Maximum Peak Intensity*
2	7,044	3.0310	3069	2.8912	104
6	7,046	---	---	---	---
20	7,114	3.0336	8780	2.8980	713
7969	7,264	3.0324	6806	---	---
30	7,344	---	---	---	---
31	7,350	3.0300	2611	2.8857	1362
34	7,366	3.0284	14738	---	---
36	7,378	3.0314	3114	2.8868	1884
8710	7,633	---	---	---	---
52	8,084	3.0259	5550	---	---
53	8,088	3.0269	6241	---	---
59	8,124	3.0307	11194	---	---
60	8,128	3.0290	5991	---	---
68	8,934	3.0272	11990	2.8886	1714
69	8,944	3.0359	2070	2.8914	289
76	8,989	3.0300	6480	2.8866	1149
80	10,153	3.0262	7157	2.8847	1122
89	10,217	3.0302	6922	2.8870	1267
95	10,978	3.0277	5184	2.8836	1069
104	11,028	3.0239	4436	2.8819	1756
110	11068	3.0296	1697	2.8860	930
148	14,951	3.0248	1332	2.8818	2652
155	16,083	3.0329	342	2.8846	8082
156	16,087	3.0280	562	2.8843	6480
171	17,176	3.0297	790	2.8825	4422
172	17,178	3.0278	441	2.8841	3306
175	17,959	---	---	2.8860	5776
F-39	17,960	3.0311	3036	2.8822	3192
Standard deviation of error in measurement †		0.0024	97	0.0033	59

* Maximum peak intensity; average counts per second.

† Average standard deviation of two samples; each was re-packed and run five separate times.

--- indicates no data

Table 6.--Microprobe analyses of iron-bearing calcite cements

Sample	Area	Spot	Molecular %*		
			$CaCO_3$	$MgCO_3$	$FeCO_3$
		A†	98.0	1.7	0.3
		B†	98.0	1.7	.3
		C	96.8	1.3	1.9
Wagon	4	D	96.7	1.3	2.0
Wheel		E	97.3	1.3	1.5
148		F	97.4	1.1	1.5
		H	96.6	1.3	2.1
		J	97.1	1.2	1.8
		C†	98.2	1.7	.1
	1	D	96.4	1.5	2.1
		E	96.6	1.4	2.0
		I	97.0	1.0	2.1
Wagon		J	97.5	1.0	1.5
Wheel	1	K	97.0	1.1	1.9
156		L	97.2	1.1	1.8
		M	97.1	1.0	1.9
		Average	97.0	1.2	1.9
		Maximum	97.5	1.5	2.1
		Minimum	96.4	1.0	1.5

* Calculated from weight % of oxide; each value is an average of two 20 second counting periods; values less than about 5 molecular % are within ± 10%.

† Iron-free calcite not included in total averaging.

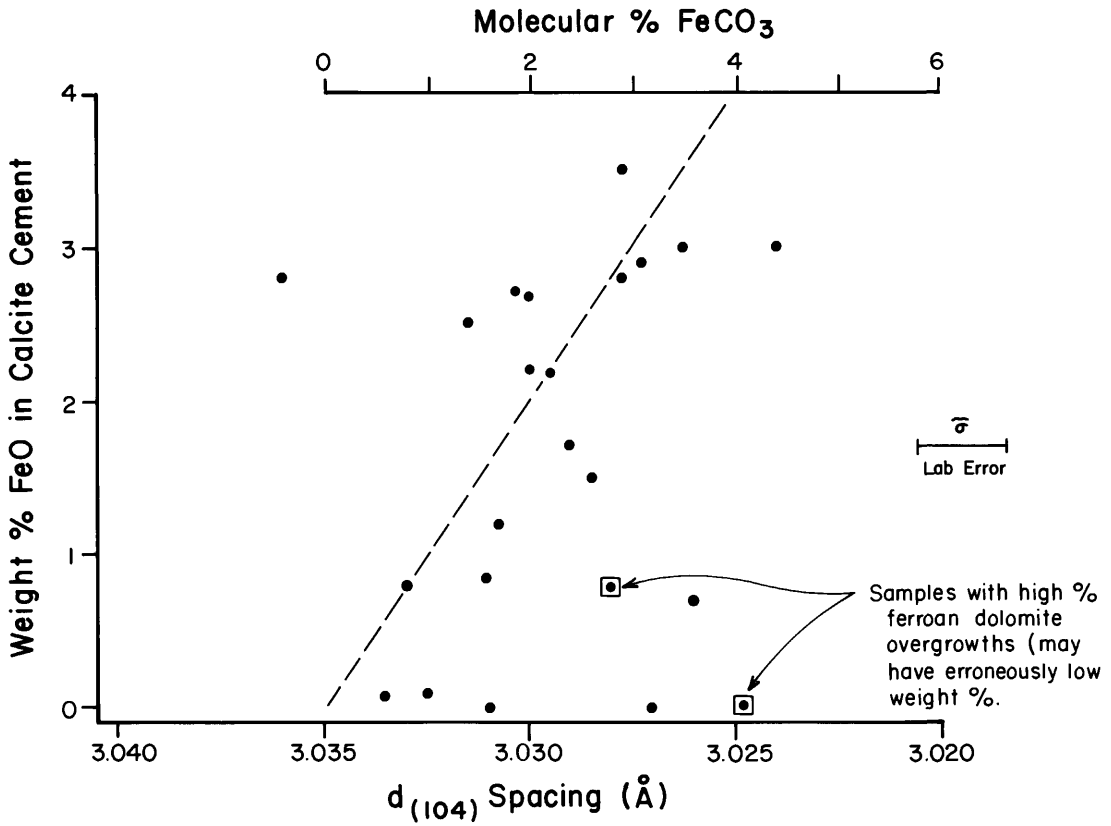

Figure 20--Relationship between $d_{(104)}$ spacing for calcite (data in Table 5) and weight % FeO in Wagon Wheel sandstones. The $d_{(104)}$ is related to molecular % $FeCO_3$ using work of Matsumoto et al, (1978). Weight % FeO was calculated from petrographic data in Table 3 and work of Lindholm and Finkelman (1972):

$$\frac{(\%\ \text{Fe-free calcite} \times 0)+(\%\ \text{Fe-poor calcite} \times 1.5)+(\%\ \text{Fe-rich calcite} \times 3.5)}{(\%\ \text{Fe-free calcite})+(\%\ \text{Fe-poor calcite})+(\%\ \text{Fe-rich calcite})} \times 100$$

At low percentages of calcite, the difference between weight %FeO and molecular %$FeCO_3$ is small. Dashed line shows equal percentages of FeO and $FeCO_3$.

dissolution and reprecipitation. Zoning, which is less common than dissolution-reprecipitation features, also shows that the outer or later stages of pore filling cement have higher iron concentrations (fig. 18d). The boundary between zones is usually wide and diffuse suggesting a gradual increase of iron in the later stages of cementation.

The evolution of carbonate cements from iron-free to later iron-rich varieties is a commonly reported paragenetic sequence (Boles, 1978; Land and Dutton, 1978; Nash and Pitman, 1975; Pitman and others 1982) and one that is observed at all depths in the northern Green River Basin. Surprisingly, the percentage of iron-bearing calcite appears to be maximized at a depth of about 11,000 feet (fig. 21). Even though the iron concentrations are low and difficult to measure, this trend is independently substantiated both from point count data and X-ray diffraction analysis. The reason that the concentration of iron-calicte is maximized near 11,000 ft remains unclear even though there are several possible sources of iron. Boles (1978) suggests that much of the Fe^{2+} in ankerites of the Wilcox Formation (southwest Texas), may come from the conversion of smectite to illite. Although this conversion is prominent near 7,100 ft in the Wagon Wheel well (Pollastro, 1983), it is not clear why iron from this source would be favored over iron derived from the breakdown of unstable ferro-magnesium grains in the first-cycle arkose above 7,100 ft. A decrease in iron-calcite below 11,000 ft may result from more effective competition for Fe^{2+} by ankerite and Fe-dolomite. Boles (1978) used theoretical calculations to demonstrate that the reaction of calcite to ankerite (presumably incudes Fe-dolomite) is favored by high temperature. Although little ankerite has been observed in the deep rocks of the basin, some of the Fe^{2+} possibly is being consumed by overgrowths of ferroan dolomite. However, the amount of Fe-dolomite is small and not detectable from X-ray analysis.

Stable Isotopes

A major problem in studying the stable isotope composition of carbonate minerals in clastic rocks is the separation of an adequate quantity of a particular phase for analysis. One way to partly avoid this problem is to correlate a large number of bulk isotopic analyses with their carbonate mineralogy, which has been petrographically determined.

In the sandstones of the northern Green River Basin, the amount of calcite cement is a major factor in controlling bulk isotopic compositions. Samples containing a high percentage of cement have a wide range of isotopic values, whereas samples containing a high percentage of detrital grains have a relatively narrow range of values (fig. 22). Most samples have isotopic compositions that are more negative than the average value for the detrital limestone grains. The reason for the triangular distribution of points in figure 22 becomes clear when samples that have more than 90 percent cement are plotted versus depth (fig. 23). With increasing depth, $\delta^{18}O$ and $\delta^{13}C$ values of the cements become less negative and approach the values of the detrital

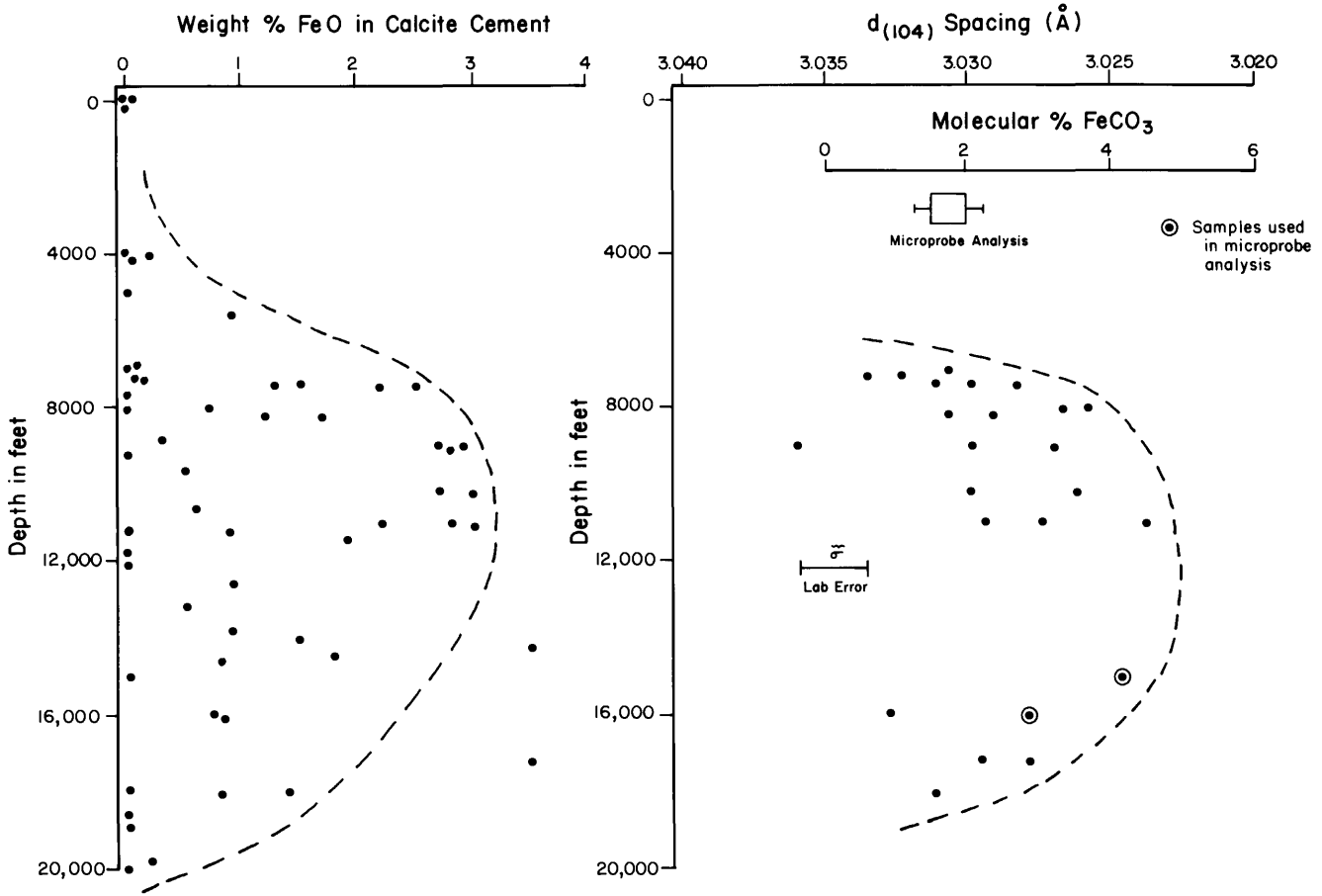

Figure 21--Relationship of depth to weight percent FeO in calcite cements from 5 wells and depth to $d_{(104)}$ spacing of bulk calcite in Wagon Wheel #1. Dashed lines are the approximate maximum concentrations of iron. Weight percent FeO calculated from data in table 3 (see text and fig. 20 for details). The $d_{(104)}$ spacing (data from table 5) is related to molecular percent $FeCO_3$ using work of Matsumoto and others, (1978). Range of microprobe analyses (with error bars) for iron-bearing calcite cements is from data in table 6.

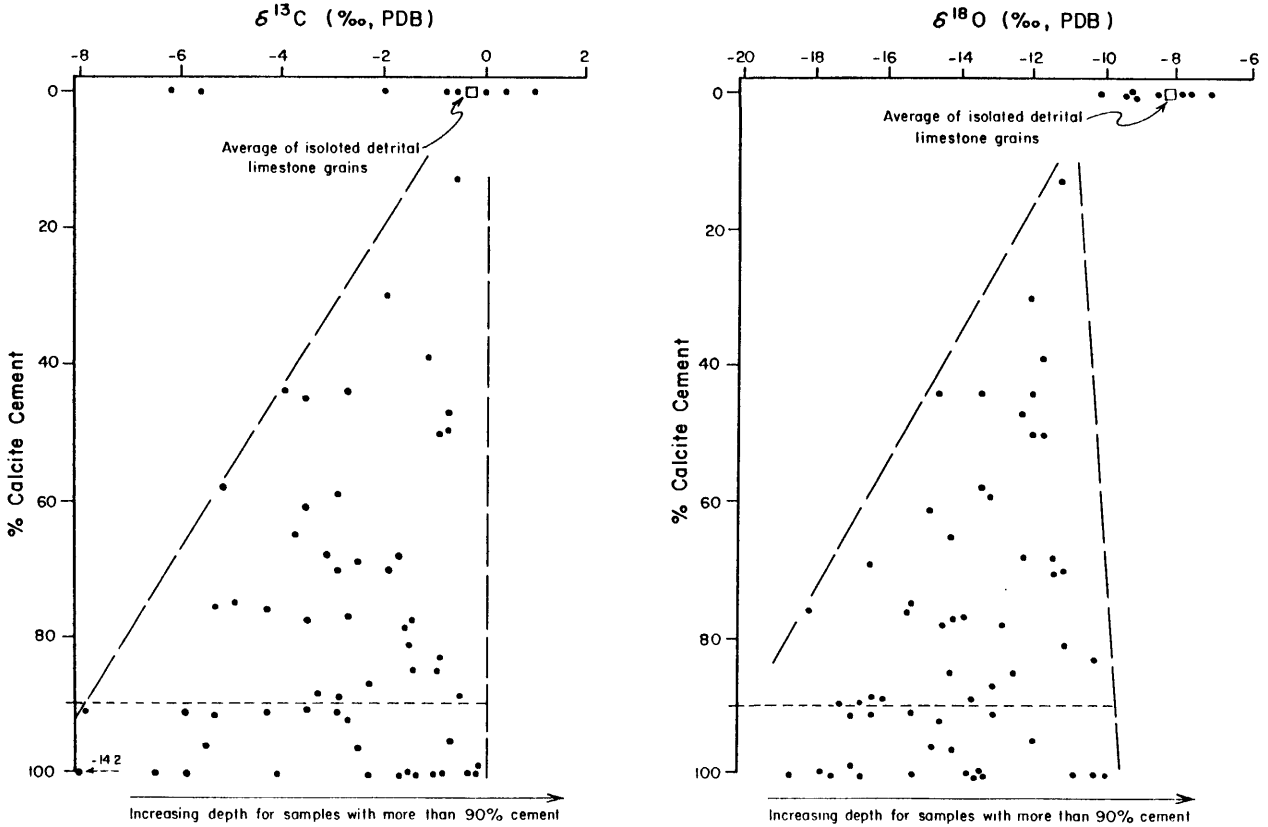

Figure 22--Plots show % calcite cement versus $\delta^{13}C$ and $\delta^{18}O$. Dashed lines are the approximate limits of the lightest and heaviest isotopic compositions. In samples with 0% cement, the calcite consists only of detrital limestone grains. The % calcite cement was calculated from data in Table 3 as follows:

$$\frac{(\%\ \text{Fe-free calcite})+(\%\ \text{Fe-poor calcite})+(\%\ \text{Fe-rich calcite})}{(\%\ \text{Fe-free calcite})+(\%\ \text{Fe-poor calcite})+(\%\ \text{Fe-rich calcite})+(\%\ \text{Detrital calcite})}$$

Samples with over 90% cement are solid dots in Figure 23.

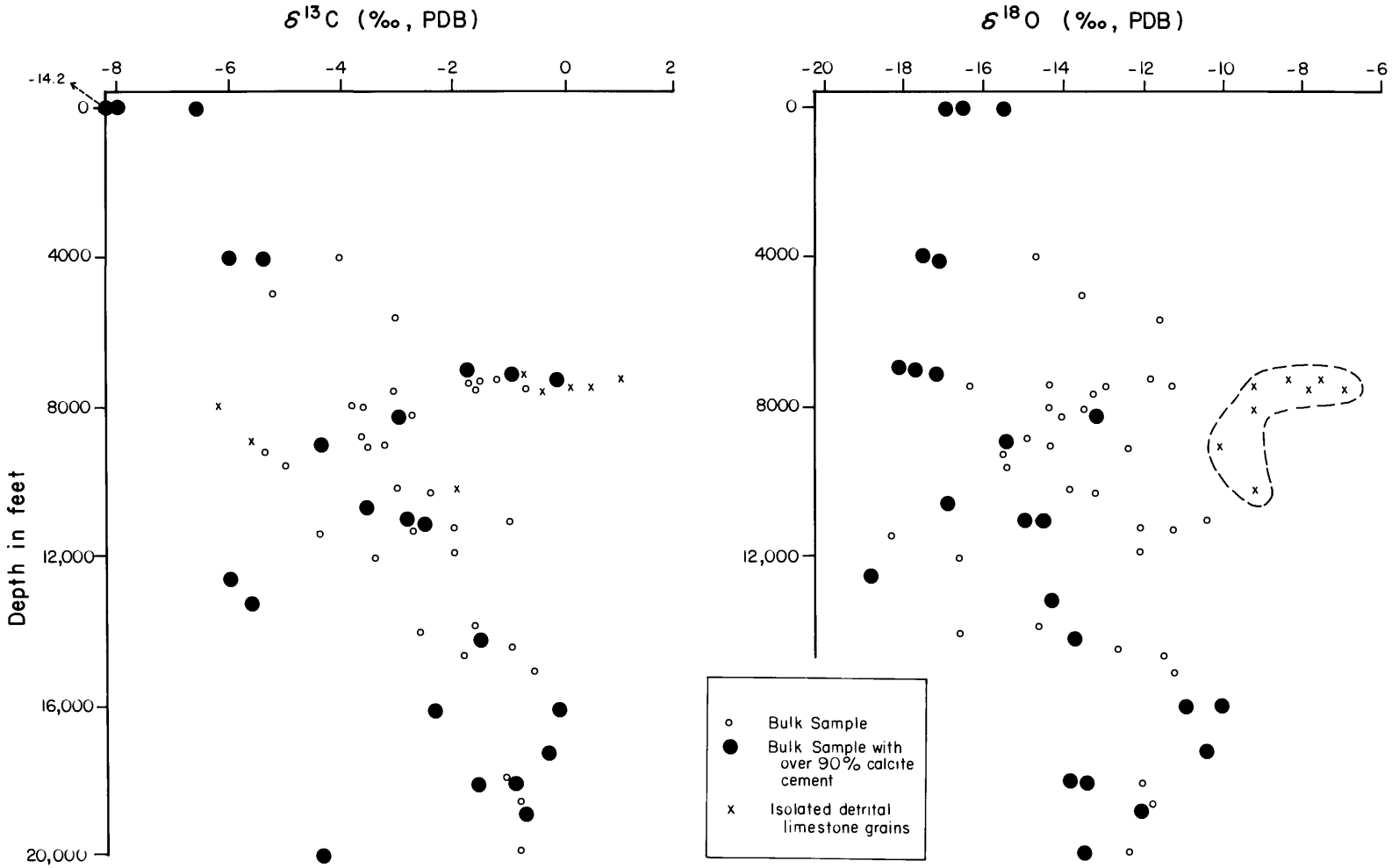

Figure 23--Relationship of depth to $\delta^{13}C$ and $\delta^{18}O$ in calcite from sandstones. Data are listed in Tables 3 and 4.

grains. Thus, while the isotopic composition of the detrital grains remains about the same, the composition of the cement changes with depth.

Although isolated and analyzed from only a few thin zones, detrital limestone grains are inferred to have similar isotopic compositions at all depths. This inferrence is supported by the fact that maximum and minimum isotopic values of the bulk samples converge near the average isotopic value of the grains (fig. 22). Note that $\delta^{18}O$ for the average detrital grains is slightly less negative than the convergence point. This suggests that recrystallized detrital grains represent an isotopic end-member in most sandstones. At any depth there is a continuum in isotopic compositions from the detrital end-member to the cement end-member. Although this continuum leads to a triangular plot of data in figure 22, it causes most of the scatter in figure 23.

There is no apparent relationship between the amount of iron in the cements and their isotopic composition. Low-iron concentrations and small differences in isotopic values may prevent recognition of such a relationship. However, the lack of a relationship is more likely because the iron content and isotopic composition of the cements change in non-corresponding ways with depth. As $\delta^{13}C$ and $\delta^{18}O$ generally become less negative with depth, iron concentrations increase down to about 11,000 feet but then decrease below this depth.

Dolomite

The total amount of dolomite increases with depth or formation age to a maximum of about 26 percent but averages around 8 percent, which is less than the average for total calcite. Morphologically, there are two types of dolomite grains (table 3): 1) Grains referred to as "detrital dolomite" show visible evidence of transportation prior to deposition but contain no overgrowths. They consist mostly of well rounded polycrystalline grains, but subangular, monocrystalline grains are common in the older and finer grained sandstones. 2) Grains referred to as "rhombic dolomite" are also detrital grains, but they have been diagenetically modified by overgrowths of authigenic dolomite.

There is a distinct absence of either dolomitic or ankeritic cement, and with few exceptions all authigenic dolomite occurs as overgrowths on grains of detrital dolomite. It is virtually impossible to obtain actual isotopic values for the overgrowths because they constitute only a small percentage of total dolomite. Instead, rhombic dolomite is used to characterize relative shifts in the isotopic values of authigenic dolomite. Small euhedral dolomite rhombs, which occur as minor replacements in chert fragments, also are present but they are volumetrically insignificant.

Detrital Dolomite

Detrital dolomite includes polycrystalline grains ranging from 0.5 to 4.0 mm in diameter and smaller monocrystalline grains which are from 0.1 to 0.5 mm in diameter. Large well-rounded polycrystalline dolomite grains are most common in the coarse fractions of the Tertiary and uppermost Cretaceous sandstones (fig. 18a) but are rare in the older and finer grained sandstones of the lower Lance and Rock Springs formations. In fine grained sandstones the detrital dolomite fraction consists mostly of monocrystalline grains which display a subhedral, rhombic morphology. In places, clusters of these crystals form small uncemented aggregates. Although most monocrystalline grains show signs of rounding and abrasion, some have a remarkably well-preserved rhombic shape; a fact that has led to controversy over their origin. Sabins (1962) concluded that monocrystalline dolomite grains found in Cretaceous sandstones and siltstones of the Western Interior formed at the sediment-water interface prior to final burial of the sediment. On the other hand, Gautier (1981) concluded that the distribution, intergranular relationships, and morphology of analogous grains in the Eagle Sandstone of Montana, strongly suggested a detrital origin.

The vertical sampling through the Tertiary and Upper Cretaceous sandstones and siltstones offers the opportunity to follow a transition from rounded polycrystalline dolomite grains, which are clearly detrital in origin, to the controversial monocrystalline, rhombic-shaped grains. Most of the polycrystalline grains have a coarse texture and consist of euhedral and subhedral rhomboid crystals which are 0.1 to 0.5 mm in size. It is not coincidental that most monocrystalline rhombic grains also are in this size range. Slightly abraded dolomite rhombs are not uncommon in fine grained sandstones and siltstones that are associated with the coarse sandstones containing polycrystalline grains. Thin-sections of some of the sandstones in the Lance Formation, contain both monocrystalline grains and small, rounded polycrystalline grains. These observations provide further evidence of a detrital origin for monocrystalline grains.

Particle size of the sediment and crystal size of the eroded dolomite are two main factors controlling the distribution of monocrystalline and polycrystalline grains. Amsbury (1962) shows that coarsely crystalline dolomites are friable and weather into mostly loose crystals which compose a major portion of the stream sediment in central Texas. He notes that the size of the dolomite crystals in the weathering rocks determines the size fraction of the sediments that contain the most dolomite. In the northern Green River Basin, it seems probable that dolomite could have eroded into both single crytals and polycrystalline grains which later disintegrated to single crystals. The small aggregates of monocrystalline grains may be a good example of the latter. Thus, the preservation of many monocrystalline grains could result from partial transportation within polycrystalline grains and from decreased abrasion to small sized particles.

Large polycrystalline grains from several zones were isolated for isotopic analysis (table 4). Unfortunately, the isotopic composition of dolomites that crop out near the the basin have not been reported. A comparison of these grains to other Paleozoic dolomites makes little sense because a review of the literature shows that there is no consistent trend with age for the isotopic composition of dolomite. The good correlation between $\delta^{13}C$ and $\delta^{18}O$ for these grains suggests that they may have undergone partial recrystallization with meteoric waters (fig. 19). The fact that the isotopic composition of these grains is less variable than the isotopic composition of the detrital limestone grains is consistent with the experimental results of Epstein and others (1964) indicating that dolomite is much less susceptible to recrystallization in water than is calcite.

Rhombic Dolomite

In this report the term rhombic dolomite is used to describe monocrystalline detrital grains that have been diagenetically altered by the addition of dolomitic overgrowths. These overgrowths, which are usually iron-bearing, commonly enhance the crystalline appearance of the detrital grains to nearly perfect rhombohedra (fig. 24). In many instances the overgrowths are thin and difficult to recognize even with proper staining techniques. Part of the controversy over the origin of monocrystalline rhombs in the Cretaceous rocks of the Western Interior may stem from the fact that authigenic overgrowths, which enhance crystallinity, are difficult to recognize.

Rhombic dolomite grains become more abundant with increasing stratigraphic age (fig. 25). However, the reason for this is obscured because the grains consist of both a detrital core and an authigenic overgrowth. On one hand there are more monocrystalline detrital grains in the Upper Cretaceous rocks than in the Tertiary rocks, but on the other hand the higher temperatures with increased depth often favor the precipitation of dolomite. Although most of the samples having an abundance of rhombic dolomite come from Upper Cretaceous rocks below 15,000 ft, two samples from the same rocks, which are about 6,000 ft deep on the flank of the basin, also have a high percentage of these grains (arrows, fig. 25). This strongly suggests that depth of burial is not a major requirement for the development of dolomitic overgrowths. Apparently, monocrystalline dolomite provides the best substrate for the precipitation of authigenic dolomite, which is noticeably absent on other grains including rounded polycrystalline dolomite. Thus, the occurrence of rhombic dolomite appears to be controlled more by the sedimentologic factors that control the occurrence of monocrystalline dolomite than by increased burial temperatures.

Microprobe analyses of several rhombic dolomite grains (table 7) show that the detrital cores are nearly homogeneous and stoichiometric in composition. However, the composition of overgrowths on the same grain and between grains is highly variable. While there is only minor variation in the percentage of calcium, percentages of iron and magnesium show large, inverse

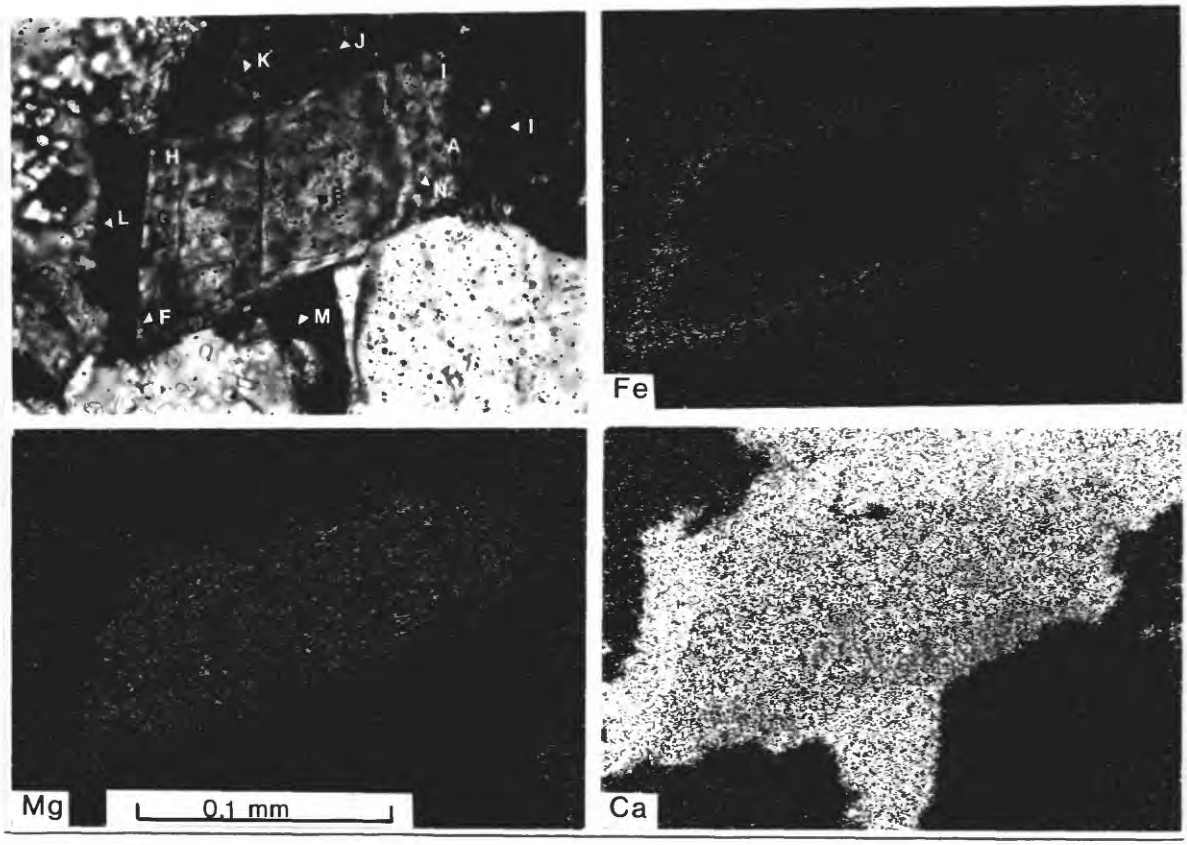

Figure 24--Grain of rhombic dolomite shows monocrystalline detrital core (points B-E, N) surrounded by an authigenic overgrowth of ferroan dolomite. The overgrowth is stained light blue and the grain is surrounded by iron-bearing calcite cement (mauve). X-ray immage maps of Fe, Mg, and Ca show the areas of detrital core, overgrowth, and calcite cement. Sample is from Wagon Wheel 156, area 1. Microprobe points A-I, N are listed in table 7; points I-M are in table 6.

Table 7.--Microprobe analysis of rhombic dolomite grains

Sample	Grain	Molecular %*							
		Detrital Core				Authigenic Overgrowth			
		Spot	$CaCO_3$	$MgCO_3$	$FeCO_3$	Spot	$CaCO_3$	$MgCO_3$	$FeCO_3$
Wagon Wheel 148	1	A	52.1	47.5	0.4	B	46.3	10.0	43.7
		H	48.8	51.1	.2	F	62.6	6.0	31.4
						G	49.9	48.4	1.7
	3	B	50.7	48.9	.4	A	50.6	46.8	2.6
Wagon Wheel 156	1	B†	51.2	46.9	2.0	A	65.4	19.1	15.5
		C	50.9	48.9	0.1	F	56.9	24.8	18.3
		D	51.0	48.8	.3	G	51.9	42.2	5.9
		E	50.5	48.4	1.0	H	56.4	28.2	15.0
		N	52.1	47.7	.3	I	54.7	36.8	8.6
	2	C†	51.7	45.0	3.3	A	56.4	28.1	15.5
		D	50.0	50.0	0.0	B	52.5	43.4	4.1
	3	A	50.7	48.2	1.1	B	57.9	22.6	19.5
		C	50.5	48.4	1.1	F	51.2	47.2	1.6
		D	50.4	48.5	1.1	G	54.1	37.9	8.0
		E	50.6	48.8	0.5	H	63.4	19.1	17.5
		I	51.0	48.8	.1	K	59.3	22.2	18.5
		J	50.8	48.9	.3	L	51.8	44.7	3.5
		O	50.2	49.7	.1	M	56.7	26.1	17.2
		P	51.1	48.8	.1	Q	67.2	18.0	14.9
		S	51.9	47.9	.1	U	58.4	22.0	19.6
		T	51.4	48.3	.3	W	58.1	22.0	19.8
		V	51.6	48.3	.1	Y	59.4	21.5	19.1
	4					A	58.0	24.6	17.5
						B	58.6	22.5	19.0
	5	A	50.9	49.1	0.0	B	57.7	22.8	19.5
		E	51.4	48.5	.1	C	58.4	22.7	19.0
		F	51.1	48.2	.8	D	59.6	22.3	18.0
	AVERAGE		50.9	48.7	0.4		56.7	27.9	15.4
	MAXIMUM		52.1	51.1	1.1		67.2	48.4	43.7
	MINIMUM		48.8	47.5	.0		49.9	6.0	1.6

* Calculated from weight % of oxide; each value is one 20 second counting period; values between 5 and 1 molecular % are within ± 10%; values less than 1 molecular % are below background levels.

† Authigenic dolomite filling a microfracture in detrital core; not included in averaging.

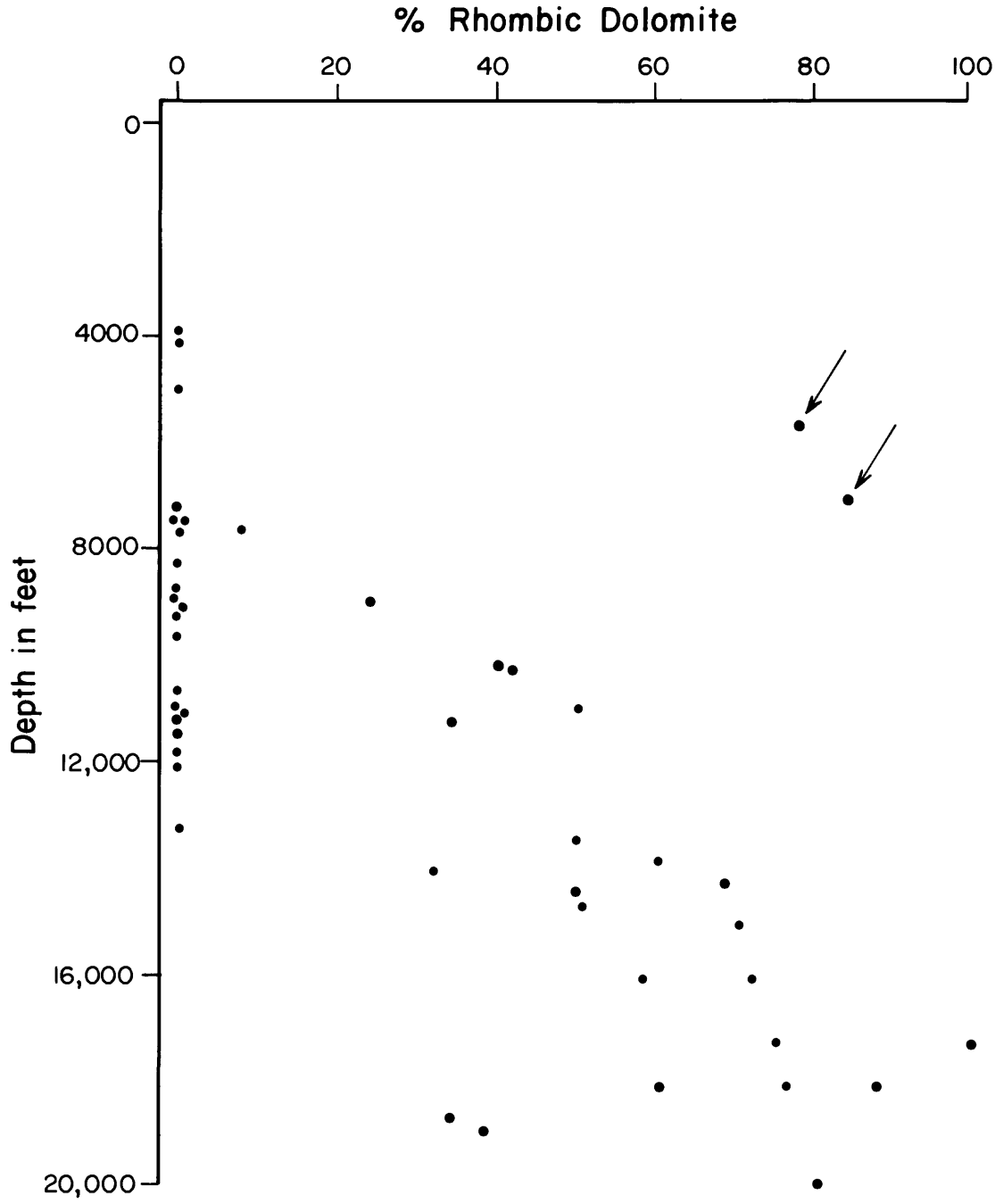

Figure 25--Plot shows increase of rhombic dolomite with increasing stratigraphic age or depth. Arrows indicate samples 16 and 19 which come from Upper Cretaceous rocks in Bar Cross #63-21. The % rhombic dolomite was calculated from data in Table 3 as follows:

$$\frac{\%\text{ rhombic dolomite (core and overgrowth)}}{(\%\text{ rhombic dolomite})+(\%\text{ detrital dolomite})} \times 100$$

variations. In most overgrowths iron is randomly distributed, but in places iron increases in concentration away from the detrital core. The overgrowths, which average 15.4 percent in $FeCO_3$, are well within the confines of a non-standardized definition for ferroan dolomite established by several authors (Boles, 1978; Dickson, 1966). In addition to overgrowths, some rhombic grains have microfractures filled with ferroan-dolomite which are assumed to be authigenic (fig. 26).

Although informative, microprobe analyses of a few exemplary grains do not represent the bulk composition that may be aquired from X-ray analysis. Measured $d_{(104)}$ spacing of dolomite averages 2.8862 Å and has a standard deviation that is barely larger than the standard deviation of the error in measurement (table 5). This suggests that the bulk composition of the dolomite is practically stoichiometric and that iron substitution in the authigenic phase is volumetrically insignificant. Although less than analytical error, a shift in d-spacing occurs between samples rich in rhorbic dolomite and samples rich in detrital dolomite (fig. 27). However, this shift is opposite of the expected one that should occur towards ferroan dolomite if the rhombic dolomite contained significant amounts of iron. The inverse relationship between iron and magnesium concentrations may nullify relative shifts in d-spacing. In this respect, X-ray analysis sheds little light on the composition of the dolomitic phases.

Stable Isotopes

In five wells, the isotopic compositions of dolomite show a remarkably good correlation (0.89) between values of $\delta^{13}C$ and $\delta^{18}O$ (fig. 28). The fact fact that all samples, regardless of age or depth, cluster around a linear regression line suggests diagenesis in the presence of meteoric waters. Samples containing more than 50 percent rhombic dolomite have more negative values of $\delta^{13}C$ and $\delta^{18}O$ than samples containing more than 50 percent detrital dolomite. The isotopic composition dolomite generally becomes more negative or lighter with an increasing percentage of rhombic dolomite. For rhombic dolomite, the detrital cores and authigenic overgrowths cannot be separated, and direct measurement of their isotopic compositions is impossible. One technique for estimating the isotopic composition of the overgrowths is to extrapolate a plot of percent overgrowth (100x overgrowth/total dolomite) versus $\delta^{13}C$ or $\delta^{18}O$. However, this was unsuccessful because 1) the overgrowths constitute a relatively small percentage of the total dolomite, and 2) their isotopic compositions change with depth.

The negative shift in $\delta^{13}C$ and $\delta^{18}O$ (fig. 28) can be attributed to compositional changes in the dolomitic overgrowths if it is assumed that most of the detrital cores in the rhombic grains have nearly the same isotopic composition. This assumption has support of some indirect evidence. Several samples, (squares, fig. 28) that come from different formations and contain mostly monocrystalline, detrital dolomite (rhombic dolomite without overgrowths) have similar but relatively positive isotopic values. In

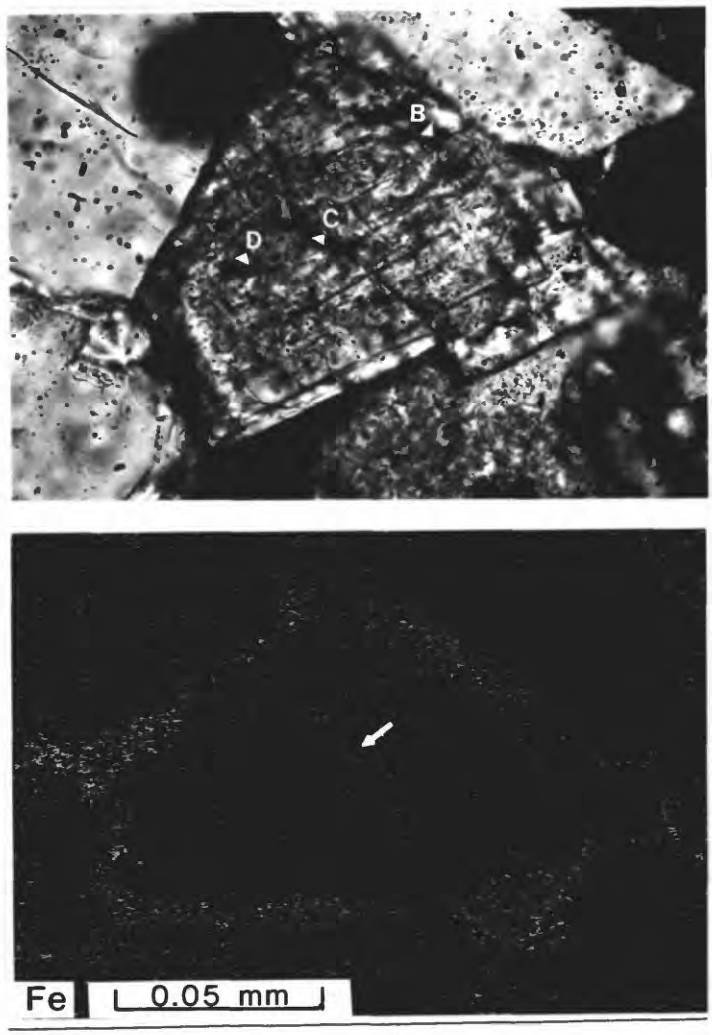

Figure 26--A microfracture (F) filled with ferroan dolomite cuts the detrital core of a rhombic dolomite grain. X-ray immage map of Fe shows microfracture and ferroan dolomite overgrowth which surrounds the detrital core. Microprobe points A-D are listed in Table 7 for sample Wagon Wheel 156, area 2.

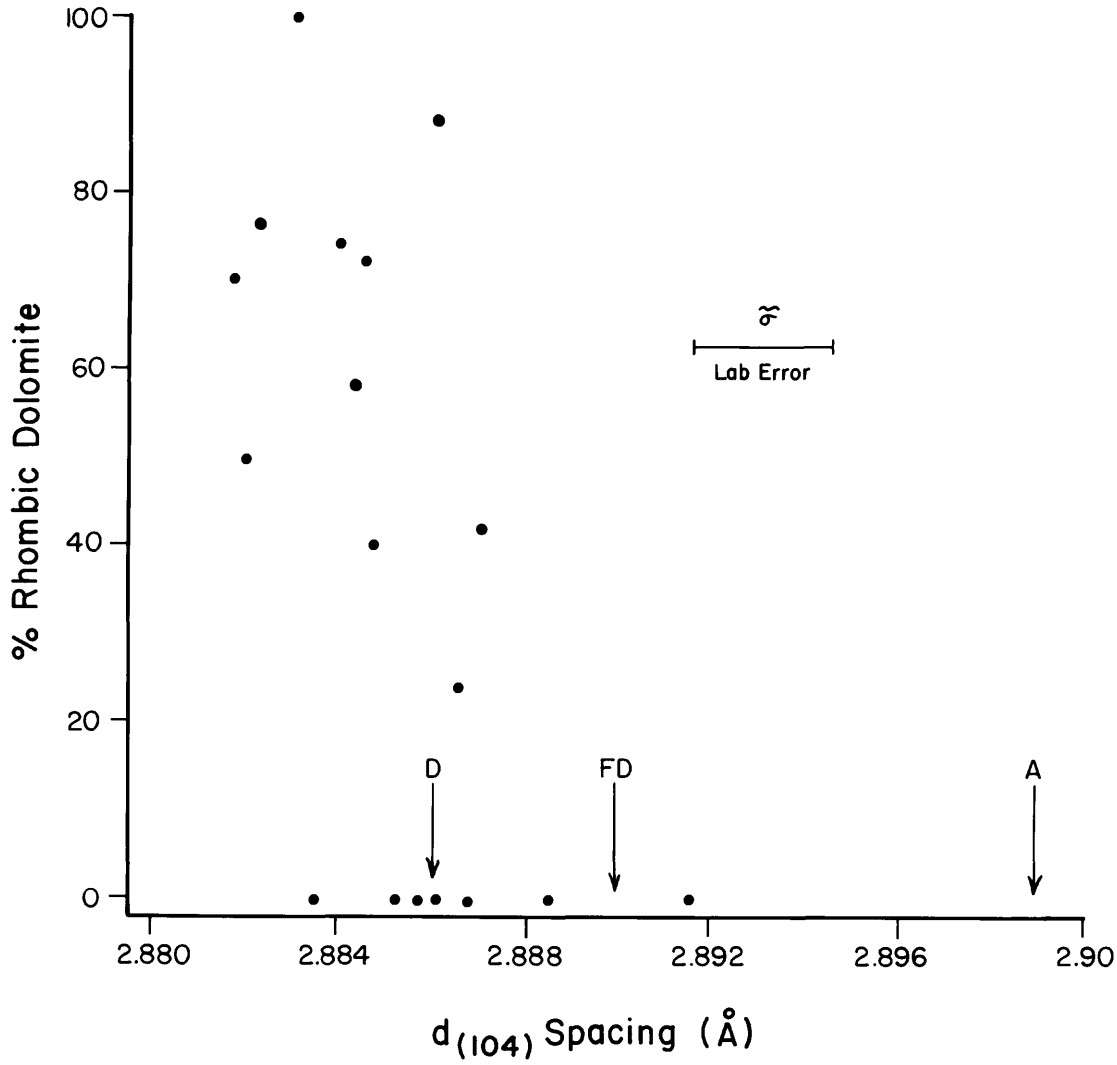

Figure 27--Plots show % rhombic dolomite versus $d_{(104)}$ spacing of dolomite in sandstones from Wagon Wheel #1. The ASTM $d_{(104)}$ spacing for dolomite (D) is 2.886Å, and for ankerite (A) it is 2.899Å. The $d_{(104)}$ spacing for ferroan dolomite (FD) is 2.890Å (Boles, 1978). See caption of Figure 25 for calculation of % rhombic dolomite.

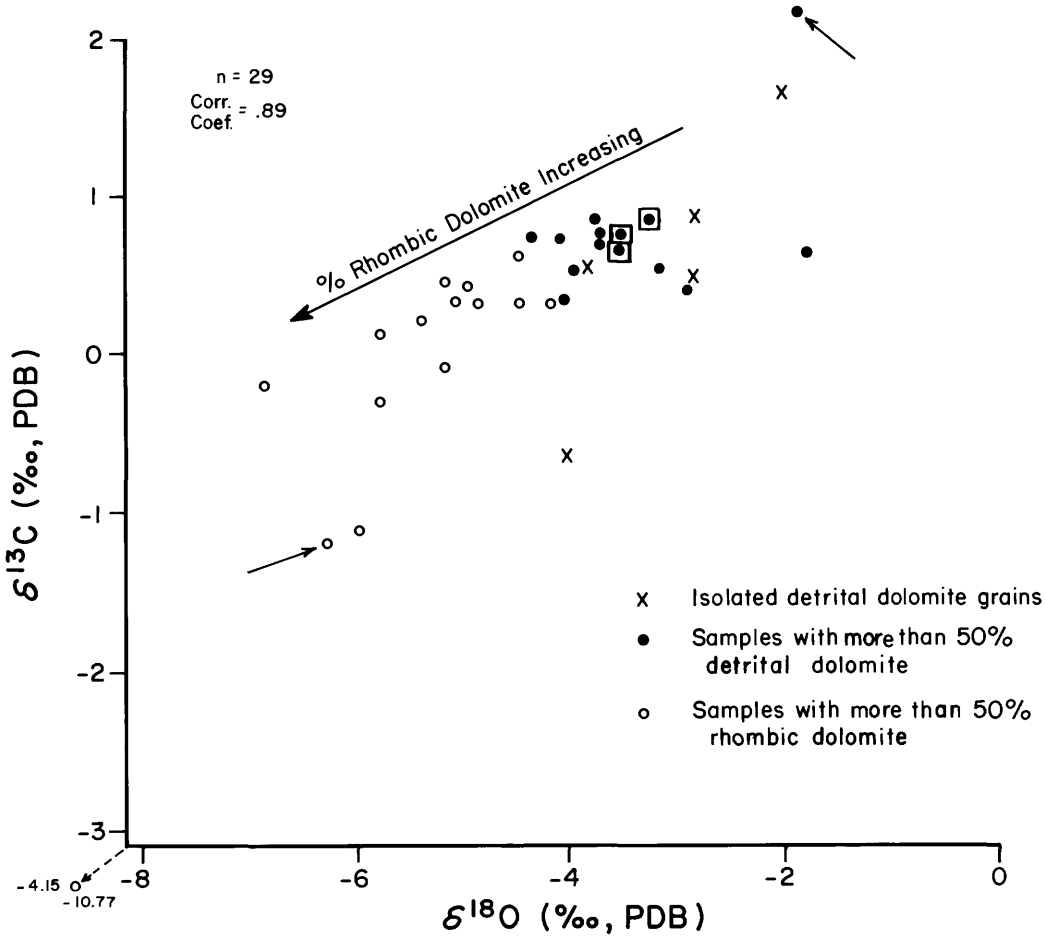

Figure 28--Plot of $\delta^{13}C$ versus $\delta^{18}O$ for dolomite samples in Tables 3 and 4. Arrows indicate samples 13 and 16 from Bar Cross #63-21. Squares are samples 89 and 110 from Wagon Wheel #1 and sample 6 from Mesa #1 all of which have a high percentage of monocrystalline dolomite. Correlation coefficient does not include isolated detrital grains.

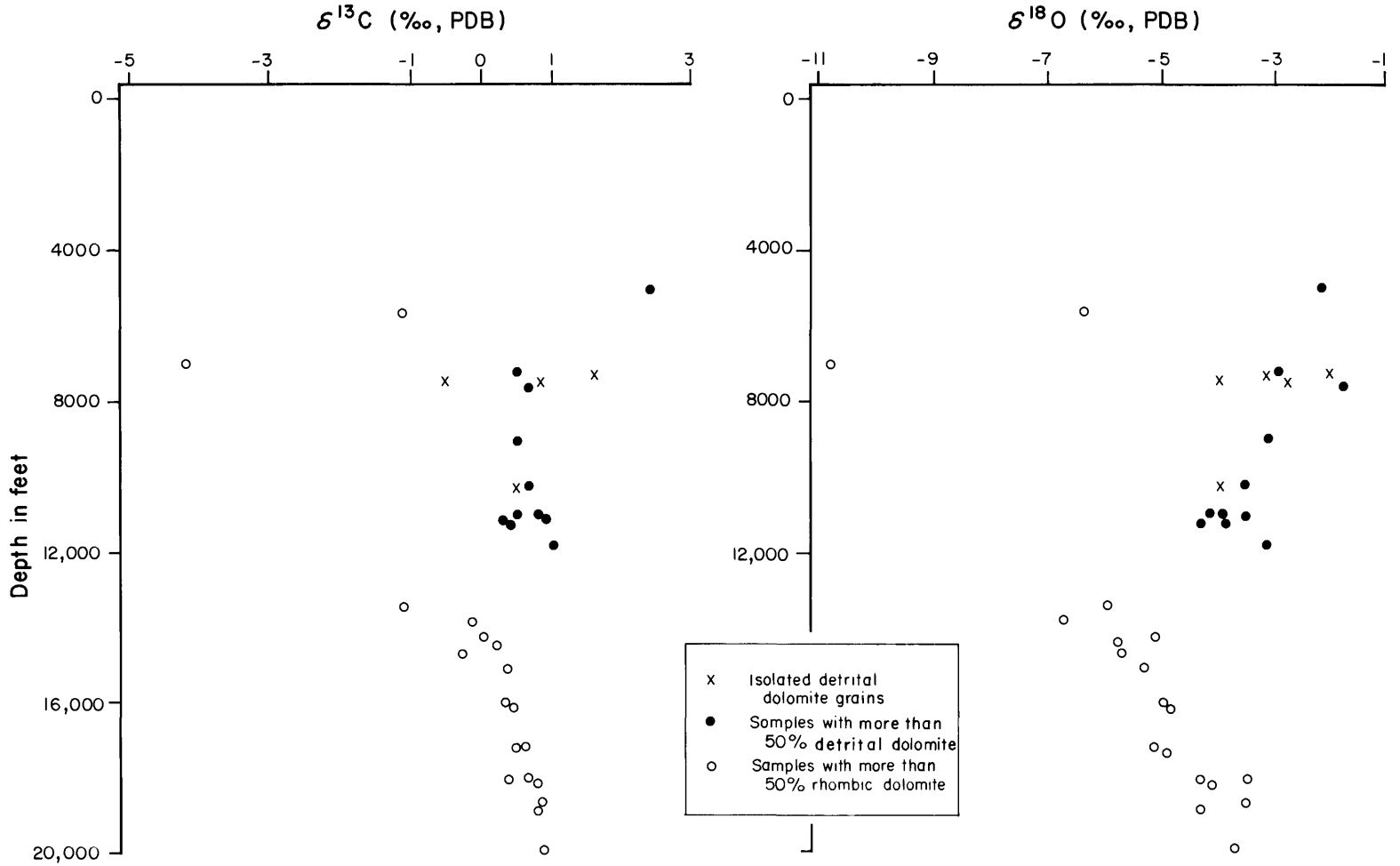

Figure 29--Relationship of depth to $\delta^{13}C$ and $\delta^{18}O$ in dolomite from sandstones. Data are listed in Tables 3 and 4.

addition, one sample containing monocrystalline detrital dolomite is in the same formation and 500 ft from another sample that is much more negative and contains mostly rhombic dolomite (arrows, fig. 28). While not conclusive, these observations strongly suggest that the addition of dolomitic overgrowths on monocrystalline, detrital grains causes a negative shift in bulk isotopic composition.

The relationship of depth to the isotopic composition of dolomite is complex because rhombic-rich and detrital-rich samples form two distinct trends (fig. 29). The lack of detrital dolomite below about 12,000 ft is largely the result of the fine grained sedimentation, which favors rhombic dolomite in Upper Cretaceous rocks. The two rhombic-rich samples near 6,000 ft (fig. 29) come from Upper Cretaceous rocks on the west flank of the basin. $\delta^{13}C$ and $\delta^{18}O$ have similar variations with depth except that shifts in $\delta^{18}O$ are greater in magnitude. With increasing depth, $\delta^{13}C$ of the detrital group remains nearly constant and close to the average value of the hand-picked, detrital grains. For the rhombic group, $\delta^{13}C$ becomes less negative with depth until it is nearly identical to the detrital group. On the other hand, the $\delta^{18}O$ of both groups approaches $\delta^{18}O \simeq -4^{o}/oo$ from opposite directions.

Isotopic shifts in the rhombic dolomite group are interpreted as resulting from changes in the isotopic composition of the overgrowths. Although generally more negative than detrital dolomite, $\delta^{13}C$ and $\delta^{18}O$ of the overgrowths also become less negative with depth. This is similar to the trend for calcite cement. However, the negative trend of $\delta^{18}O$ in the detrital dolomite group is surprising because the polycrystalline grains, which constitute most of this group, lack visible signs of recrystallization. Because it would be highly coincidental if this trend were the result of depositional variations, it must be concluded that the polycrystalline grains have been modified after burial. In addition, there is a slight hint that $\delta^{18}O$ of two rhombic-rich samples above the zone of overpressuring also become more negative with depth. From these observations one possible conclusion is that diagenetic conditions in the normally pressured rocks favor a negative trend with depth for $\delta^{18}O$ in both the rhombic and detrital groups. However, to confirm such a trend for the rhombic dolomite group, more sampling on the flank of the basin is necessary.

SHALES

To better understand the diagenesis of the carbonate minerals in sandstones, carbonate-rich shales were selected from Wagon Wheel core and analyzed (table 8). In this case, the term shale is used as a class name and also includes mudstones, which lack the fine laminations or fissility of a true shale.

Interbedded sandstones and shales undergo different diagenesis mainly because of differences in composition and grain size. After initial compaction and dewatering, shales are left with little permeability, whereas adjacent sandstones may act as conduits for large volumes of water. Consequently, much of the diagenesis in shales takes place in a restricted hydrologic system, while sandstone diagenesis takes place in a more open hydrologic system - one that is modified by waters from a variety of external sources. Some of these differences in the diagenetic regimes should be reflected in the isotopic composition of the carbonates.

Carbonate Mineralogy

In the selected shale samples (table 8), total calcite averages about 6.9 percent and total dolomite averages about 6.8 percent. The amount of dolomite increases with increasing depth or stratigraphic age, but the amount of calcite shows no systematic variation (fig. 30). Although visual evidence is not possible, it is reasonable to assume that the increase in the amount of dolomite in the shales is similar to the increase that occurs in the sandstones and results largely from an influx of detrital, monocrystalline dolomite grains in the Upper Cretaceous sediments. Presumably, these dolomite grains also act as substrates for the precipitation of authigenic dolomite. The absence of carbonate-rich shales in core above 7,100 ft probably results from a dearth of carbonate material in the arkosic debris that was shed during the late Paleocene and early Eocene.

X-ray analyses show that the d-spacings of carbonate minerals do not vary significantly as a function of depth (table 8). This may simply indicate that, as in the sandstones, there are no major trace-element substitutions in the carbonates of the shales. However, equal substitutions of iron and magnesium as well as the small number of analyses could obscure subtle shifts in d-spacing.

It is assumed that the shallower shales consist mostly of detrital components and contain few authigenic minerals relative to the deeper shales. This is because the low porosity and permeability in most shales prevent the influx of large volumes of saturated water and hence the precipitation of externally derived pore-filling materials. However, with increasing burial and time, more and more of the detrital components within the shale dissolve and form authigenic minerals which not only replace portions of the detrital grains but also fill pores.

Stable Isotopes

Since petrographic and X-ray analyses provide no characterization of the carbonate minerals in the shales, it is only possible to examine the bulk isotopic compositions of calcite and dolomite as a function of depth and compare this to the sandstones (fig. 31). Generally, the range of $\delta^{13}C$ and $\delta^{18}O$ for calcites in the shales is smaller than that for calcite cements in the sandstones. There are two possible reasons for this. First, there is a

Table 8.--Selected shale samples from Wagon Wheel core; X-ray analysis of carbonate minerals, isotopic composition of carbonate minerals and organic carbon

Sample number	Depth (ft)	Temperature °C	Isotopic Ratios (°/oo, PDB)					% TOC	X-Ray Analysis*					
			Calcite		Dolomite		Organic Carbon		Calcite			Dolomite		
			$\delta^{13}C$	$\delta^{18}O$	$\delta^{13}C$	$\delta^{18}O$	$\delta^{13}C$		$d_{(104)}$ Å	Maximum Peak Intensity	Weight† %	$d_{(104)}$ Å	Maximum Peak Intensity	Weight† %
24	7,125	61	-1.60	-11.39	---	---	-25.12	0.25	3.0257	1362	4.2	---	---	0.0
26	7,130	61	-1.40	-11.56	---	---	-25.55	2.31	3.0342	2873	6.1	---	---	0.0
38	7,384	62	-2.16	-9.82	0.34	-8.30	-25.01	1.47	3.0280	3969	6.6	2.8844	1640	3.5
39	7,388	62	-2.18	-9.76	---	---	-25.15	2.03	3.0295	4789	12.9	2.8875	1391	4.0
41	7,395	62	-1.96	9.62	0.34	-7.33	-25.39	1.20	3.0291	4070	10.9	2.8844	1789	3.9
48	8,066	67	-3.50	-11.10	0.59	-7.54	-26.04	.19	3.0339	3102	7.3	2.8853	2440	3.5
50	8,073	67	-3.71	-11.36	---	---	-26.02	.72	3.0287	2266	6.0	2.8819	1303	2.0
63	8,135	68	-6.72	-10.09	---	---	-25.60	1.18	3.0317	4369	8.4	2.8858	1815	1.0
79	10,145	81	---	---	-0.27	-6.36	-26.13	.44	3.0326	331	.5	2.8830	3931	7.4
103	11,024	87	-2.12	-10.75	---	---	-26.22	.99	3.0322	502	1.8	2.8946	2777	1.0
112	11,068	87	.00	-7.99	0.12	-5.50	-26.75	.32	3.0279	3881	9.8	2.8859	2411	6.2
135	14,897	113	-1.27	-11.01	-0.14	-5.47	-26.15	1.37	3.0319	3058	8.9	2.8865	6872	14.0
139	14,918	114	---	---	-0.19	-7.16	-25.70	4.87	3.03.6	586	1.0	2.8838	7056	15.7
141	14,923	114	-0.47	-11.13	-0.13	-6.80	-26.26	.75	3.0313	2314	6.9	2.8829	5685	13.6
159	16,101	122	-0.78	-12.11	0.24	-5.96	-25.80	1.50	3.0350	1568	3.9	2.8871	7293	11.4
164	16,115	122	---	---	0.27	-5.06	-25.82	1.05	---	---	1.5	---	---	12.4
170	17,173	129	-2.12	-13.22	0.45	-4.59	-26.86	.31	3.0250	4251	12.5	2.8861	5089	10.9
176	17,961	134	-0.40	-12.18	0.65	-4.57	-26.21	.77	3.0309	2510	9.2	2.8853	7903	12.5

* See methods section and Table 5 for analytical error.
† Weight difference of bulk sample by dissolution in 5% HCl after one hour for calcite and after 24 hours for dolomite.
--- indicates no data.

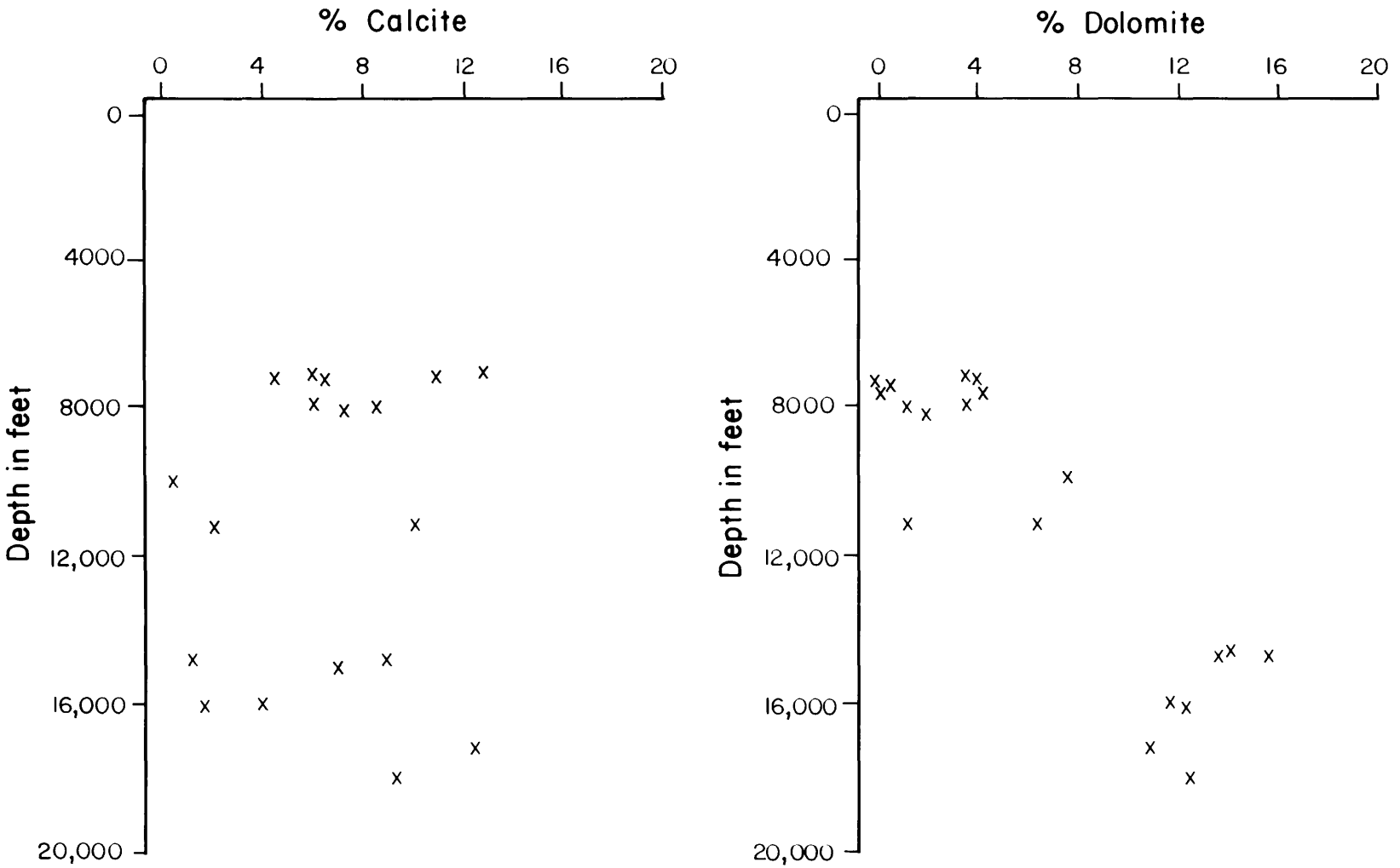

Figure 30. Plots show depth versus % total calcite and % total dolomite in selected shales from Wagon Wheel #1. Data are from Table 8.

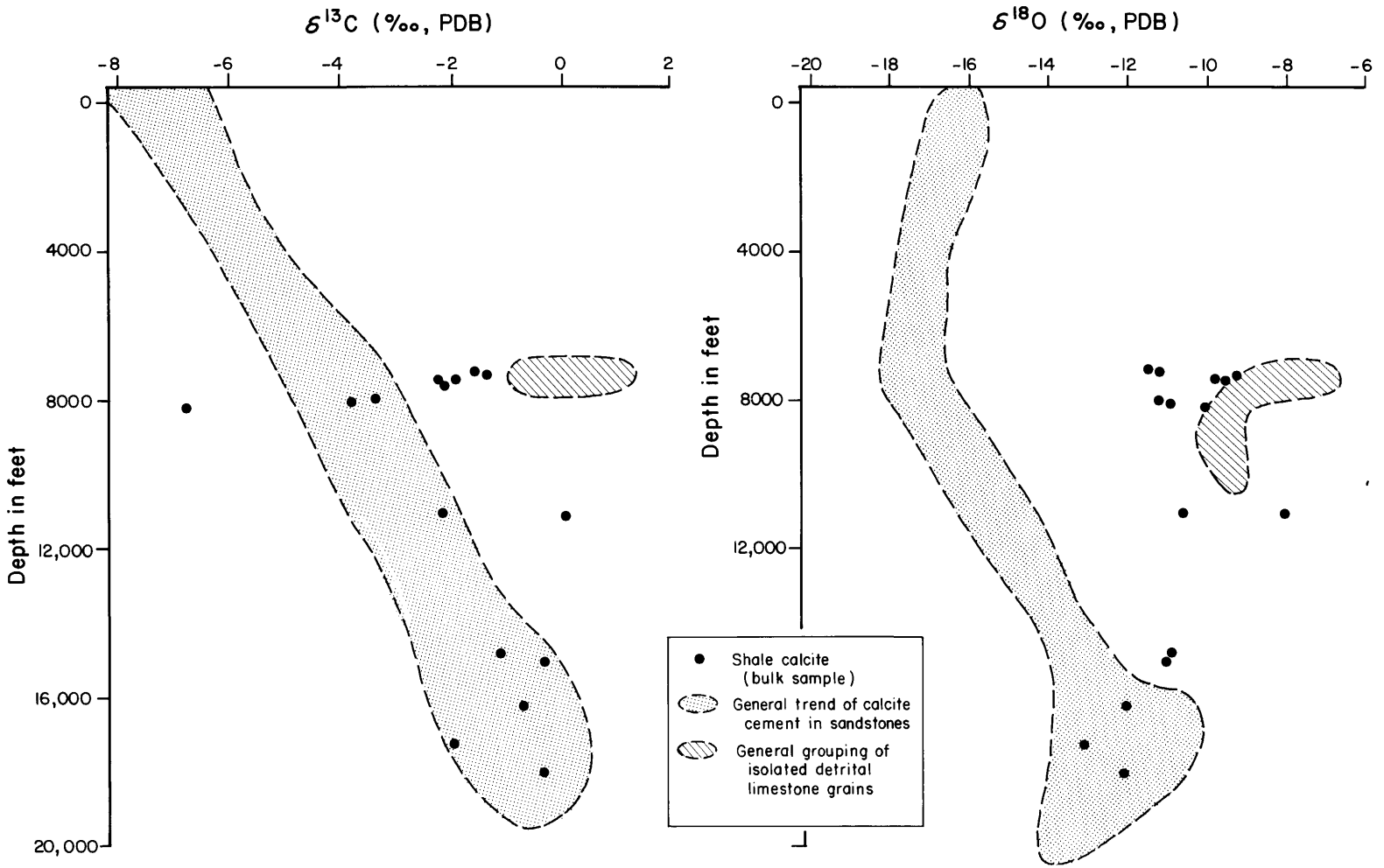

Figure 31--Plots of depth versus $\delta^{13}C$ and $\delta^{18}O$ in bulk calcite (solid dots) of selected shales from Wagon Wheel #1. Data are listed in table 8. For comparison with figure 23, shaded areas indicate general grouping of isolated detrital grains and calcite cements in sandstones.

relatively small number of shale samples coming from a single well whereas the 54 sandstone samples come from five wells. Second, although shale diagenesis varies with time, it takes place in a restricted geochemical environment and is not controlled by wide variety of pore waters with different isotopic compositions. Similar to the sandstones, $\delta^{13}C$ of the shales becomes more positive with increasing depth, but unlike the sandstones $\delta^{18}O$ becomes slightly more negative with increasing depth (fig. 31). There is no correlation between $\delta^{13}C$ and $\delta^{18}O$ for either calcite or dolomite. This implies that there has been little systematic influence of meteoric waters on the diagenesis of the carbonate minerals.

For dolomite, variations in $\delta^{13}C$ and $\delta^{18}O$ as a function of depth are similar to those for the rhombic dolomite group in sandstones (fig. 32). This similarity is not surprising because rhombic dolomite is the most common constituent in the finer grained sandstones and therefore should be the major constituent in shales. The $\delta^{13}C$ of shale dolomite shows no variation with depth and has a range of about 0.9°/oo, which centers near 0.0°/oo, PDB. This suggests that the dolomite either does not recrystallize with burial or if it does recrystallize, it acquires carbon only from local detrital dolomite grains. On the other hand, $\delta^{18}O$ of the dolomite becomes less negative with increasing depth which suggests partial reequilibration at elevated temperatures with pore fluids in the shales.

Organic Carbon

In the Tertiary and Upper Cretaceous rocks of the Green River Basin there is no systematic variation between the stratigraphic units and the amount of total organic carbon (TOC) in shales (Law, 1984). For 257 shale samples from the basin, the average TOC is 2.0 percent (Law, 1984), which is somewhat higher than 1.2 percent - the average for 18 Wagon Wheel shales (table 8). However, this is not surprising because of the small number of Wagon Wheel samples and the variation in TOC between adjacent samples. Because of the relatively low TOC and low volume of shale in the rocks, much of the gas in the sandstones probably originates from the more organic-rich beds associated with coal-bearing zones (Law, 1984).

In the Wagon Wheel shales, the $\delta^{13}C$ of bulk organic matter becomes slightly more negative with increasing depth or stratigraphic age (fig. 33). The largest incremental shift in $\delta^{13}C$ occurs between the Tertiary and Upper Cretaceous samples (between samples 41 and 48, table 8). For five Tertiary samples the average $\delta^{13}C$ is -25.24°/oo, while the average for thirteen Upper Cretaceous samples is -26.08°/oo. This shift of 0.84°/oo, although small, is significantly greater than laboratory error (±0.15°/oo). For all of the samples, the average $\delta^{13}C$ is -25.84, which is consistent with a $\delta^{13}C$ of -25 to -26 (PDB) for humic acids of modern soils (Hoefs, 1980).

The observation that $\delta^{13}C$ of sedimentary organic matter becomes more negative with increasing age has been observed by several workers (Degens, 1969; Oehler and others 1972; Welte and others 1975). This negative shift in

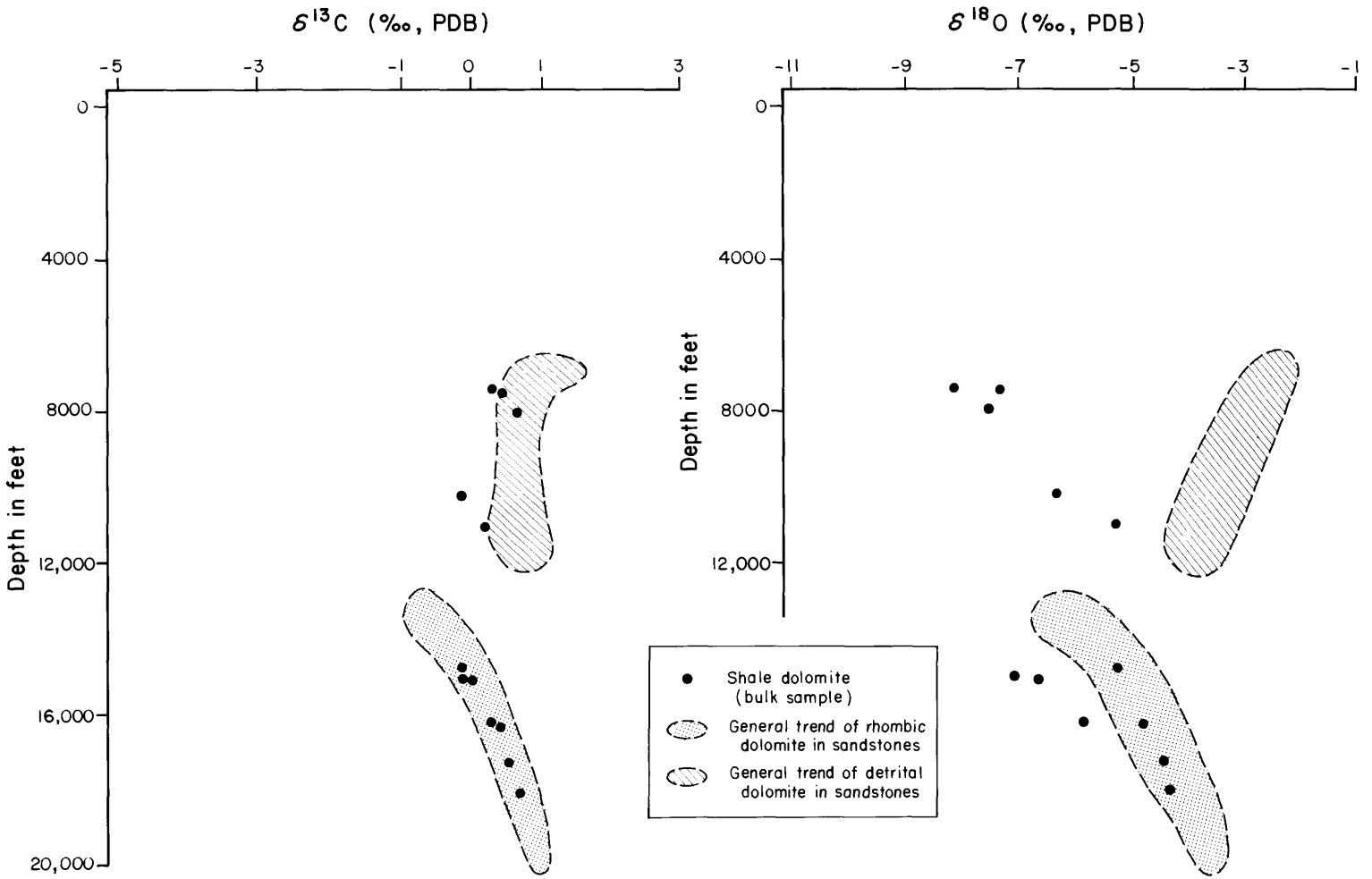

Figure 32--Plots of depth versus $\delta^{13}C$ and $\delta^{18}O$ in dolomite from selected shales. Data are listed in Table 8. For comparison with Figure 29, shaded areas indicate general grouping of dolomites in sandstones.

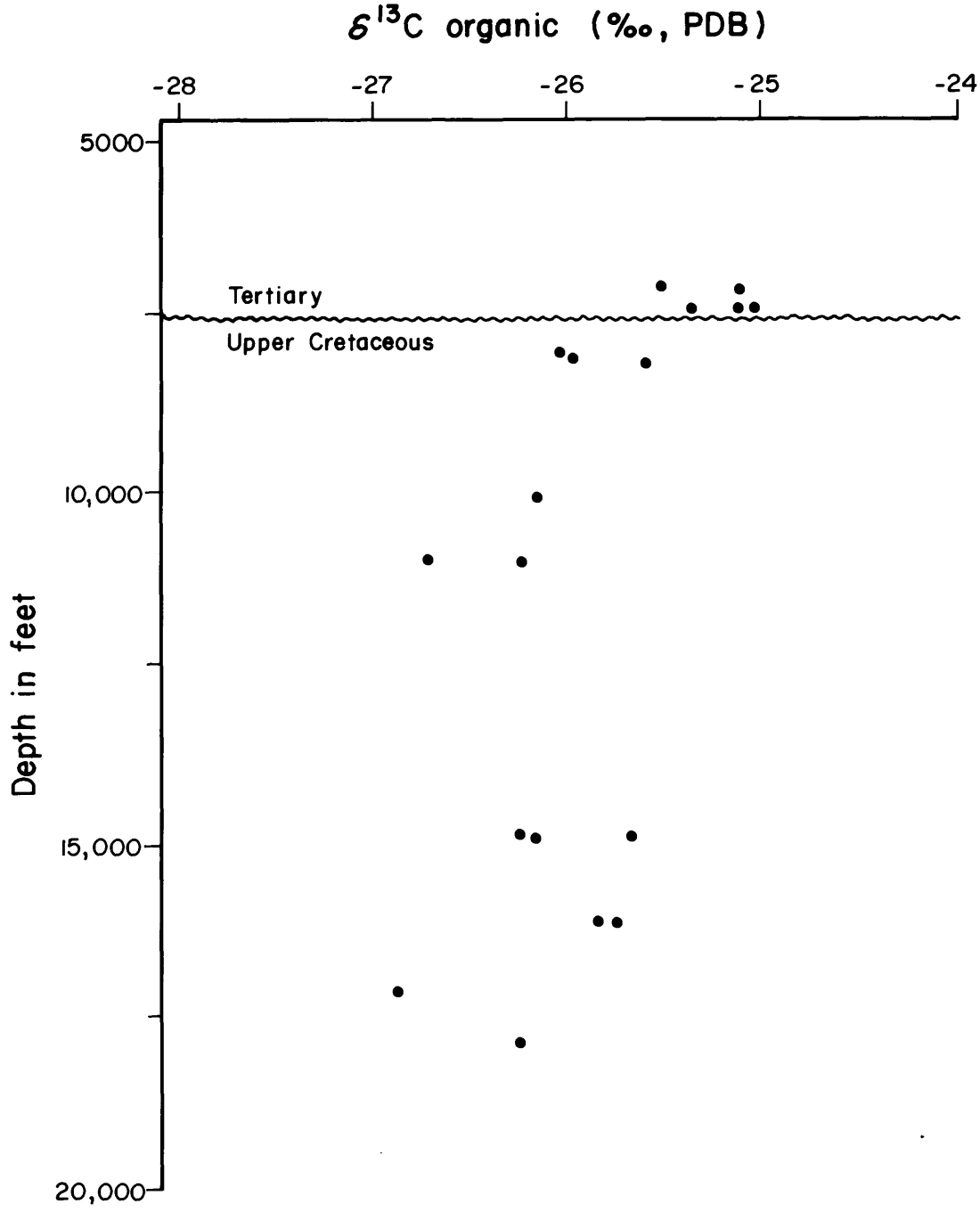

Figure 33--Plot shows depth versus $\delta^{13}C$ of organic carbon in Wagon Wheel #1 shale samples. Data are listed in Table 8. In Wagon Wheel #1, the Tertiary-Cretaceous boundary is at approximately 7,600 ft deep (Law, 1981).

$\delta^{13}C$, which is most prominent in rock from Pennsylvanian to Devonian in age, is thought to reflect the decrease in photosynthetic activity as land plants became less abundant through past geological ages (Welte and others 1975). However, a negative shift in the $\delta^{13}C$ of organic matter reflecting a global decrease in photosynthetic activity has not been reported across the Tertiary-Cretaceous boundary.

The small but significant shift in $\delta^{13}C$ near the Tertiary-Cretaceous boundary in the northern Green River Basin (fig. 33) may reflect changes in the isotopic composition of the carbon in the flora which contributed the organic matter. Wood and most terrestrial plants utilizing the C_4 photosynthetic pathway, have $\delta^{13}C$ values from -22 to -28°/oo PDB (Craig, 1953). On the other hand, plants which utilize C_3 pathways (tropical grasses such as corn, sugarcane, and millet) have $\delta^{13}C$ values from -12 to -14°/oo PDB (Bender, 1968). It is possible that the Cretaceous sediments of the basin received organic matter entirely from C_4-plants, whereas the Tertiary sediments may have received a small amount of organic detritus from C_3-plants. Such a change in the flora not only could cause the observed shift in $\delta^{13}C$ but also would be consistent with the paleoecology of the basin and the evolution of the grasses beginning in the early Tertiary.

There are two reasons why the $\delta^{13}C$ shift in figure 33 is probably not the result of maturation processes. First, a gradual rather than an abrupt shift is expected from maturation effects because maximum burial and temperature occurred after Eocene time (Dickinson and Law in preparation). Second, the release of volatiles during maturation is commonly expected to cause the $\delta^{13}C$ of organic matter to become more positive. However, Jackson and others (1978) note that because of the heterogeneity of organic matter, bulk isotopic analyses of organic carbon in most sedimentary rocks are often difficult to interpret. In view of this, maturation effects cannot be completely ruled out even though the slight but abrupt shift in $\delta^{13}C$ near the Tertiary-Cretaceous boundary is more consistent with a change in the isotopic composition of the flora.

FRACTURES

Subsurface fractures may represent the best chance for non-stimulated or natural recovery of gas from low permeability reservoirs in the northern Green River Basin. Although I found that most of the fractures were filled with cement, there may be large areas in the basin where they are open and without cement. For example, open fractures in the Piceance Basin (west-central Colorado) provide the only explanation for the high permeability that is observed in some of the tight-gas reservoirs (C. W. Spencer oral commun., 1983).

The literature on cement-filled fractures in sedimentary rocks is sparse. Many fractures are obviously associated with structural features, but many are not and lack a clear explanation for their origin. One theory, which lacks evidence, holds that high fluid pressures associated with hydrocarbon

generation induce fracturing. A better understanding of the basic questions concerning the opening and cementation of fractures is necessary before they can be successfully exploited for oil or gas. In addition, if the same fluids migrate through both fractures and sandstones, fracture cementation may be related to some of the cementation in sandstones which causes major reductions in porosity and permeability.

Occurrence

Numerous cement-filled fractures are present in the Wagon Wheel and Wasp wells but are absent in core from the other three wells which were examined for this study. These fractures occur mainly in sandstones and siltstones and are rare in the mudstones. In fact, many of the fractures in the sandstones terminate at the contact with mudstones and clay clasts.

Although they are found only in the overpressured zones, the fractures are not ubiquitous in sandstones and siltstones but occur in small numbers within discrete zones. Fractures may be straight or tortuous and range from microscopic to a half-inch in width. Most fractures are essentially perpendicular to bedding but some thin and discontinuous ones follow bedding surfaces.

The highest concentration of fractures are found in the two deepest intervals of Wagon Wheel core. Steeply dipping beds and seismic data (Martin and Shaughnessy, 1969) indicate that these fractures are associated with faulting. They are oriented in several directions and may cross-cut each other or merge to form a continuous vein. In this respect these fractures are quite distinct from the more solitary ones found in the other cores. These cursory observations suggest that two different mechanisms caused fracturing in the basin. One mechanism is tectonic and the other, for lack of a better hypothesis, may be related to excessive fluid pressures.

Fracture Filling Cements

In decreasing order of abundance, calcite, dickite, barite, and quartz fill the fractures and leave few visible voids. In addition to these minerals, an opaque residue, probably bitumen, coats many of the crystals in the fractures. The distribution of these minerals appears to be partly controlled by the composition of the surrounding formation. For example, calcite-filled fractures are dominant in most of the Cretaceous formations which are litharenites and contain various amounts of carbonate. However, fractures in the Ericson sandstone, which is a quartz arenite, are filled only with dickite and a minor amount of quartz. Presumably, calicte-filled fractures are absent because the Ericson lacks carbonate minerals.

In most of the fractures the distinct crystals, which result from unrestricted growth, suggest precipitation as void-filling cement. For voids to form, the wall-rock must have been well lithified before fracturing. In the larger fractures, single calcite crystals may reach a quarter-inch in

length. There is no evidence for displacive growth such as the kind described by Watts (1978) and Marshal (1982) in fibrous calcite veins.

Although it is impossible to determine paragenesis of unconnected fractures from petrographic evidence, the sequence of mineralization within individual fractures is roughly the same. Where present, quartz lines fracture walls and usually occurs as well developed crystals that protrude into either calcite or dickite (fig. 34a). In most places calcite and dickite interpenetrate (fig. 34b). This obscures their paragenetic relationship because such a contact could result either if dickite precipitated first and calcite precipitated around it or if calcite precipitated first and dickite replaced it. However, quartz which is not penetrated by calcite, is penetrated by dickite in some places (fig. 34c). Although this suggests that dickite may precede calcite cementation, the relationship between quartz and dickite appears to be one of co-precipitation rather than replacement because both minerals have well developed crystals and the quartz does not have a corroded texture. Commonly, barite is found in the middle of fractures and surrounded by calcite, and this relationship suggests that barite is the last mineral to precipitate (fig. 34d). Thus, the general order of precipitation within individual fractures appears to be 1) quartz followed by 2) dickite, 3) calcite, and 4) barite.

One major exception to this sequence has been found in sample F-35 where several void-filling quartz crystals, surrounded by calcite, are clearly the last to precipitate. These quartz crystals are important because they contain fluid inclusions that have yielded a reliable temperature. C. E. Barker (oral commun. 1983), determined a minimum temperature for quartz precipitation of 130°C, which is about 10 degrees hotter than the present temperature at this depth.

Other than a few solution surfaces, the dissolution of fracture-filling calcite has been minor, and there is little textural evidence for recrystallization. However, bitumen, which coats barite and calcite crystals (fig. 34d), indicates that in some places cementation was episodic at least during the precipitation of the bitumen. The equant crystals protruding into cavities suggest that at the time of coring, there may or may not have been active precipitation but that dissolution was not active.

Stable Isotopes

Table 9 gives carbon and oxygen isotopic ratios of calcite sampled from widely spaced and different fractures. To check for homogeneity within fractures, a wide calcite vein was analyzed by microprobe and sampled in five places for isotopic analysis (fig. 35). There is no apparent trend in $\delta^{13}C$ across the fracture but the small difference in $\delta^{18}O$ between the inner and outer parts of the vein is greater than analytical error. Examination of the same fracture using cathodoluminescence shows banding and large color variations that must result from small compositional differences in trace elements, which cannot be detected by the microprobe. This test shows that

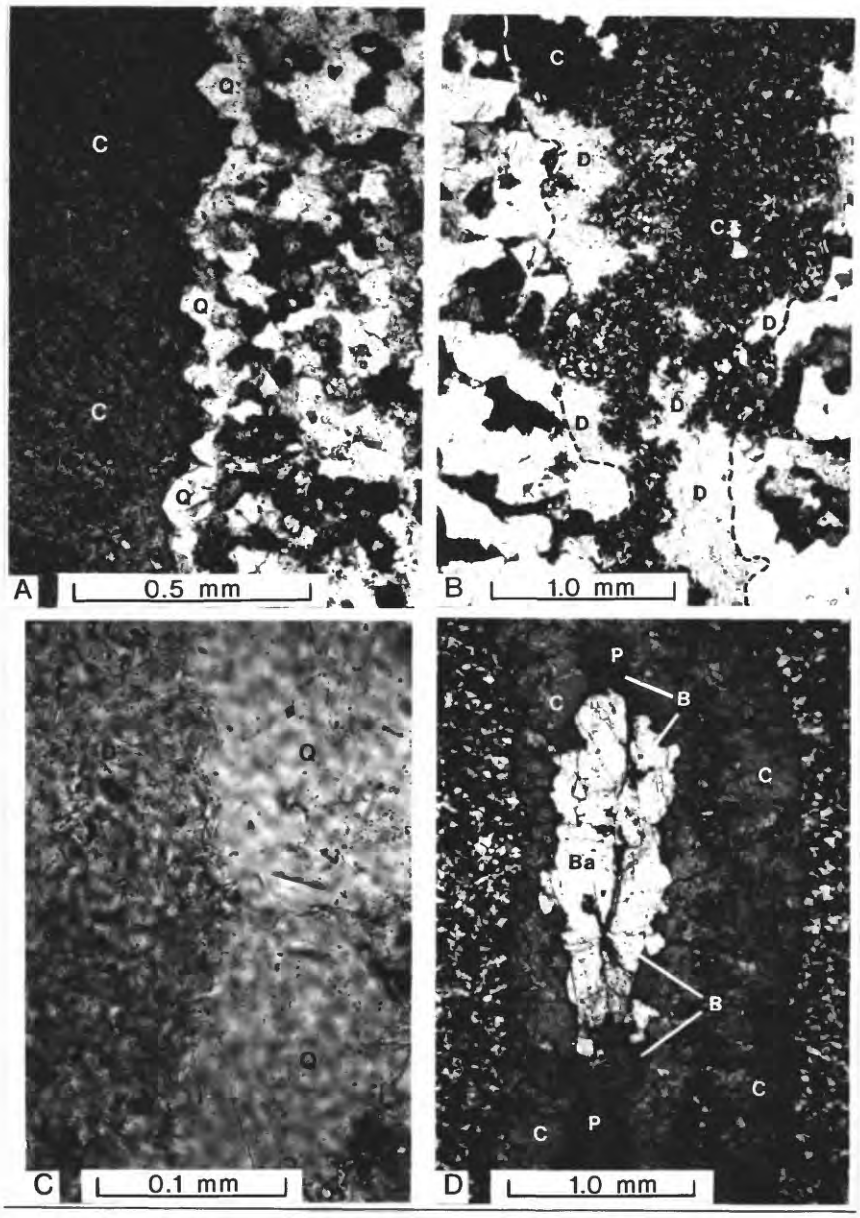

Figure 34--Photomicrographs showing the paragenetic relationships of fracture-filling cements in Wagon Wheel #1 and WASP 1-A. A) Equant crystals of quartz (Q) line fracture walls and suggest precipitation in a void prior to calcite (C, stained pink) cementation. B) Interpenetrating contact between calcite (C, stained pink), which appears dark, and "books" of dickite (D) crystals which are light in color. Dashed lines mark the boundary of the fracture walls. C) Intergrowth of quartz (Q) and dickite (D). Quartz lines the walls of the fracture. "Books" of dickite crystals are surrounded by quartz. (Plane light.) D) Barite (Ba) is surrounded by calcite (C, stained pink) and fills the center of the vein. Cavities (P, blue epoxy) are lined with bitumen (B). Equant crystals of calcite protrude into the cavities.

Table 9.--Calcite cement in fractures

Well	Sample Number	Depth (feet)	Temperature (°C)	Isotopic Ratios (°/oo PDB) $\delta^{13}C$	$\delta^{18}O$
	F-6	8,096	67	-5.50	-15.83
	60	8,128	67	-4.85	-16.19
	69	8,944	73	-5.05	-14.89
	F-11	8,959	73	-5.49	-15.32
	F-14	10,155	81	-4.04	-13.01
EPNG	F-18	10,235	82	-3.96	-12.88
Wagon	F-19	10,993	87	-3.19	-13.07
Wheel #1	F-21	11,000	87	-3.33	-12.66
	F-35	16,119	122	-1.67	-15.32
	167	16,121	122	-0.92	-14.75
	168	17,169	129	-1.26	-14.25
	171	17,176	129	-1.43†	-14.75†
	172	17,179	129	-1.48	-14.69
	F-39	17,960	134	-1.37	-15.11
	F-40	17,966	134	-1.12	-14.42
	26	11,333	107	-7.14	-17.77
	65	11,592	110	-7.34*	-17.63*
	216	13,026	122	-1.79	-16.72
	275	13,433	126	-1.97*	-16.10*
	288	13,482	126	-1.69	-15.29
Belco	304	13,591	127	-0.75	-16.47
WASP 1-A	307	13,612	127	-0.68	-16.30
	354	13,987	131	-0.82	-16.15
	360	14,032	131	-2.15*	-15.55*
	363	14,043	131	-1.77	-15.19
	394	14,193	132	-2.63	-15.64
	396	14,198	132	-2.69*	-16.52*

* Unpublished data from Donald L. Gautier
† Average of 5 values

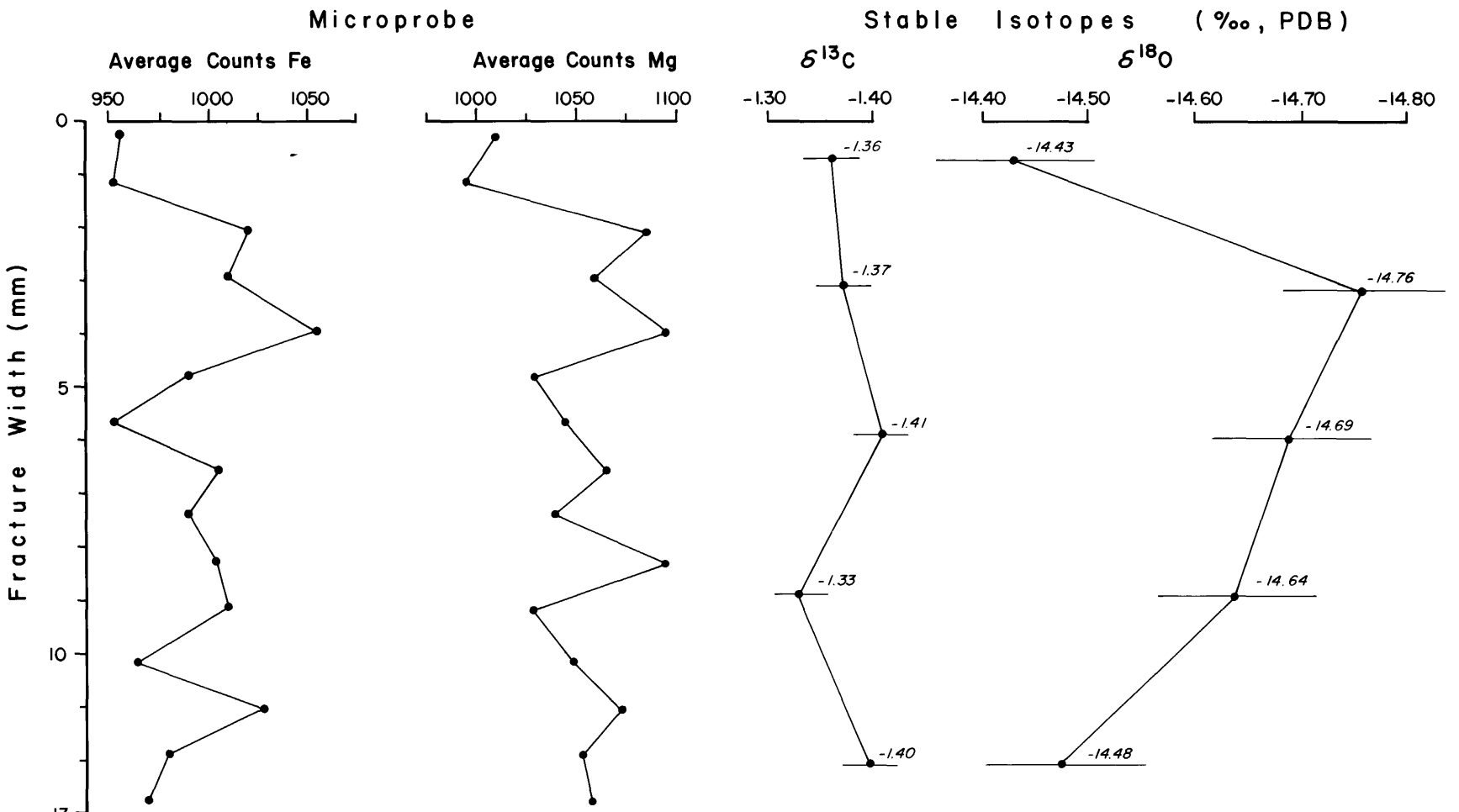

Figure 35--Points indicate trace element and isotopic analyses of calcite across a fracture (Wagon Wheel 171) 13 mm wide. Microprobe points represent the average count for two 20 second counting periods. At these low concentrations of Mg and Fe, error is ± 10% of the average count value, and therefore the variations are not significant. Error bars indicate that the shift in $\delta^{18}O$ is significant.

variations in isotopic compositions between fractures are much greater than variations within fractures.

Interpretations

Isotopic values between fracture calcites and sandstone calcites are remarkably similar (fig. 36). This similarity and the apparent control by the composition of the surrounding formation on fracture mineralogy, strongly suggest that local wall-rock materials were the source for fracture filling cements. Fracture calcites would have a different isotopic composition if transport fluids came either from deep seated waters or from meteoric waters. In general, $\delta^{13}C$ and $\delta^{18}O$ of the fracture calcites are more negative than the bulk analyses of the sandstone calcites which include the isotopically heavy, detrital limestone grains. However, sandstone cements and fracture calcite have roughly the same isotopic composition.

Among closely spaced fractures, significant variations of $1^{o}/oo$ for $\delta^{18}O$ and by $0.2^{o}/oo$ for $\delta^{13}C$ indicate that many fractures were not connected during cementation. An extreme example of this is the difference in isotopic composition between samples F-35 and 167 (table 9), which are only 2 feet apart. Variations on this scale are not probable if all the fractures opened at the same time and conducted the same fluid. Therefore, it is reasonable to assume that the fractures opened at different times because if they all opened at the same time, they probably would have been connected and conducted the same fluid. The slight decrease in $\delta^{18}O$ towards the center of a fracture can only result from changes in temperature or isotopic composition of the waters or a combination of both. However, changes in the $\delta^{18}O$ of the waters seems least likely because there is no corresponding change in $\delta^{13}C$. Thus, the decrease in $\delta^{18}O$ suggests that calcite may have precipitated at a slightly higher temperature in the center of some fractures.

The temporal relationship of hydrocarbon generation to fracture opening is of major importance if the fractures are to be considered as potential reservoirs. Although many of the fractures opened and filled episodically, several lines of reasoning suggest that opening, as a whole, is a recent feature and not a product of Laramide tectonism. First, it is clear that the sandstones were well lithified before fracturing and that the fractures did not form during early diagenesis. Second, fluid inclusion evidence, although sparse, suggests that precipitation of the latest cement occurred near present temperatures or slightly hotter. Third, and perhaps the most compelling evidence for recent fracturing, is the existance of cavities which appear to be in the process of filling with cement.

The rate at which the fractures filled depended largely on the composition and flow of fluids. Two things suggest that filling was probably a rapid geological process. First, there is no petrographic evidence for repeated dissolution and precipitation which might be expected if the fractures filled slowly. Second, the small elemental variations in calcite within a single fracture suggest that precipitation occurred under nearly

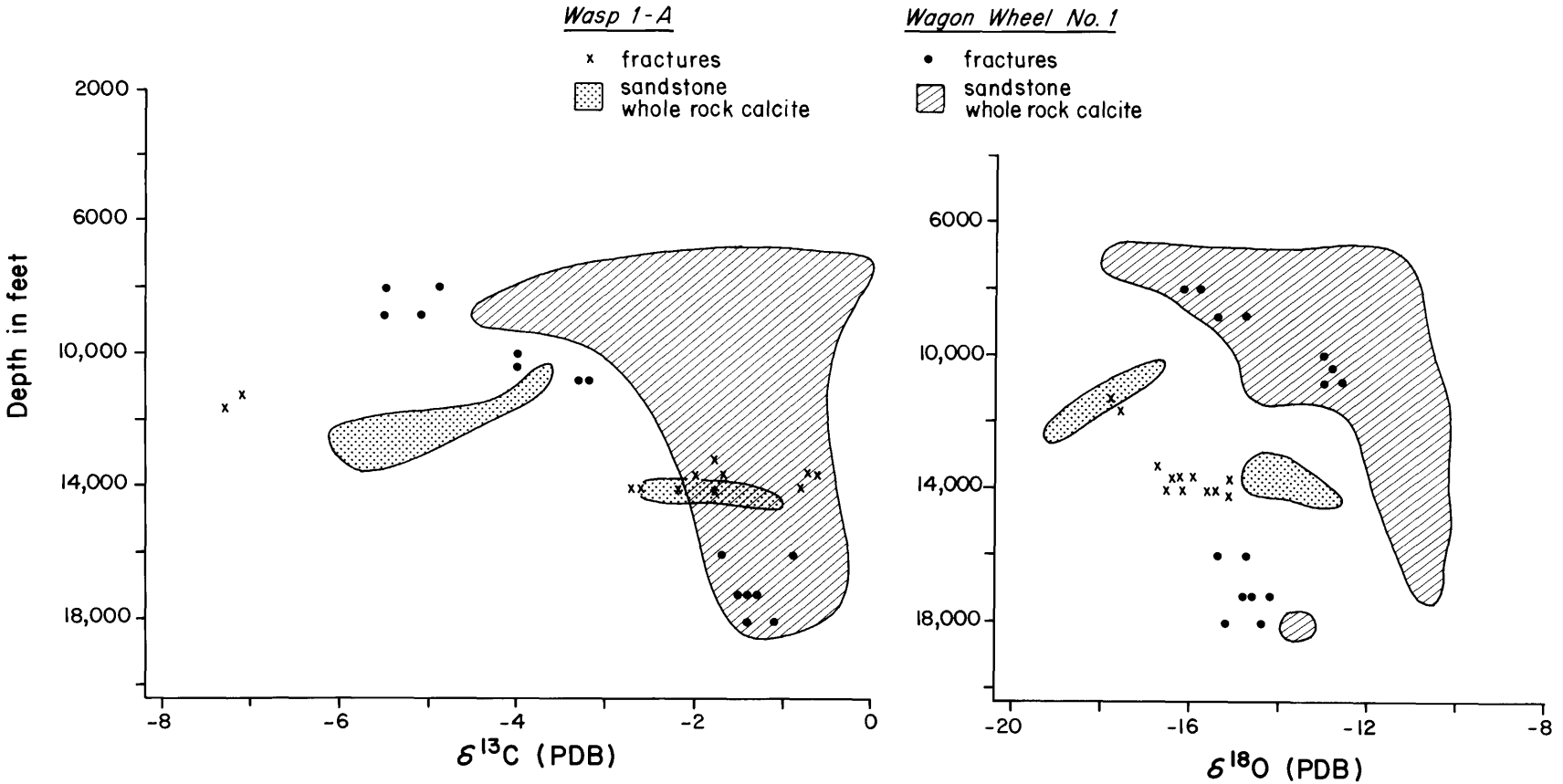

Figure 36. Plots of depth versus $\delta^{13}C$ and $\delta^{18}O$ in fracture-filling calcite cement from Wagon Wheel #1 and WASP 1-A. Data are listed in Table 9. For comparison, shaded areas indicate general grouping of calcites in sandstones, Figure 23.

constant conditions. Any geological changes that could alter these conditions must have occurred at a rate slower than fracture filling.

In summary, isotopic and petrographic evidence indicate that fracturing in the Upper Cretaceous rocks is a recent event and that precipitation of cement is a relatively rapid geologic process. However, these observations pose additional problems. If fracturing is recent and methane is currently being generated, then these concurrent processes imply that the fractures should make good reservoirs. But at present, there is no evidence from drilling tests that natural fractures enhance reservoir properties of overpressured sandstones. The reason may be that fractures provide only a small, and temporary reservoir before they are filled with cement. Surprisingly, the presence of natural gas does not inhibit cementation. Additional evidence for the presence of gas during cementation is illustrated by the abundant methane inclusions found in all of the fracture filling calcites (C. E. Barker oral commun., 1983). Another problem concerns the apparent rapid rate at which fractures fill with cement. The isotopic composition of fracture calcite suggests migrating fluids aquired the materials, which precipitated in the fractures, from local sandstones. It is paradoxical that seemingly large volumes of solute are needed to fill the fractures with cement, yet the fractures reside in sandstones where the flow rates are so slow that diffusion may be the dominant process.

MODELS FOR ISOTOPIC FRACTIONATION

During chemical reactions, differences in mass among stable isotopes cause a redistribution or fractionation of these atoms in the molecules of chemical substances. Both oxygen and carbon isotopes are fractionated by a variety of natural processes, which may work individually or collectively. Fractionation by the process of isotope exchange--a special case of chemical equilibrium--is temperature dependent and plays a major role in determining the oxygen isotopic composition of mineral phases and pore fluids during burial. On the other hand, large kinetic fractionations caused by living organisms can mask the effects of temperature on carbon isotope fractionation. Consequently, in carbonate minerals carbon isotopes often reveal the source of carbon, whereas oxygen isotopes are informative about temperatures of precipitation.

Recent evidence indicates that carbonate diagenesis takes place by dissolution and reprecipitation and not by solid-state diffusion (Land, 1980). Because of this, stable isotopes in authigenic carbonate minerals contain a history of the fluid composition and temperature of precipitation. In many studies, different generations of calcite cement, which have been fortuitously preserved, show a variety of trends in oxygen and carbon isotopic ratios. The principles of isotope fractionation can be used to interpret these trends and shed light on the isotopic composition of the fluids and temperature of precipitation.

In this section, several models will be used to demonstrate how the oxygen isotopic composition of calcite varies depending on the oxygen isotopes in the fluid and the temperature of precipitation. These models will be used for the interpretation of isotopic trends in the northern Green River Basin.

Oxygen

The oxygen isotope exchange reaction between calcite and water is

$$CaC^{16}O_3 + 3H_2{}^{18}O \rightleftarrows CaC^{18}O_3 + H_2{}^{16}O.$$

From experimental work, O'Neil and others (1969) established a fractionation equation that describes the distribution of oxygen isotopes in this reaction. It is

$$10^3 \ln \alpha_{\text{calcite-water}} = 2.78(10^6\ T^{-2}) - 3.39,$$

where T is temperature in degrees Kelvin and

$$\alpha_{\text{calcite-water}} = \frac{\delta^{18}O_{\text{calcite}} + 1000}{\delta^{18}O_{\text{water}} + 1000}.$$

This equation shows the relationship between the temperature of precipitation, the $\delta^{18}O$ of calcite, and $\delta^{18}O$ of solution from which the calcite precipitates. If two of these variables are known the third may be calculated. To simplify the equation, approximate values of $10^3 \ln \alpha$ may be found by the difference in δ values. This is because of the fact that $10^3 \ln (1.00x) \simeq x$. For example, if $\delta^{18}O_{\text{calcite}} = 10$ and $\delta^{18}O_{\text{water}} = 5$ then $\alpha_{\text{calcite-water}} = 1.00489$ and $10^3 \ln \alpha_{\text{calcite-water}} = 4.96$. The value 4.96 is close to $\delta^{18}O_{\text{calcite}}$ minus $\delta^{18}O_{\text{water}}$ or 5. This approximation is within experimental error and therefore can be used for most applications of the equation.

Caution must be used in applying the experimental data of O'Neil and others (1969) because there is no real evidence that natural systems represent the equilibrium described by the above equation. It is only an assumption that isotopic equilibrium exists between calcite and water. In addition because dissolved salts affect oxygen isotope activity in water, many of the experimentally observed mineral-water fractionations may be too high by 0.3°/oo to 1.0°/oo (Truesdell, 1974).

The simplified oxygen fractionation equation (from the O'Neil and others 1969 equation) for calcite and water is

$$\delta^{18}O_{calcite} - \delta^{18}O_{water} = 2.78(10^6\ T^{-2}) - 3.39.$$

Although mostly used for geothermometry, the equation is useful to this discussion because it demonstrates that the $\delta^{18}O$ value of calcite ultimately depends only on $\delta^{18}O_{water}$ and temperature. By holding one of these three variables constant and substituting reasonable values for the second, the third variable may be calculated. Plots of the substituted values versus the calculated values yield three end-member models (fig. 37). These models illustrate the changes in $\delta^{18}O_{water}$ and temperature that are necessary to cause shifts in the oxygen isotopic composition of successive generations of calcite cement. They do not deal with the other geological factors that control $\delta^{18}O_{water}$ and temperature.

A - Constant Temperature

At constant temperature, calculated $\delta^{18}O$ values for calcite are directly proportional to the substituted $\delta^{18}O$ values of water (fig. 37a). Below 500°C, calcite will always be enriched in ^{18}O with respect to the water from which it precipitates.

For a given sedimentary formation, long-term constant temperature could be a difficult condition to maintain, but in veins and fractures the geologically rapid precipitation of calcite should occur at nearly constant temperature. If vein-filling calcite is assumed to have precipitated as a single event, then variations in $\delta^{18}O$ of the calcite can be attributed mostly to variations in the $\delta^{18}O$ of the formation water. Marshall (1982) suggests that the variations in $\delta^{18}O$ of vein-filling calcites from Jurassic shales in Britain resulted from pore water evolution.

B - Constant $\delta^{18}O_{water}$

If $\delta^{18}O$ of water is held constant, then with increasing temperature the $\delta^{18}O$ values of successive calcite precipitates become more negative; in other words, the calcites become lighter or enriched in ^{16}O (fig. 37b). Numerous studies (Milliken and others 1981; Dickson and Coleman, 1980; Matter and others 1975; Lawrence, 1973) have found a general decrease in $\delta^{18}O$ of bulk carbonates with increasing temperature or depth of burial. For this to happen, figure 37b would suggest that $\delta^{18}O$ of the water remained relatively constant as successive generations of calcite precipitated at higher temperatures.

C - Constant $\delta^{18}O_{calcite}$

For $\delta^{18}O$ of precipitated calcite to remain the same with increasing temperatures, figure 37c shows that $\delta^{18}O_{water}$ must become more positive; that is the water must become heavier or enriched in ^{18}O. In limestones or quartz-

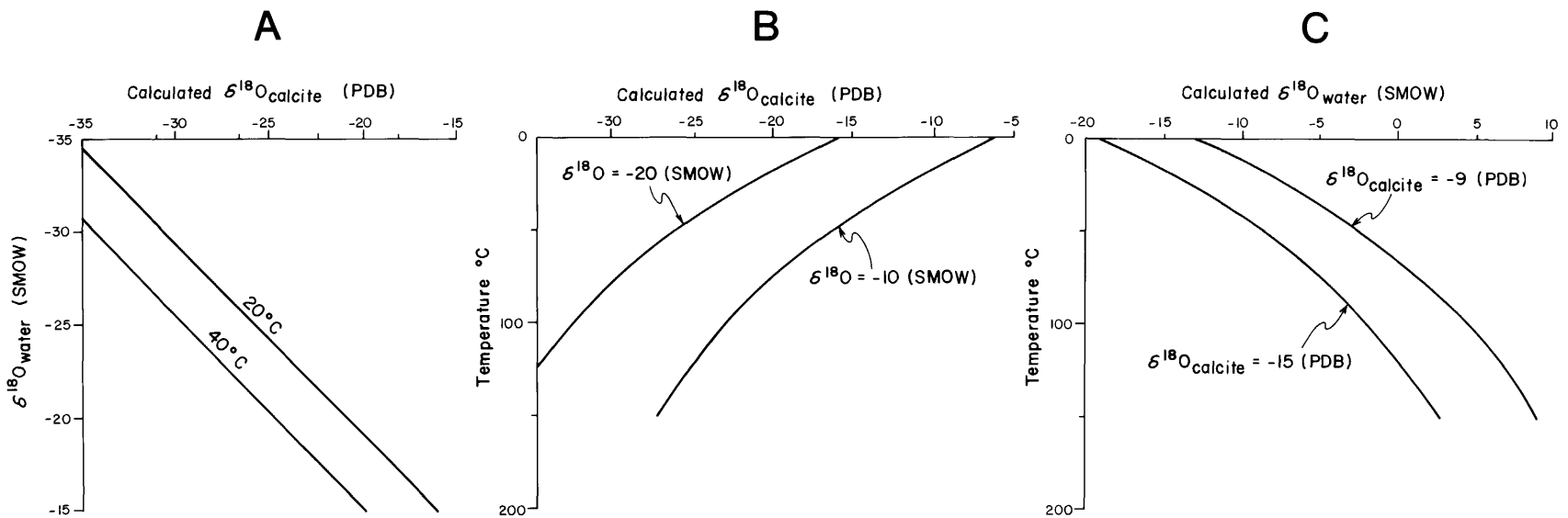

Figure 37--Plots were constructed by substituting values of interest on the abscissa and using the equation $\delta^{18}O_{calcite}-\delta^{18}O_{water} = 2.78(10^6T^{-2}) - 2.89$ from Friedman and O'Neil (1977) to calculate: A) $\delta^{18}O_{calcite}$ at constant temperature, B) $\delta^{18}O_{calcite}$ from constant $\delta^{18}O_{water}$, and C) $\delta^{18}O_{water}$ from constant $\delta^{18}O_{calcite}$. Note that $\delta^{18}O_{calcite}$ is plotted in °/oo, PDB after conversion from °/oo, SMOW.

rich sandstones, migrating pore waters should become enriched in ^{18}O with increasing depth. In a classic study covering four basins, Clayton and others (1966) found that $\delta^{18}O$ of formation waters fell to within 2°/oo of an equilibrium line constructed for a $\delta^{18}O_{calcite} = -6.4$ (PDB) at all observed temperatures. They suggested that the major cause of ^{18}O enriched waters was limestone-water equilibration at elevated temperatures.

Because the above models are end-members, complexities arise when the variables that were held constant are allowed to change. In model B, if the $\delta^{18}O$ composition of the water were changing with temperature, then the calculated $\delta^{18}O_{calcite}$ would deviate from the equilibium line. The relative amount of change between variables is an important consideration. For example, with increasing depth or temperature in the subsurface, assume that calcite dissolves and reprecipitates so the bulk of it is always near isotopic equilibrium with surrounding pore fluids. If $\delta^{18}O_{calcite}$ is found to become more negative by 1°/oo per 10°C, the shift in $\delta^{18}O_{water}$ must be relatively small (fig. 38, curve A). On the other hand, if $\delta^{18}O_{calcite}$ becomes more positive by 1°/oo per 10°C, the shift in $\delta^{18}O_{water}$ with increasing depth must be large (fig. 38, curve B). Respectively, curves A and B of figure 38 are somewhat analogous to models B and C.

Controls on $\delta^{18}O_{water}$

The main factors that determine $\delta^{18}O$ of the pore waters are as follows: 1) the initial $\delta^{18}O$ of the water, 2) the $\delta^{18}O$ of the solids with which pore fluids may exchange, 3) the extent of equilibration between water and rock, and 4) the temperature of equilibration.

The initial $\delta^{18}O$ of the pore water depends on the environment in which the sediments are deposited. Marine waters have $\delta^{18}O$ values close to 0°/oo (SMOW), whereas the $\delta^{18}O$ of rainwater normally is determined by a Rayleigh distillation. This process is a vapor-liquid fractionation that occurs during evaporation and condensation of atmospheric moisture (for discussion see Hoefs, 1980 p. 103 or Drever, 1982 p. 338). Initially, pore waters react with the enclosing sediment, but later during burial diagenesis and uplift they are mixed with water from different sources. The amount of mixing depends on the hydrology of the basin, and the porosity and permeability of the sediment.

The initial $\delta^{18}O$ of the solids depends on the source material prior to deposition. After deposition, these solids not only dissolve and contribute oxygen to the pore waters but also play a major part in controlling the type of authigenic minerals that precipitate. In a closed system, modifications to the $\delta^{18}O$ of the pore waters result from the isotopic fractionation that occurs during the precipitation of authigenic minerals. The proportions and types of the solids are also important. For example, isotopic exchange, which proceeds by dissolution and precipitation, is much more rapid between calcite and water than between silicate and water (Clayton and others 1966).

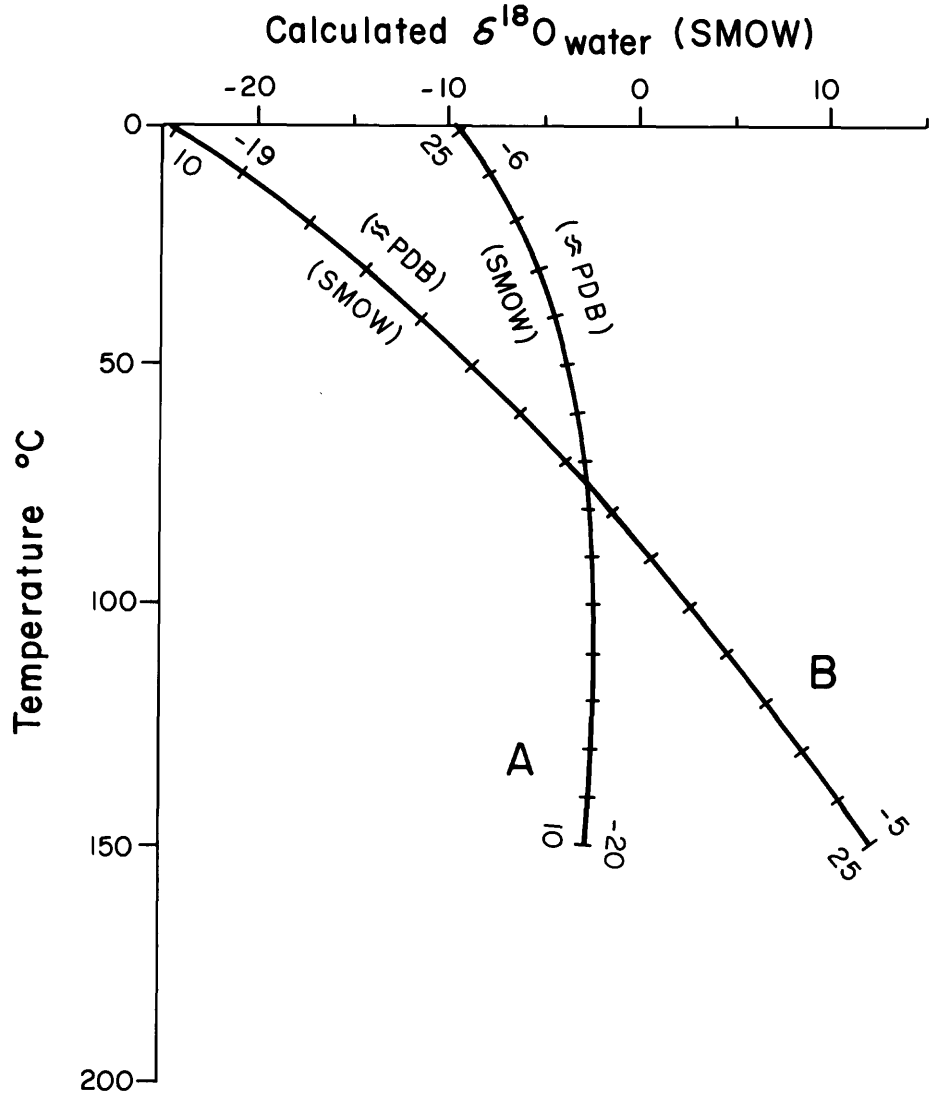

Figure 38--Plots shows relative amounts of change between variables in the equation: $\delta^{18}O_{calcite} - \delta^{18}O_{water} = 2.87(10^6T^{-2}) - 2.89$ (Friedman and O'Neil, 1977). A) If $\delta^{18}O_{calcite}$ becomes more negative by $1^o/oo$ per 10^oC then the shift in $\delta^{18}O_{water}$ must be small. In this case the water/rock ratio is high. B) If $\delta^{18}O_{calcite}$ becomes more positive by $1^o/oo$ per 10^oC there would be a large shift in $\delta^{18}O_{water}$. The water/rock ratio would be low in this case.

The magnitude of oxygen isotope fractionation between two minerals in isotopic equilibrium depends on temperature. Fractionation factors become smaller with increasing temperature. Thus, at low temperatures there will be a large difference in $\delta^{18}O$ between an authigenic mineral and the water from which it precipitates but at high temperatures there will be a smaller difference.

Shifts in $\delta^{18}O_{water}$ also depend on the mass ratio of water to rock. If water is flowing rapidly through an aquifer, the shift in $\delta^{18}O_{water}$ is likely to be small. Conversely, if pore water is almost stagnant, the effective water-rock ratio will be small, and large shifts in $\delta^{18}O_{water}$ can be expected. Thus, curve A (fig. 38) is more likely to result where the water-rock ratio is large and mineral-water exchange has little effect on the isotopic composition of the pore waters. Curve B (fig. 38) would be likely to result where pore waters are stagnant. This model strongly implies that in open flow systems, the $\delta^{18}O$ of successive calcite precipitates becomes more negative with increasing temperature, but in restricted systems the $\delta^{18}O$ of calcites should become more positive with increasing temperature.

As discussed previously, the extent to which diagenetic reactions modify the $\delta^{18}O$ of pore waters depends largely on the volume of water to rock. Variable flow rates and mixing of large volumes of subsurface waters make prediction of $\delta^{18}O_{water}$ virtually impossible for open hydrochemical systems. However, in closed systems, known fractionation equations for a variety of mineral-water reactions can be used to predict $\delta^{18}O_{water}$ at temperatures of interest.

In the northern Green River Basin the $\delta^{18}O$ of near-surface waters is known but that of deeper waters is not. In this case, predictive modeling of $\delta^{18}O_{water}$ may offer a partial solution. With increasing depth, the decrease in porosity and permeability (figs. 4-7) indicates a parallel decrease in fluid movement. By definition, the overpressured zone provides compelling evidence for a highly restricted hydrochemical system, which for the purpose of modeling is assumed to be closed.

Modeling of $\delta^{18}O_{water}$

In a closed system, the change in $\delta^{18}O$ of pore waters caused by diagenetic reactions at elevated temperatures can be determined by the simultaneous solution of a mass balance equation for oxygen and an isotopic fractionation equation for oxygen. If the mole fraction (x_1) and isotopic composition of a component of the sediment (δ_a) and of the pore water (δ_b) prior to diagenesis are known, as well as the isotopic fractionation factor (α_b^c), between the authigenic precipitate and the pore water, the $\delta^{18}O$ of the authigenic precipitate (δ_c) and the pore water (δ_d) may be calculated as follows (Lawrence and others 1976):

$$\delta_d = \frac{x_1\delta_a + (1 - x_1)\delta_b - 1000x_1(\alpha_d^c - 1)}{x_1(\alpha_d^c - 1) + 1}$$

$$\delta_c = 1000(\alpha_d^c - 1) + \alpha_d^c \cdot \delta_d$$

where

x_1 = mole fraction of oxygen in the solid phase before alteration.
$(1-x_1)$ = mole fraction of oxygen in the pore water phase.
δ_a = $\delta^{18}O$ of the solid phase before alteration.
δ_b = $\delta^{18}O$ of the pore water before alteration.
δ_c = $\delta^{18}O$ of the precipitated phase.
δ_{d_c} = $\delta^{18}O$ of the pore water after alteration.
α_d = fractionation factor between the precipitated phase and pore water.

With these equations, two models (fig. 39) are constructed to simulate changes in $\delta^{18}O_{water}$ that occur as a result of diagenetic reactions in the deep sandstones of the basin. Three basic diagenetic reactions, which from petrographic evidence seem likely to occur, are used in the models to modify $\delta^{18}O_{water}$. These reactions include: 1) the recrystallization of detrital calcite and calcite cement, 2) the dissolution of detrital quartz and silicified volcanic rock fragments (VRF) with subsequent reprecipitation of chert and quartz cement, and 3) the precipitation of illite/smectite with components derived from shale (detrital quartz, detrital feldspar, and detrital clay). It is emphasized that the equations used for modeling consider only the transfer of oxygen molecules in the three diagenetic reactions. In addition, each model requires a closed system (no input of external oxygen) and assumes complete isotopic equilibration of the authigenic products with the pore fluids. Clearly, an open hydrochemical system would make it impossible to calculate the input variables δ_b and x_1.

Figure 39 is a schematic illustration of how δ_c and δ_d are calculated in the models. Although calcite is used as an example in the figure, quartz and illite/smectite are treated in the same manner. Values of the variables used for modeling are listed in table 10. The sequence in both models is started with measured variables at the surface. Calculated variables are then used at each successive increment of depth. Model A used the same δ_a for dissolution and precipitation at each increment of burial, but Model B used the preceding δ_d (authigenic precipitate) for δ_a at each step of dissolution and precipitation. Petrographic evidence suggests that both pathways of dissolution and preciptation occur at least for calcite.

Curves in figure 40 illustrate the results of modeling by showing the values of δ_d and δ_c as a function of depth. As burial diagenesis proceeds with increasing temperature, ^{18}O is transferred to the pore waters while the authigenic products become slightly depleted. Although the models use one

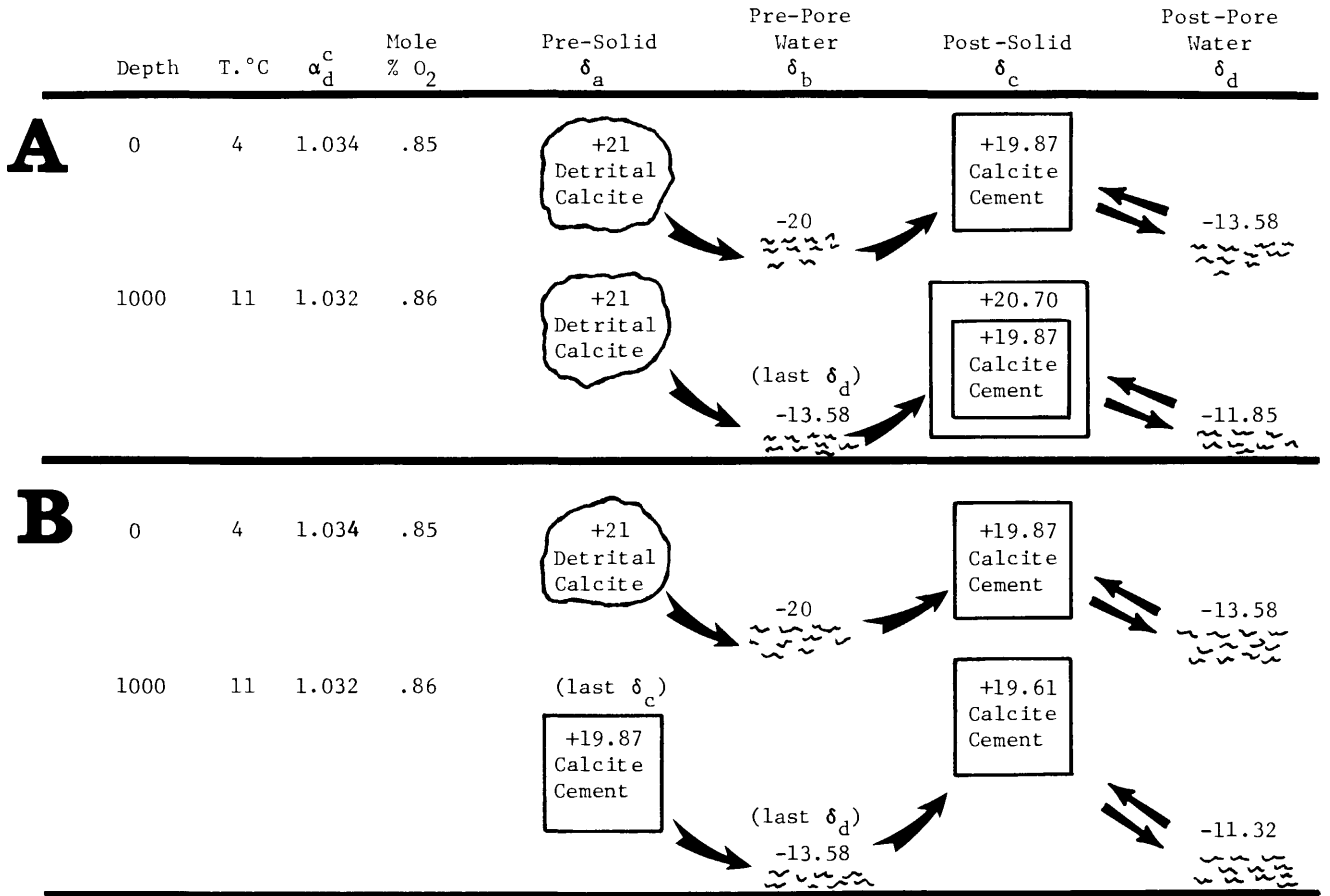

Figure 39--Schematic diagram of two closed system models used for material balance calculations. Values of δ_a, δ_b, δ_c, δ_d are $\delta^{18}O$ in °/oo, SMOW. See text for definitions. Models assume equilibrium between δ_c and δ_d at each depth. In this example the calcite-water reaction is considered, but the other diagenetic reactions are similar. In model A, detrital calcite supplies the only oxygen to the pore water. In model B, detrital calcite makes the initial contribution of oxygen to the pore water but authigenic calcite contributes the remainder.

Table 10.--Variables used for material balance equations

Variable		Equation or Value	Remarks
Temperature gradient used to calculate α_d^c.		$T^oC = 4 + .0072$ (Depth in Feet.)	Average temperature gradient in northern Green River Basin calculated from Law and Smith (1983).
Isotope fractionation equations used to calculate α_d^c (fractionations between authigenic phase and the pore water).		$10^3 \ln \alpha_{Calcite-Water} = 2.78(10^6 T^{-2}) - 2.89$	Friedman and O'Neil, 1977; T = temperature in ^oK.
		$10^3 \ln \alpha_{Quartz-Water} = 3.38(10^6 T^{-2}) - 2.90$	Friedman and O'Neil, 1977
		$10^3 \ln \alpha_{I/S-Water} = (2.43 + .24E)(10^6 T^{-2}) - 4.82$	Yeh and Savin, 1977; I/S = Illite-smectite; E = % expandability.
δ_a	($\delta^{18}O$ of the solid phase before diagenetic alteration)	Detrital carbonate = $+21^o/oo$	Average value for detrital carbonate grains in the sandstone.
		Detrital quartz = $+20^o/oo$ (50% VRF quartz and 50% igneous quartz)	Volcanic rock fragment (VRF) Quartz = $+29^o/oo$, an estimate of silicified VRF's by near-surface water ($\delta^{18}O = -7$ at 20^oC) in the in the Eocene and Oligocene; Igneous quartz = $+11^o/oo$ (Hoefs, 1980).
		Shale = $+18.6^o/oo$	Average of 2 shales from the Green River Formation (Savin and Epstein, 1970). Highly positive values may reflect isotopic exchange with highly negative $\delta^{18}O$ waters of the area.
δ_b	($\delta^{18}O$ of pore water before alteration)	Northern Green River Basin average near-surface water = $-20^o/oo$	Average of 7 samples (Table 1); Pliocene and older rocks probably had more positive pore water.
x_i	(Mole frsction of oxygen in solid before alteration)	.85 to .95 (20% to 7% porosity, decreases with depth)	At any porosity x_i has roughly the same value for a diverse group of minerals. Values estimated from Table 1 of Lawrence et al, (1976). The x_i is the same for each reaction but changes with porosity.
$(1-x_i)$	(Mole fraction of oxygen in pore water)	.15 to .05	Values would be close to 1 if porosities were high.
δ_c	($\delta^{18}O$ of the precipitated phase)	Calculated values plotted versus depth in Figure 40.	Model B uses these values to calculate a "new" pore water at each depth.
δ_d	($\delta^{18}O$ of pore water after alteration	Calculated values plotted versus depth in Figure 40.	By definition of a closed system, each "old" δ_d value is used to calculate the "new" one.

Note: All isotope values are $^o/oo$ relative to SMOW.

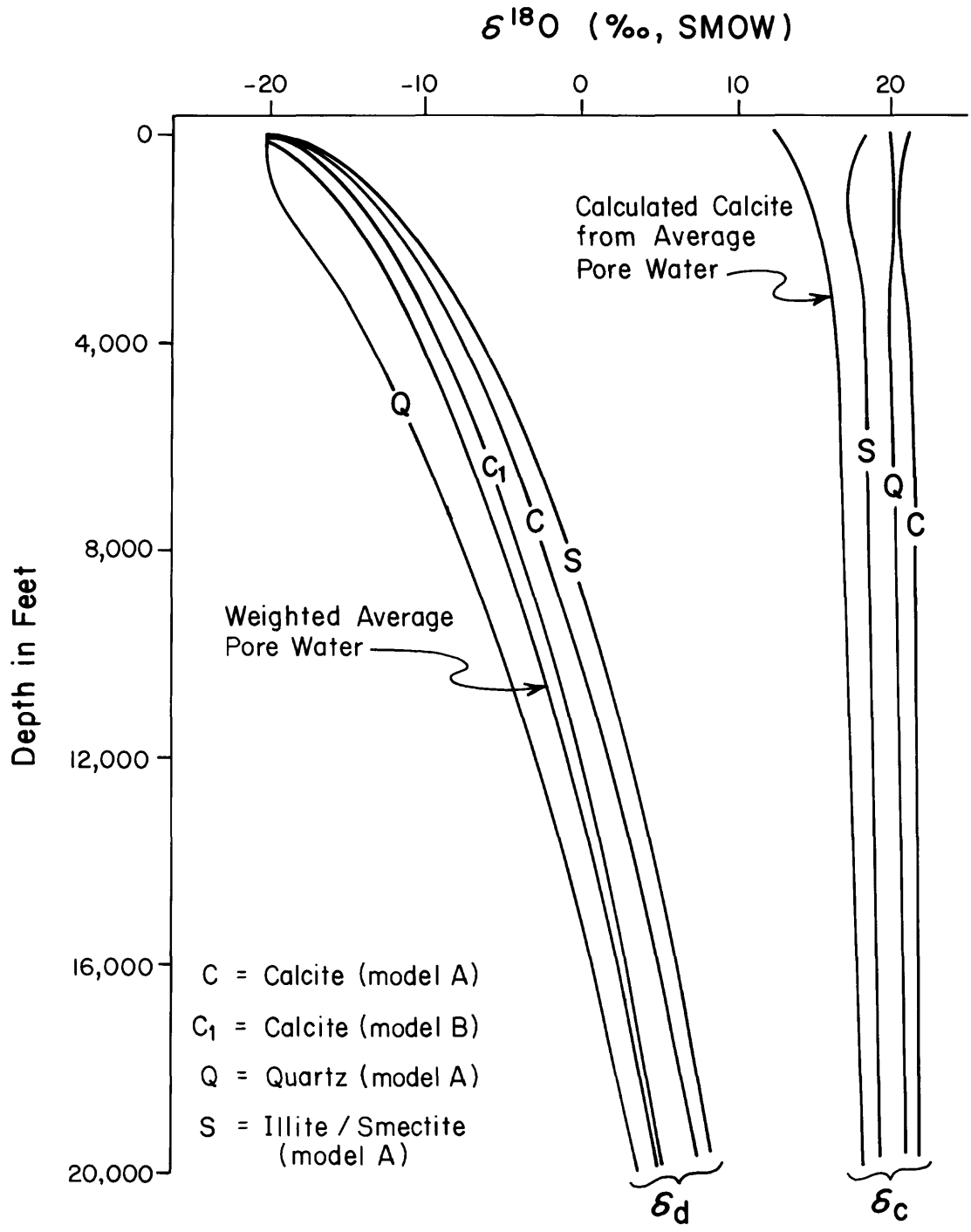

Figure 40--Predictive modeling of $\delta^{18}O$ for pore waters (δ_d) in equilibrium with precipitated phases (δ_c). Three mineral-water reactions which may occur in deep sandstones are considered. For comparison, δ_d of the calcite-water reaction is shown for models A and B. Although used to calculate the weighted average pore water, curves Q_1 and S_1 of model B are not shown.

cycle of dissolution and precipitation for every 1,000 feet, the number of cycles or depth increment hardly affects the shapes and values of the curves. In addition, there is a relatively small difference in the δ_d produced by each of the diagenetic reactions. Thus, despite large variations in the method of modeling, the curves remain remarkably similar. This demonstrates how the relatively large oxygen reservoir in the rock controls the relatively small oxygen reservoir in the pore water. In other words, when the water/rock ratio is low, the $\delta^{18}O$ of pore water is controlled largely by the $\delta^{18}O$ of the rock.

In theory, the diagenetic contribution of oxygen from the rock to the pore water at each depth increment is a summation of all the diagenetic reactions. Because of this it is necessary to consider the relative composition of the rock because it governs most of the diagenetic reactions that take place. From X-ray analyses and petrographic work on Wagon Wheel core, a rough estimate of bulk composition for Upper Cretaceous rocks is 15 percent carbonate, 50 percent quartz, and 35 percent shale. Using these percentages to weight the values of δ_d from Models A and B, I calculated an average $\delta^{18}O$ for descending pore waters (fig. 40). However, the small differences in δ_d between the diagenetic reactions permit considerable deviation in bulk composition before there is a significant change in the averaged water. Also shown in figure 40 is a curve of the calculated $\delta^{18}O$ for calcite which would precipitate in equilibrium with these waters. The difference between this curve and the curve for recrystallized calcite (curve C, δ_c; fig. 40) demonstrates the necessity of considering the combined contribution of oxygen from several diagenetic reactions.

These simple models can be criticized on a number of points. Many other diagenetic reactions and variations of the models could be considered for valid improvements. However, the general shape and trend of the averaged water curve would probably remain the same, but values along the curve would be different. Regardless of the particular mineral-water reaction, the curves in figure 40 are largely the result of a closed system with low porosity and a decrease in the oxygen isotopic fractionation with increasing temperature. Without measuring isotopic ratios in silicate minerals, I used published data to estimate the best possible $\delta^{18}O$ values for the initial minerals. Also it is likely that the initial $\delta^{18}O$ of the pore water was less negative and probably between $-10^{o}/oo$ and $-5^{o}/oo$ shortly after deposition in the Paleocene and Eocene. Conceivably, these errors are large, and could alter the final value of the averaged pore water.

In addition to questionable input values, there are several inherent flaws in the models. First, they assume that the authigenic precipitate reaches homogeneous equilibration with the solution at each step. At temperatures less than $70^{o}C$, complete isotopic equilibration is not expected (Yeh and Savin, 1977). Second, mineral-water reaction rates have not been considered. For example, it is difficult to estimate how the relatively rapid, calcite-water exchange modifies pore fluids that are mostly in contact with silicate minerals. Third, the models assume a closed system throughout

geologic time. Even in the northern Green River Basin pore fluids migrate and escape, yet the degree of pore water mixing would be virtually impossible to estimate. Perhaps the most serious flaw is that the models do not use an averaged pore water for the input $\delta^{18}O_{water}$ (δ_d) at each step. Essentially, the simplified method which was used, averaged the $\delta^{18}O$ of six pore waters (one from each model) after the reactions had occurred. Because of this, the authigenic precipitates and the pore waters have slightly incorrect $\delta^{18}O$ values at each step of dissolution and precititation. Although these flaws could with some effort be eliminated to improve the validity of the models, the general trends in $\delta^{18}O$ are likely to remain the same as long as a closed system with low porosity is specified.

Carbon

In general, $\delta^{13}C$ is most useful for understanding the origin of carbon in sedimentary carbonate minerals. This is because the kinetic (non-equilibrium) fractionations caused mainly by living organisms, allow discrimination between light (^{13}C depleted) carbon derived from organic matter and heavy (^{13}C enriched) carbon derived from limestones. Organic matter (plant and animal) in sedimentary rocks has a $\delta^{13}C$ value that is usually more negative than $-20^{o}/oo$ (PDB), while marine limestones have average $\delta^{13}C$ values near $0^{o}/oo$ (PDB). The carbon in CO_2 that comes from decaying and thermally maturing organic matter has roughly the same $\delta^{13}C$ as its parent organic matter. The carbon in atmospheric CO_2 has a $\delta^{13}C$ value of approximately $-7^{o}/oo$ (PDB). The isotopic compositions of sedimentary carbonates reflect the mixing or dominance of carbon from these three sources.

Carbon isotopes are not useful geothermometers because the kinetic fractionations are large and usually mask the smaller fractionations that result from equilibrium processes. Nevertheless, fractionation factors for carbon isotope exchange have been determined for carbonate equilibria, and depending on the system, temperature may effect the concentration of carbon isotopes in pore waters and calcite precipitates.

Equations relating temperature to carbon isotope fractionation between carbonate species are as follows:

$$10^3 \ln \alpha_{CO_{2(g)}\text{-}CaCO_3} = 7.6663(10^3\ T^{-1}) - 2.9880(10^6\ T^{-2}) - 2.4612$$

theoretically calculated up to high temperatures by Bottinga (1968);

$$10^3 \ln \alpha_{HCO^-_{3(aq)}\text{-}CO_{2(g)}} = 9.552(10^3\ T^{-1}) - 24.10$$

experimentally determined from 5^{o} to $125^{o}C$ by Mook and others (1974); and

$$10^3 \ln \alpha_{CO^=_{3(aq)}\text{-}CO_{2(g)}} = 1.410(10^6\ T^{-2}) - 8.371$$

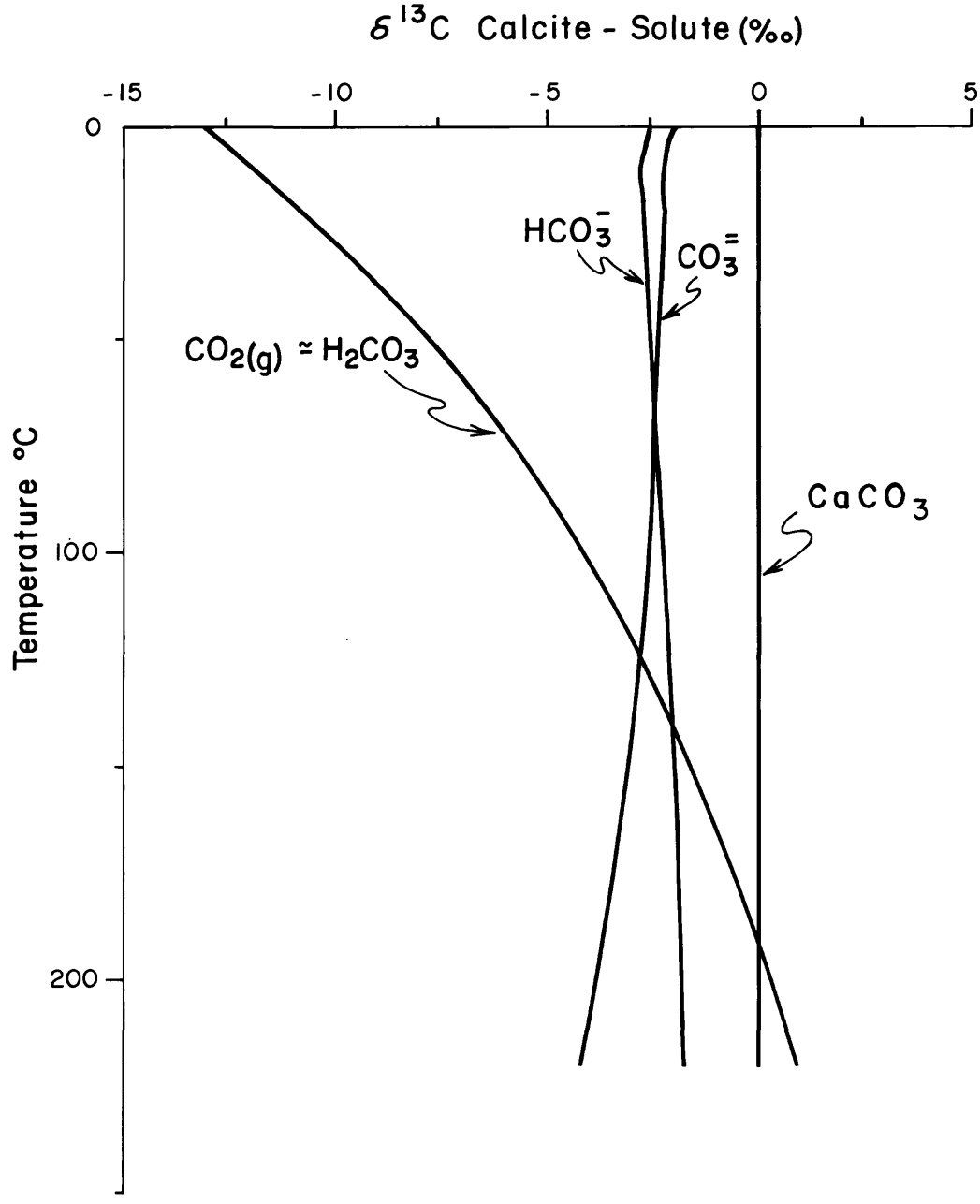

Figure 41--Temperature dependence of carbon isotope fractionation for carbon solute species with respect to $CaCO_3$. The abscissa is the difference in $\delta^{13}C$ between the solute species and $CaCO_3$ using $CO_{2(g)}$ for reference (modified from Robinson, 1975).

determined by least squares regression of theoretical data from Thode and others (1965).

The ^{13}C fractionation between $H_2CO_{3(aq)}$ and $CO_{2(g)}$ is less than 1.0°/oo, so for this discussion $H_2CO_{3(aq)}$ will be isotopically approximated as $CO_{2(g)}$.

Using $CO_{2(g)}$ for reference, enrichment factors of these species have been calculated relative to calcite and plotted versus temperature in figure 41. Notice that temperature has little effect on the magnitude of fractionation between calcite and HCO_3^- and $CO_2^=$ dominant solutions, and calcite is enriched in ^{13}C relative to these species by 2.5 - 3.0°/oo. On the other hand, temperature will cause a shift in the $\delta^{13}C$ of calcites precipitated from solutions dominated by H_2CO_3. If the $\delta^{13}C$ of these solutions remains the same, then with increasing temperature, calcite precipitates should have more negative $\delta^{13}C$ values.

Several factors control the isotopic composition of carbon in authigenic carbonate minerals. 1) The $\delta^{13}C$ of CO_2 gas in equilibrium with carbonate species in solution, 2) the $\delta^{13}C$ of the carbonate species in solution, 3) the pH, which affects the abundance of each carbonate species in solution, and 4) the temperature of equilibration. In most cases kinetic fractionations by living organisms cause large variations in the $\delta^{13}C$ of both CO_2 gas and solute species. By comparison carbon fractionations caused by temperature are small but should be considered where sedimentary systems are isolated from biological processes.

DISCUSSION

In this section I will demonstrate that isotopic variations in the carbonate minerals of the sandstones, shales, and fractures exhibit consistent trends which result from predictable changes with increasing depth in both the temperature and the isotopic composition of pore water. To make this interpretation, it is necessary to assume that some portion of the total carbonate undergoes recrystallization by a process of dissolution and reprecipitation. This assumption is reasonable because modification of isotopic composition occurs mainly by isotopic exchange between pore fluids and authigenic precipitates (Land, 1980). Thus, with burial the bulk composition of carbonate cement is continually modified, either by the addition of new cement or by the recrystallization of old cement.

The northern Green River Basin is unique because of two relatively predictable hydrochemical regimes in the subsurface. With increasing depth there is a transition from a normally-pressured, open hydrochemical system to an overpressured, restricted hydrochemical system. Between these two systems, there is a predictable shift in the isotopic composition of the pore waters. This is because when water/rock ratios are high, as in the normally pressured zone, water-rock diagenetic reactions cause little modification to the isotopic composition of the fluids. However, with increasing depth, drastic reductions in porosity and permeability cause increased stagnation of the pore

waters and lower the water/rock ratio. In the overpressured zone water-rock diagenetic reactions are expected to cause significant modification to the isotopic composition of the pore fluids.

A discussion of calcite is followed by a discussion of dolomite. Both carbon and oxygen isotopes show similar trends for somewhat similar reasons, but carbon is easier to understand because temperature-dependent fractionations cause little modification to $\delta^{13}C$.

Calcite

The positive shift with depth in $\delta^{13}C$ of calcite cements in the sandstones and fractures (figs. 23 and 36) may be interpreted as resulting from a similar shift in $\delta^{13}C$ of the pore waters. The average $\delta^{13}C$ ($-9.7^{o}/oo$) of calcite cements sampled from outcrops is similar to the average $\delta^{13}C$ ($-8.6^{o}/oo$) for near-surface waters. Although figure 41 indicates a 2 - $3^{o}/oo$ enrichment in ^{13}C for calcite precipitating in equilibrium with bicarbonate-rich waters, this fractionation is probably not observed because the cement and water samples come from different locations and are unrelated. The average $\delta^{13}C$ of near-surface waters suggests that most of the carbon in the dissolved species comes from atmospheric CO_2. This is supported by the fact that only minor amounts of carbon are available either from detrital carbonate, which is scarce in the arkosic aquifers, or from organic carbon, which is not abundant in the thin soils of the basin. With increasing depth two things happen to change the $\delta^{13}C$ of carbon species in the pore waters: 1) the percentage of detrital carbonate increases in the sandstones, and 2) there is a decrease in the volume of meteoric water which penetrates to deep sandstones. Thus, dissolved carbon becomes diluted with ^{13}C from the dissolution of detrital carbonate and $\delta^{13}C$ becomes more positive with depth. The carbon in the deep calcite cements is essentially redistributed carbon from detrital carbonate grains.

There is a smaller positive shift in $\delta^{13}C$ of bulk calcite in shales when compared to the sandstone cements (fig. 31). The reason for this is not clear because both authigenic and detrital components are measured in the bulk samples. Part of the reason may be that shales are initially less permeable than sandstones and acquire smaller volumes of authigenic cements from circulating waters during early burial. It is also possible that the trend is the result of an increase in the amount of detrital marine limestone in the shales. However, the small shift in $\delta^{18}O$ of the shales (fig. 31) argues for recrystallization. It seems likely that the shales are slightly permeable to pore fluids and the calcites have partially recrystallized during burial acquiring some carbon from an external source. Although the source of ^{13}C may come from a different part of the shale which was not sampled, the acquisition of ^{13}C from an external source is necessary for a positive shift in $\delta^{13}C$ of the bulk sample.

It is surprising that there is no evidence for the addition of ^{13}C-depleted (organic) carbon to the calcite cements of the gas-bearing sandstones and shales. At depth, significant amounts of ^{12}C are expected from CO_2 produced during the thermal decarboxylation of organic matter. The lack of dissolution features in the overpressured rocks also suggests that carbonic acids are not present in significant volumes. Perhaps the volume of CO_2 produced during late stage maturation of the Type III kerogens in these rocks is simply too small to be recognized or found.

Variations with depth in $\delta^{18}O$ of authigenic carbonates reflect changes in temperature of precipitation and changes in $\delta^{18}O$ of pore waters. With increasing depth and temperature, the positve trend in $\delta^{18}O$ of the calcite cements is opposite from the negative trend observed by a number of workers (Dickson and Coleman, 1980; Hudson, 1977; Milliken and others 1981; Pitman and others 1982). This seemingly uncommon trend is thought to result from a large positive shift in the $\delta^{18}O$ of pore water which compensates for the negative shift that might result from increasing temperatures. Although deep pore waters from the northern Green River Basin area have not been recovered, the low water/rock ratio implied by the low permeability of overpressured rocks strongly suggests that $\delta^{18}O$ of the pore waters becomes more positve with increasing depth. There are at least three possible reasons for this. 1) Near-surface waters, which have a relatively negative $\delta^{18}O$ (-20^{o}/oo, SMOW), are excluded from the overpressured sandstones. 2) Meteoric waters during deposition of the Tertiary and Upper Cretaceous sediments (fig. 13 and 14) were less negative than present meteoric waters. 3) With increasing temperatures during progressive burial, isotopic fractionations in most carbonate and silicate diagenetic reactions cause a net transfer of ^{16}O to diagenetic products and ^{18}O to water. Because of low circulation rates, pore waters in the deep sandstones should be isotopically modified by these reactions.

In the previous section, the average $\delta^{18}O$ of deep pore waters in the basin was predicted by using a closed system model and an estimated bulk rock composition of 15 percent calcite, 50 percent quartz, and 35 percent shale. However, these values are now bracketed with a range of values because the bulk composition of the rock is one variable that plays a major part in controlling the average composition of pore water. In this discussion, rocks having a bulk composition of 10-20 percent calcite, 60-40 percent quartz, and 30-40 percent shale are used to find a range of averaged pore waters from the models which were previously used. $\delta^{18}O$ values of measured calcite cements and bulk calcite in shales are compared to $\delta^{18}O$ of calcites which are calculated to be in equilibrium with predicted pore waters (fig. 42).

Figure 42 illustrates a number of points by showing how measured calcites relate to a closed system model that should be applicable to the overpressured zone. Using the mean annual surface temperature ($4^{o}C$) and $\delta^{18}O$ (-20^{o}/oo, SMOW) for near-surface water in the basin, the calculated $\delta^{18}O$ for an equilibrated calcite is -17^{o}/oo (PDB)--a value that closely agrees with the

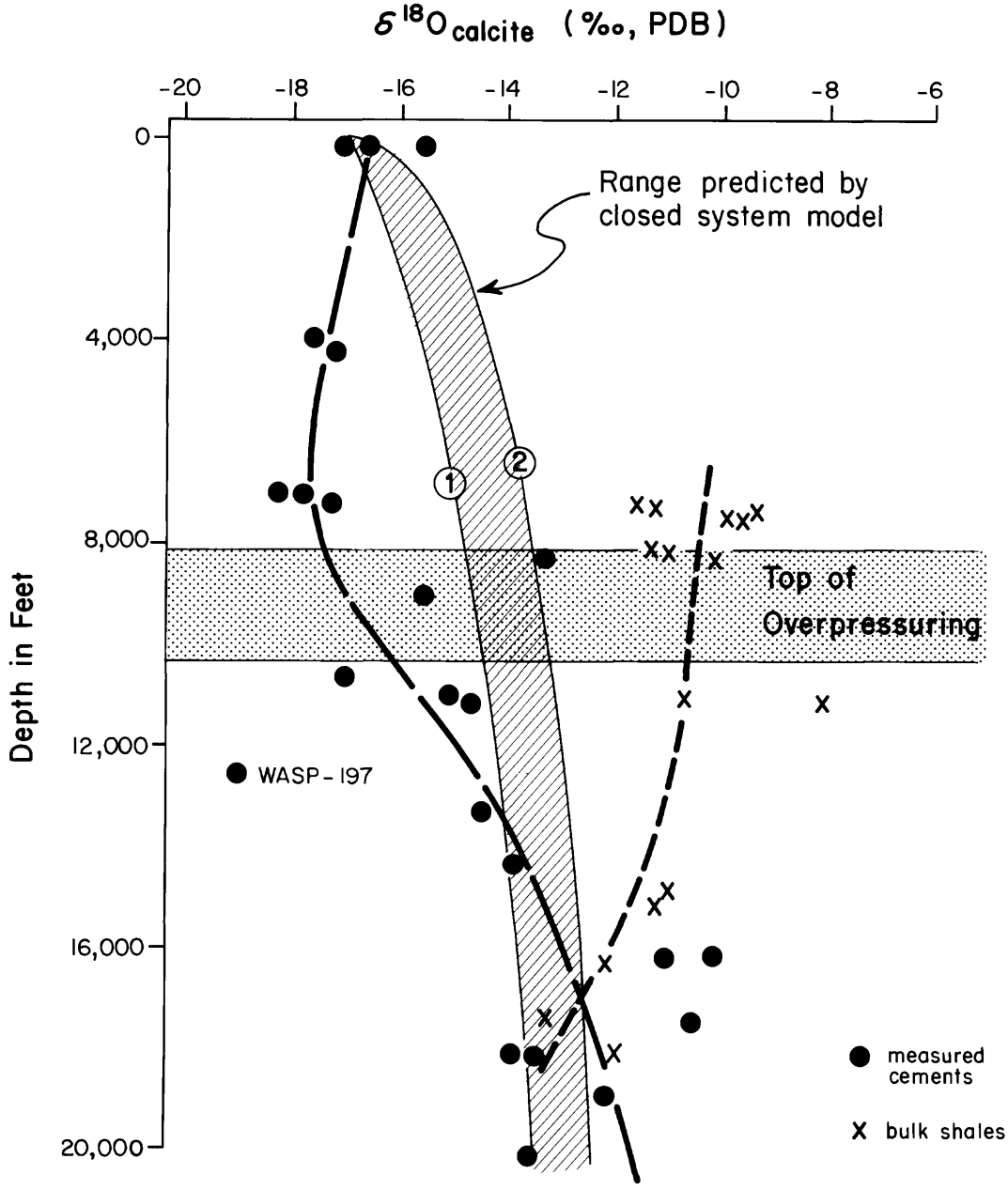

Figure 42--The $\delta^{18}O$ of calcite cements in sandstones (fig. 23) and bulk calcite in shales (fig. 31) are compared to calcite in equilibrium with modeled pore waters for a closed system. Curve 1 uses a bulk rock composition of 10 percent calcite, 60 percent quartz, and 30 percent shales; curve 2 uses 20 percent calcite, 40 percent quartz and 40 percent clay. See text for details. Dashed curves show approximate trends in the sandstones and shales. The cement in sample WASP - 197 (photomicrograph in fig. 9d) shows no visual evidence of recrystallization. The top of overpressuring, which differs in four wells, is represented by a zone.

average of measured $\delta^{18}O$ (-16.4°/oo) in calcite cements from outcrop. This evidence indicates that calcite cements in sandstones at the surface are in equilibrium with present near-surface conditions. In the normally pressured zone, the $\delta^{18}O$ values of the measured cements deviate from the closed system model and become slightly more negative with depth. This suggests that negative trends in $\delta^{18}O$ of authigenic calcites may be indicators of open hydrochemical systems. Near the top of overpressuring there is a reversal in trend, and $\delta^{18}O$ of the measured cements approaches the closed system model in the overpressured zone. WASP-197 is an excellent example in which the calcite cement has failed to recrystallize. In this sample there is no petrographic evidence for dissolution and reprecipitation (fig. 9d). Consequently, it is not surprising that in this calcite both $\delta^{13}C$ and $\delta^{18}O$ are off the general depth-trend and more representative of the isotopic values observed at shallow depths. In addition, if present porosities are used as a guide (figs. 4, 5, and 6), the minus-cement porosity (24 percent) of this sample suggests that cementation took place between 2,000 and 3,000 ft deep.

For bulk shale samples, the trend in $\delta^{18}O$ suggests that the carbonate minerals recrystallize and approach the isotopic composition of calcite in a closed system. Unfortunately, carbonate-rich shales could not be found at the surface because of the dominance of arkosic detritus.

Figure 42 also illustrates that the starting isotopic composition of the carbonate is important in determining the direction of isotopic trends with depth. For example, the $\delta^{18}O$ of carbonate in sandstones and shales converges toward a value of about -13°/oo. However, the initial $\delta^{18}O$ of the sandstone cement is about -17°/oo, whereas in the shales the initial carbonate, which is mostly detrital, has a $\delta^{18}O$ of about -8.6°/oo. Thus, with recrystallization both positive and negative trends can develop in the same hydrochemical system (sandstones and shales are hydrologically closed in the overpressured zone).

Dolomite

The consistency of $\delta^{13}C$ in dolomite (figs. 29 and 32) indicates either a lack of recrystallization with burial or recrystallization with acquisition of carbon from local detrital carbonate grains. However, the slight modification in $\delta^{18}O$ of dolomite argues for some recrystallization with burial. The variability in isotopic composition of dolomite is expected to be less than that for calcite because dolomite is much less susceptible to recrystallization in water than is calcite (Epstein and others 1964).

The trend with depth for $\delta^{18}O$ in dolomite (figs. 29 and 32) is difficult to interpret for two reasons. (1) First, the relation between $\delta^{18}O_{water}$ and dolomite at diagenetic temperatures (less than 300°C) is poorly understood (Land, 1980). (2) Second, bulk isotopic compositions obscure the absolute values of $\delta^{18}O$ for authigenic dolomite. From figure 29 it appears that the addition of authigenic dolomite causes the bulk composition of rhombic dolomite to become isotopically lighter. Although this says nothing about variations of $\delta^{18}O$ in authigenic dolomite, it does imply that a small portion of the total dolomite equilibrates with burial.

CONCLUSION

The observed trends in isotopic composition of the carbonate minerals would be very difficult to explain without assuming recrystallization by dissolution and reprecipitation. By this process the carbonates may alter their composition and approach equilibrium with geochemical conditions that continually change during burial. Although this mechanism appears to fit the data best, it is necessary to mention at least one alternative process which has been considered but not discussed.

It is possible that most cementation took place near the surface under changing conditions as the basin evolved, and during burial there was little diagenetic alteration of the carbonates. Conceivably, this could explain the general trend of $\delta^{18}O$, because meteoric waters in the basin have probably become progressively more negative since Late Cretaceous (figs. 12-14). However, the reversal in $\delta^{18}O$ near the top of overpressuring would require an additional explanation. Perhaps the most convincing evidence against this mechanism is the positive shift in $\delta^{13}C$ which is observed with increasing depth. If cementation had occurred near the surface, the $\delta^{13}C$ of the Upper Cretaceous cements should be more negative than $-8.6^{o}/oo$ (average of outcrop cements) because of the lush vegetation that could have supplied large volumes of light carbon. Presently, there is no trace of such cements left in the deep sandstones.

One reason for the reasonably well defined trends in $\delta^{13}C$ and $\delta^{18}O$ of the carbonates may be a long residence time of burial. Burial curves reconstructed from vitrinite reflectance indicate rapid burial from the Late Cretaceous to Eocene. However, from Eocene to Pliocene there was little tectonic activity for 40 m.y., and this may have allowed equilibration of many diagenetic reactions. Minor changes during the last 5 m.y. of post-Pliocene uplift probably could not be resolved from the present quantity of isotopic data.

ACKNOWLEDGEMENTS

This study was funded by the Department of Energy (Morgantown Energy Technology Center) in conjuction with the Western Tight Gas Sands Project at the U.S. Geological Survey. The initial report served as a Ph.D. dissertation at the University of Colorado.

I am deeply grateful to Prof. Donald D. Runnells at the University of Colorado for continual encouragement and guidance throughout the course of this work. Special thanks are given to Donald L. Gautier who provided helpful discussion and criticism and made this study possible at the U.S. Geological Survey. I benefited greatly from discussions with Ben E. Law, Richard M. Pollastro, Charles W. Spencer, Neely H. Bostick, Richard P. Major, Lynton S. Land and Irving Friedman.

I appreciate the technical assistance provided by many personnel of the U.S. Geological Survey. Access to the carbonate extraction line and mass spectrometer was provided by George E. Claypool and Charles N. Threlkeld. April Vuletich analyzed the isotopic composition of organic matter in the shales. Richard Pollastro and Gene Whitney provided laboratory facilities and access to the X-ray diffractometer. Ralph Christian lent assistance on the micorprobe and Jim Nitche assisted with the operation of the SEM. Marjorie Cunningham and Helen Colburn prepared the manuscript for publication.

REFERENCES

Ahmed, U., Holland, M. T., and Schatz, J. F., 1981, Resource evaluation and production research on tight sands in the Pinedale unit, Sublette County, Wyoming: Unpublished Report, Gas. Research Institute, Chicago, Illinois, 157 p.

Amsbury, D. L., 1962, Detrital dolomite in central Texas: Journal Sedimentary Petrology, v. 32, p. 5-14.

Armstrong, F. C., and Oriel, S. S., 1965, Tectonic development of Idaho-Wyoming thrust belt: American Association of Petroleum Geologists Bulletin, v. 49, p. 1847-1866.

Bathurst, R. G. C., 1975, Carbonate Sediments and Their Diagenesis, (2nd enlarged ed.): New York, Elsevier, 658 p.

Bender, M. M., 1968, Mass spectrometric studies of carbon 13 variations in corn and other grasses: Radiocarbon, v. 10, no. 2, p. 468-472.

Boles, J. R., 1978, Active ankerite cementation in the subsurface Eocene of southwest Texas: Contributions Mineralogy and Petrology, v. 68, p. 1322.

Bottinga, Y., 1968, Calculation of fractionation factors for carbon and oxygen exchange in the system calcite-carbon dioxide-water: Journal Physics Chemistry, v. 72, p. 800-808.

Bucurel, H. G., 1981, Section B-B´, subsurface correlations of some Upper Cretaceous and Tertiary rocks, Great Divide Basin, Wyoming: U.S. Geological Survey Open-File Report 82-456, 2 sheets.

Clayton, R. N., Friedman, I., Graf, D. L., Mayeda, T. K., Meents, W. F., and Shimp, N. F., 1966, The origin of saline formation waters: I. Isotopic composition: Journal Geophysical Research, v. 71, p. 3869-3882.

Craig, Harmon, 1953, The geochemistry of stable carbon isotopes: Geochimica et Cosmochimica Acta, v. 3, p. 53-92.

Degens, E. T., 1969, Biogeochemistry of stable carbon isotopes, in, Eglinton, G., and Murphy M. T. J., eds., Organic Geochemistry: Springer, Heidelberg, p. 304-329.

Deines, P., Langmuir, D., and Harmon, R. S., 1974, Stable carbon isotope ratios and the existence of a gas phase in the evolution of carbonate ground water: Geocimica et Cosmochimica Acta, v. 38, p. 1147-1164.

Dickinson, W. W., and Gautier, D. L., 1983, Diagenesis of nonmarine rocks and gas entrapment in northern Green River Basin, Wyoming (abs.): American Association of Petroleum Geologists Bulletin, v. 67, p. 450.

Dickson, J. A. D., 1966, Carbonate identification and genesis as revealed by staining: Journal of Sedimentary Petrology, v. 36, p. 491-505.

Dickson, J. A. D., and Coleman, M. L., 1980, Changes in carbon and oxygen isotope composition during limestone diagenesis: Sedimentology, v. 27, p. 107-118.

Dorr, J. A., Spearing, D. R., and Steidman, J. R., 1977, Defformation and deposition between a foreland uplift and an impinging thrust belt; Hoback Basin, Wyoming: Geological Society of America Memoir 177, 82 p.

Dott, R. H., and Batten, R. L., 1981, Evolution of the earth: 3rd Ed., McGraw-Hill, New York, 573 p.

Drever, J. I., 1982, The geochemistry of natural waters: New Jersey, Prentice-Hall, 388 p.

Epstein, S., Graf, D. L., and Degens, E. T., 1964, Oxygen isotope studies on the origin of dolomite, in H. Craig and others eds., Isotopic and cosmic chemistry: North Holland Publishing Company, Amsterdam, p. 169-180.

Erickson, J. M., 1978, Bivalve mollusk range extensions in the Fox Hills Formation (Maestrichtian) of North and South Dakota and their implications for the Late Cretaceous geologic history of the Williston Basin: Annual Proceedings North Dakota Academy of Science, v. 32, part II, p. 79-89.

Faure, G., 1977, Principles of isotope geology: Wiley, New York, 464 p.

Folk, R. L., 1965, Some aspects of recrystallization in ancient limestones, in Pray, L. C., and Murray, R. C., eds., Dolomitization and Limestone Diagenesis: A Symposium, Society Economic Paleontologists Mineralogists, Special Publication 13, p. 14-48.

Friedman, I., 1970, Some investigations of the deposition of travertine from hot springs -I. The isotopic chemistry of travertine-depositing spring: Geochimica et Cosmochimica Acta, v. 34, p. 1330-1315.

Friedman, I., and O'Neil, J. R., 1977, Compilation of stable isotope fractionation factors of geochemical interests, in M. Fleischer, ed., Data of Geochemistry: U.S. Geological Survey Professional Paper 440-KK, 6th Ed.

Friedman, I., Redfield, A. C., Schoen, B., and Harris, J., 1964, The variation in the deuterium content of natural waters in the hydrologic cycle: Review of Geophysics, v. 2, p. 177-224.

Gardner, L. R., 1972, Origin of Morman Mesa caliche, Clark County, Nevada: Geological Society of American Bulletin, v. 83, p. 143-155.

Garrels, R. M., and Christ, C. L., 1965, Solutions, minerals and equilibria: Freeman, Cooper and Company, San Francisco, 450 p.

Gat, J. R., 1971, Comments on the stable isotpe method in regional ground water investigations: Water Resources Research, v. 7, p. 980-993.

Gautier, D. L., 1981, Petrology of the Eagle Sandstone, Bearpaw Mountains area, north-central Montana: U.S. Geological Survey Bulletin 1521, 54 p.

Hoefs, J., 1980, Stable isotope geochemistry, 2nd ed., Springer-Verlag, New York, 208 p.

Hudson, J. D., 1977, Stable isotopes and limestone lithification: Joural Geological Society London, v. 133, p. 637-660.

Jackson, T. A., Fritz, P., and Drimmie, R., 1978, Stable carbon isotope ratios and chemical properties of kerogen and extractable organic matter in pre-Phanerozoic and Phanerozoic sediments--their interrelations and possible paleobiological significance: Chemical Geology, v. 21, p. 335-350.

Jonas, E. C., and McBride, E. F., 1977, Diagenesis of sandstone and shale; application to exploration for hydrocarbons: Continuing Education Program Publication No. 1, Department of Geology, University Texas, Austin, Texas, 165 p.

Keith, M. L., and Weber, J. N., 1964, Carbon and oxygen isotopic composition of selected limestones and fossils: Geochimica et Cosmochimica Acta, v. 28, p. 1787-1816.

Land, L., 1980, The isotopic and trace element geochemistry of dolomite: the state of the art, in Zenger, D. H., Dunham, J. B., and Ethington, R. A., eds., Concepts and Models of Dolomitization: Society of Economic Paleontologists and Mineralogists Special Publication 28, p. 87-110.

Land, L. S., and Dutton, S. P., 1978, Cementation of a Pennsylvanian deltaic sandstone, isotopic data: Journal of Sedimentary Petrology, v. 48, p. 1167-1176.

Law, B. E., 1981, Section C-C′ subsurface correlations of some Upper Cretaceous and Tertiary rocks, northern Green River Basin, Wyoming: U.S. Geological Survey Open-File Report 81-663, 2 sheets.

_____1984, Relationships of source rock, thermal maturity, and overpressuring to gas generation and occurrence in low-permeability Upper Cretaceous and lower Tertiary rocks, Greater Green River basin, Wyoming, Colorado, and Utah, in Woodward, J., Meissner, F., and Clayton, J., eds., Symposium on hydrocarbon source rocks of the greater Rocky Mountain region: Rocky Mountain Association of Geologists, p. 469-490.

Law, B. E., and Smith, C. R., 1983, Subsurface temperature map showing depth to 180° Fahrenheit in the Greater Green River basin, Wyoming, Colorado, and Utah: U.S. Geological Survey Miscellaneous Field Studies Map MF-504.

Law, B. E., Spencer, C. W., and Bostick, N. H., 1980, Evaluation of organic matter, subsurface temperature, and pressure with regard to gas generation in low-permeability Upper Cretaceous and lower Tertiary sandstones in Pacific Creek area, Sublette and Sweetwater Counties, Wyoming: The Mountain Geologist, v. 17, no. 2, p. 23-25.

Lawrence, J. R., 1973, Interstitial water studies, Leg 15--Stable oxygen and carbon isotope variations in water, carbonates, and silicates from the Venezuela Basin (Site 149) and the Aves Rise (Site 148): Initial Reports of the Deep Sea Drilling Project, v. XX, U.S. Government Printing Office, p. 891-919.

Lawrence, J. R., Gieskes, J., and Anderson, T. F., 1976, Oxygen isotope material balance calculations, leg 35: Initial Reports of the Deep Sea Drilling Project, v. XXXV, U.S. Government Printing Office, p. 507-512.

Lickus, M. R., Pawlewicz, M. J., Law, B. E., and Dickinson, W. W., 1984, Thermal maturity map, northern Green River basin, Wyoming, in Law, B. E., ed., Geological characteristics of low-permeability Upper Cretaceous and lower Tertiary rocks in the Pinedale anticline area, Sublette County, Wyoming: U.S. Geological Survey Open-File Report 84-753, p. 60-65.

Lindholm, R. C., and Finkelman, R. B., 1972, Calcite staining; semiquantitative determination of ferrous iron: Journal of Sedimentary Petrology, v. 42, p. 239-242.

Love, J. D., 1960, Cenozoic sedimentation and crustal movement in Wyoming: American Journal of Science (Bradley vol.) v. 285-A, p. 204-214.

Marshall, J. D., 1982, Isotopic composition of displacive fibrous calcite veins: reversals in pore-water composition trends during burial diagenesis: Journal of Sedimentary Petrology, v. 52, p. 615-630.

Martin, W. B., and Shaughnessy, J., 1969, Project Wagon Wheel: in, Wyoming Geological Association Guidebook 1969, 21st Field Conference, Symposium on Tertiary Rocks of Wyoming, p. 145-152.

Matsumoto, R., Utada, M., and Kagami, H., 1978, Sedimentary petrology of DSDP cores from sites 362 and 363, the Walvis Ridge, and site 364, the Angola Basin, drilled on leg 40: Initial Reports of Deep Sea Drilling Project, v. XL, U.S. Government Prining Office, p. 469-483.

Matter, A., Douglas, R. G., and Perch-Nielson, K., 1975, Fossil preservation, geochemistry, and diagenesis of pelagic carbonates from Shatsky Rise, Northwest Pacific: Initial Reports of the Deep Sea Drilling Project, v. XXXII, U.S. Government Printing Office, p. 891-908.

McCrea, J. M., 1950, The isotopic chemistry of carbonates and a paleo-temperature scale: Journal of Chemistry and Physics, v. 18, p. 849-855.

McPeek, L. A., 1981, Eastern Green River Basin: a developing giant gas supply from deep, overpressured Upper Cretaceous sandstones: American Association of Petroleum Geologists Bulletin, v. 65, p. 1078-1098.

Milliken, K. L., Land, L. S., and Loucks, R. G., 1981, History of burial diagenesis determined from isotopic geochemistry, Frio Formation, Brazoria County, Texas: American Association of Petroleum Geologists Bulletin, v. 65, p. 1397-1413.

Mook, W. G., Bommerson, J. C., and Staverman, W. H., 1974, Carbon isotope fractionation between dissolved bicarbonate and gaseous carbon dioxide: Earth and Planetary Science Letters, v. 22, no. 2, p. 169-176.

Moore, R. G., 1960, A Paleocene fauna from the Hoback Formation, Wyoming [Ph.D. dissert.]: Ann Arbor, University Michigan, 169 p.

Nash, A. J., and Pittman, E. D., 1975, Ferro-magnesian calcite cement in sandstones: Journal of Sedimentary Petrology, v. 45, p. 258-272.

Oehler, D. Z., Schopf, J. W., and Kevenvolden, K. A., 1972, Carbon isotopic studies of organic matter in Precambrian rocks: Science, v. 175, p. 1246-1248.

O'Neil, J. R., Clayton, R. N., and Mayeda, T. K., 1969, Oxygen isotope fractionation in divalent metal carbonates: Journal of Chemistry Physics, v. 51, p. 5547-5558.

Pearson, F. J., and Hanshaw, B. B., 1970, Sources of dissolved carbonate in ground water and their effects on carbon-14 dating: in Isotope Hydrology, IAEA, Vienna, p. 271-286.

Pitman, J. K., and Fouch, T. D., and Goldhaber, M. B., 1982, Depositional setting and diagenetic evolution of some Tertiary unconventional reservoir rocks, Uinta Basin, Utah: American Association of Petroleum Geologists Bulletin, v. 66, p. 1581-1596.

Pollastro, R. M., 1983, The formation of illite at the expense of illite/smectite--mineralogical and morphological support for a hypothesis: Program and Abstracts, 12th Annual Meeting, The Clay Minerals Society, 32nd Annual Clay Minerals Conference, Buffalo, N.Y., p. 82.

Robinson, B. W., 1975, Carbon and oxygen isotopic equilibria in hydrothermal calcites: Geochemistry Journal, v. 9, p. 43-46.

Sabins, F. F., 1962, Grains of detrital, secondary, and primary dolomite from Cretaceous strata of the Western Interior: Geological Society of America Bulletin, v. 73, p. 1183-1196.

Savin, S. M., and Epstein, S., 1970, The oxygen and hydrogen isotope geochemistry of ocean sediments and shales: Geochimica et Cosmochimica Acta, v. 34, p. 43-63.

Schmidt, V., and McDonald, D. A., 1979, The role of secondary porosity in the course of sandstone diageneses, in Scholle, P. A., and Schluger, P. R., eds., Aspects of diagenesis: Society of Economic Paleontologists and Mineralogists Special Publication 26, p. 175-207.

Sheppard, S. M. F., Nielsen, R. L., and Taylor, H. P., 1969, Oxygen and hydrogen isotope ratios in minerals from porphyry copper deposits: Economic Geology, v. 64, p. 755-775.

Shuster, M. W., 1983, The origin and development of the northern Green River Basin; a stratigraphic and flexural approach: Unpublished Report, University of Wyoming, Laramie, 24 p.

Shuster, M. W., and Steidtmann, J. R., 1984, Origin and development of northern Green River Basin; a stratigraphic and flexural study (abs.): American Association of Petroleum Geologists Bulletin, v. 68, p. 527.

Spencer, C. W., 1983, Geologic aspects of tight gas reservoirs in the Rocky Mountain region, in 1983 SPE/DOE Symposium on Low-Permeability Gas Reservoirs, Proceedings, Denver, Colorado, March 13-16, 1983: Society of Petroleum Engineers, p. 399-408.

Taylor, H. P., 1974, The application of oxygen and hydrogen isotope studies to problems of hydrothermal alterations and ore deposition: Economic Geology, v. 69, p. 843-883.

Thode, H. G., Shima, M., Rees, C. E., and Krishnamurty, K. V., 1965, Carbon-13 isotope effects in systems containing carbon dioxide, bicarbonate, crabonate, and metal ions: Canadian Journal of Chemistry, v. 43, p. 582-595.

Thomas, R. D., and Ward, D. C., 1972, Effects of overburden pressure and water on gas permeability of tight sandstone cores: Journal of Petroleum Technology, v. 24, p. 120-124.

Truesdell, A. H., 1974, Oxygen isotope activities and concentrations in aqueous salt solutions at elevated temperatures--Consequences for isotope geochemistry: Earth and Planetary Science Letters, v. 23, no. 3, p. 38-396.

Walters, L. J., Jr., Claypool, G. E., and Choquette, P. W., 1972, Reaction rates and $\delta^{18}O$ variation for the carbonate-phosphoric acid preparation method: Geochimica et Cosmochimica Acta, v. 36, p. 129-140.

Watts, N. L., 1978, Displacive calcite; evidence from recent and ancient calcretes: Geology, v. 6, p. 699-703.

Welder, G. E., 1968, Ground-water reconnaissance of the Green River Basin southwestern Wyoming: U.S. Geological Survey Hydrologic Investigations Atlas HA-290.

Welte, D. H., Kalkreuth, W., and Hoefs, J., 1975, Age-trend in carbon isotopic composition in Paleozoic sediments: Naturwissenschaften, v. 62, p. 482-483.

Wilkinson, B. H., Buczynski, C., and Owen, R. M., 1984, Chemical control of carbonate phases: implications from upper Pennsylvanian calcite-arogonite ooids of southeastern Kansas: Journal of Sedimentary Petrology, v. 54, p. 932-947.

Yeh, H., and Savin, S. M., 1977, Mechanism of burial metamorphism of argillaceous sediments: 3. O-isotope evidence: Geological Society of America Bulletin, v. 88, p. 1321-1330.

Zeller, H. D., and Stephens, E. V., 1969, Geology of the Oregon buttes area Sweetwater, Sublette and Fremont Counties southwestern Wyoming: U.S. Geological Survey Bulletin, 1256, 60 p.